UNIVERSITY OF NAIROBI

SCHOOL OF ENGINEERING

DEPARTMENT OF ENVIRONMENTAL AND BIOSYSTEMS ENGINEERING

OPTIMIZATION OF THE PERFORMANCE OF A HYBRID SOLAR-DESICCANT DRYER

By

FRANKLINE MURIUNGI MWITI

Reg No: F56/88229/2016
(B.Sc. Biosystems Engineering, UON, 2014)

Thesis submitted to the Department of Environmental and Biosystems Engineering, University of Nairobi, in partial fulfilment of the requirements for the Degree of Master of Science in Environmental and Biosystems Engineering

NOVEMBER 2019

DECLARATION

I, Mwiti Frankline Muriungi, declare that this Thesis is my original work, and has not been presented for award of a degree in any other University.

…… ..…….……

Frankline Muriungi Mwiti **Date**

This thesis has been submitted for examination with our approval as university supervisors.

…… ..…….……

Duncan.O.Mbuge, PhD. **Date**

Department of Environmental and Biosystems Engineering

University of Nairobi

……..…….. ……..…….……

Ayub.N.Gitau, PhD **Date**

Department of Environmental and Biosystems Engineering

University of Nairobi

DECLARATION OF ORIGINALITY

Name of student:	Frankline Muriungi Mwiti
Registration:	F56 /88229 / 2016
College:	College of Architecture and Engineering
Faculty/School/Institute:	School of Engineering

1) I understand what plagiarism is and I'm aware of the university policy in this regard
2) I declare that this thesis is my original work and has not been submitted elsewhere for examination, award of a degree or publication. Where other works or my own work has been used, this has properly been acknowledged and referenced in accordance with the University of Nairobi's requirements.
3) I have not sought or used the services of any professional agencies to produce this work
4) I have not allowed and shall not allow anyone to copy my work with the intention of passing it off as his/her work
5) I understand that any false claim in respect of this work shall result in disciplinary action in accordance with University of Nairobi anti-plagiarism policy.

Signature…… Date……

DEDICATION

I dedicate this work to my parents, entire family members and mentors for their continued inspiration, encouragement and persistent support throughout my academic life.
May the almighty God bless you all

ACKNOWLEDGEMENT

I thank God for giving me the chance, strength and good health throughout the period of this research. Sincere thanks to my supervisors, Eng. Dr. Duncan O. Mbuge and Eng. Prof. Ayub.N. Gitau for their encouragement, criticism and guidance they provided during this study. I am greatly indebted for the funds and facilities awarded by Volkswagen Foundation and the University of Nairobi. I particularly thank the chairman Department of Environmental and Biosystems Engineering, Eng. Dr. Duncan O. Mbuge for his overwhelming support in the entire period of study. I appreciate and give gratitude to Dr. Franz Roman of University of Kassel-Germany for his remarkable critic during this research.

I owe gratitude debts to the technical staff of the university of Nairobi. Special thanks to Mr. Wamutitu (metal workshop technologist), Mr. Mwachoni (Process and Food Engineering lab) as well as Mr. Kahiro (Mechanical Engineering workshop), Mr. Opiyo and Mr Tomas Obwago of Science Workshop.

May the Almighty God Bless You All

ABSTRACT

A hybrid solar desiccant dryer (HSDD) was designed, developed and optimized with the aim of preconditioning the air for maize grain drying. The effect of four solar collector configurations in optimizing dryer performance was studied, comprising of (1) Radiation concentration lenses to increase solar radiation intensity and achieve high temperatures, (2) High density longitudinal finned elements for enhanced thermal contact and heat transfer rates, (3) Desiccant exhaust dehumidification conduits to enhance thermal recuperation of waste heat for regeneration into the dryer and (4) Combined effect of the three configurations.

The collectors were tested and grain drying experiments performed on a loaded HSDD with the most efficient collector configuration and results compared with open sun drying method. Temperature changes of the solar collector configurations, heat transfer rates, collector efficiencies, grain drying rates and drying time were analysed. Moreover, the HSDD experimental moisture ratio data was fitted to 18 mathematical models of dying and regressed using MATLAB (Version R2016a) to evaluate goodness of fit by comparing coefficient of determination (R^2), sum of square error (*SSE*) and root mean square error (*RMSE*).

Results showed that collector configuration with finned elements, desiccant exhaust air regeneration conduits and radiation concentration lenses had average temperature change of 8°C, 17°C and 21°C above ambient respectively; while the combined collector had the highest average temperature change of 28°C. Similarly, changes in relative humidity were 6%, 16%, 19% and 25% for finned elements surfaces, desiccant exhaust air regeneration, radiation concentration lenses and the combined collector respectively. Analysis of variance using Stratigraphic16.1 software showed statistically significant differences in temperature changes under different test configurations at 95% level of confidence. Moreover, multiple range tests indicated significant differences between the means of temperatures from the contrasted collector configurations.

The temperature and relative humidity changes increased linearly, and the rate of change was highest in the combined configuration and least in finned elements. Thermal efficiency increased with temperature changes as well as with useful heat gain and solar insolation. Useful heat gain increased to reach the maximum average values of 0.104 kJs, 0.19 kJs, 0.244 kJs and 0.289 kJs for the finned elements, desiccant exhaust air regeneration, radiation concentration lenses and the combined configurations respectively at maximum solar insolation time (13.30hrs). The average collector efficiencies were 17%, 36%, 45%, and 61% for the finned

elements, desiccant exhaust air regeneration, radiation concentration lenses, and the combined collector configuration respectively. The integrated collector configuration improved thermal efficiency from individual configurations by 44%, 25% and 16% for the longitudinal finned elements, desiccant exhaust air regeneration and radiation concentration lenses alone respectively. The combined collector set up had lowest heat loss coefficient (7.1528) while the collector with radiation concentration lenses only manifested the highest value (12.336) despite achieving high temperatures than finned elements surfaces (10.008) and desiccant exhaust regeneration (9.0295).

The HSDD achieved maize grain drying from 24.1% to 13.1% M.C (w.b) in 18 hours compared to 54 hours for open air sun drying method. Moisture removal rate increased from 0.162 kg/hr to 0.485kg/hr while the drying time was reduced by 67% using HSDD. Regressed moisture ratio datasets of the eighteen fitted mathematical models reviewed that the Two term model characterised the drying kinetics of maize grain in the HSDD with highest R^2 (0.9676) and lowest *SSE* (0.05655) and *RMSE* (0.04078) values.

The performance of the dryer was optimised by incorporating radiation concentration lenses, longitudinal finned element surfaces and desiccants exhaust regeneration system to increase drying temperatures, heat transfer and waste heat recovery for subsequent drying. This study is useful in scaling-up dryer design and prediction of tempering effects during conditioning of grain in planned drying schedules. It optimizes drying process parameters for improved dryer performance and efficiency enhancement to reduce time loss and possible grain damage during drying to benefit grain and seed industry for sustainable food security.

Keywords: *Solar collector, Grain dryer, Finned element, Exhaust regeneration, Desiccant, Radiation concentration lenses, Drying rate, Drying kinetics.*

TABLE OF CONTENTS

LIST OF FIGURES

LIST OF PLATES

LIST OF TABLES

NOMENCLATURE

%	Percent
Δ	Change
A	Area
A_c	Collector Area
ANOVA	Analysis of Variance
ASABE	American Society of Agricultural and Biological Engineers
CFD	Computational Fluid Dynamics
C_P	Specific Heat Capacity
CPV	Concentrated Photovoltaic
DEARS	Exhaust Air Desiccant Regeneration Conduit
E	Energy
EMC	Equilibrium Moisture Content
FAO	Food and Agriculture Organization of the United Nations
HSDD	Hybrid Solar Desiccant Dryer
I	Insolation
IFPRI	International Food Policy Research Institute
$\dot{m}$	Mass Flow Rate
MC	Moisture Content
M_f	Final Moisture Content
M_o	Initial Moisture Content
MPEADR	Multi-Pass Exhaust Air Desiccant Regeneration
MR	Moisture Ratio
MRR	Moisture Removal Rate
NREL	National Renewable Energy Laboratory of the United States
OSD	Open Sun Drying
PV	Photovoltaic
Q	Volume Flow Rate
Q_u	Useful Heat
R^2	Coefficient of Determination
RCL	Radiation Concentration Lenses
RH	Relative Humidity
SAP	Superabsorbent Polymer

T	Temperature
T_a	Ambient Temperature
T_i	Inside Temperature
U_L	Heat Loss Rate
W.b	Wet Basis
α	Absorption Coefficient
ΔT	Temperature Change
η	Efficiency
ρ	Density
τ	Transmission Coefficient
χ^2	Reduced Chi-square

UNITS OF MEASURE

°C	Degrees Celcius
Hrs	Hours
kg/m^3	Density
kJs	Kilojoule Second
kW	Kilowatt
m	Metres
m^2	Square metre
W	Watt

CHAPTER ONE: INTRODUCTION

1.1 Background

Integration of renewable energy technologies in post-harvest grain management operations is a significant feature in addressing energy demands, food security and climate change for agricultural livelihoods in developing countries.

It is currently estimated that 2 billion people in the world suffer from energy constraints that limit their economic development opportunities, food security and improved standards of living. Sayibu and Ampadu (2015) hold that availability of energy for industrial, domestic and agricultural applications is the most significant and captivating feature in any civilized society. Renewable energy is a feasible alternative and is gaining significant attention in agriculture due to problems associated with conventional energy sources sources (Fathima *et al*., 2014).

According to Al-Neama & Farkas (2018) and Perez & Perez (2009) solar energy has attained worldwide recognition as the most promising renewable energy source due to its availability, reliability, affordability. Furthermore, solar is a source of clean energy, environment friendly and requires little system maintenance. However, there is a global concern of weather variability as a result of climate change. For maize farmers in Kenya and in the tropics, rains coincide with harvest season and have not been spared of heavy grain losses that have seen a growing demand for energy in a modernised technology for post-harvest grain management. This creates a necessity for advancement in concentrated solar thermals and photovoltaics. In Kenya 90% of the farmers grow maize and 75% of the overall yield is produced by small scale farmers (Kang'ethe, 2011) and rely on open sun drying and ambient storage of the harvest. Majority of small-scale maize farmers retain about 58% of their harvest for subsistence consumption (Mbithi, 2000; Kenya National Bureau of Statistics, 2014).

According to Karanja (1996) Maize is the most consumed food crop in Kenya and represents 44 percent calorie intake of the daily dietary energy consumption. In the recent years maize products retail prices have been on substantial increase due to dwindling supply with the need for imports remaining into the foreseeable future due to post harvest losses. Energy requirements in grain drying and appropriate storage systems are important post-harvest operations. Recent estimates put post-harvest losses of maize in Africa at 14% to 36% of the total production and can be nearly 80% under adverse weather conditions (Tefera, 2012). This

challenge has attracted the attention establishing appropriate drying and storage facilities to reduce post-harvest losses and aflatoxin contamination (Kumar & Kalita 2017).

Maize grain drying is characterised by progressive moisture loss due to simultaneous heat and mass transfer. Usually is harvested, threshed and dried to 12%-13% w.b moisture content, a process that requires abundant source of energy (Tonui *et al*, 2014). Drying energy is supplied by mechanical dryers that operate on large amounts of fuel and electricity and thus expensive particularly for small scale maize farmers. Majority of farmers cannot afford the fossil fuels or electric dryers and only 20% of the population has access to electricity in Africa (Winkler, 2011). For this reason, the farmers practice open air-sun drying which has serious challenges when the rainy season coincides with the harvest period especially in recent times of climate change. In addition, the practice of open sun drying is such that solar radiation is only available and effective for 6 - 8 hours a day Punlek *et al.* (2009) and the energy is greatly affected by haze and sporadic atmospheric conditions (Tiwari, 2016).

Open-air sun drying (OASD) method involves a considerable daily labour and drudgery in removal and return of the grain back into the stores, discoloration of grain kernels as a result of direct solar drying. Further condensation of moisture in lower layers results to reduced transmissivity and diffusion of moisture from grain kernels which reduces drying rates. Additionally, maize kernel is a hygroscopic and tends to regain moisture during the night to attain equilibrium condition with surrounding air. As such there is need for an alternative appropriate drying method that ensures continuous drying even at low radiation hours. A hybrid system incorporating both solar and a desiccant such as superabsorbent polymer (SAP) can be explored to hasten the drying when direct solar is not available to prevent conditions that can lead to aflatoxin contamination.

According to Waewsak *et al*. (2006), renewable energy technologies can have an important role in extending post-harvest technology to farmers in the developing countries for increased productivity. Akinola *et al*. (2006) says renewable solar thermal energy has a growing awareness and acceptance in agricultural applications since it is abundant, non-polluting and inexhaustible. Solar radiation can be harnessed in a solar collector-drying system, creating a greenhouse effect within the drying system to attain appropriate temperatures for drying. This can avert post-harvest losses and improve productivity of the farmers towards better revenue (Toshniwal & Karale, 2013).

Kenya as a tropical country receives abundant solar radiation characterised by average daily insolation of between 5.5-6 kwh/m^2/day (Oloo *et al*., 2016). Al-Neama & Farkas (2018) reported that the use of solar energy was achieving greater importance in agricultural produce drying. At the same time quality controls in drying, preservation and storage became more significant aspects in processing of agricultural produce than before. Moreover, Ertekin and Yaldiz (2004) stated that open sun drying was practiced widely but is faced with problems of contamination by dirt and dust, infestation by insects, rodents and other animals. Drying of food materials should therefore be carried out in enclosed dryer equipment, to preserve the quality of the final product (Ertekin and Yaldiz, 2004).

In systems which used solar energy to dry different agricultural products, the moisture content is removed by air which heated by solar energy with a temperature range of 50^{o}C to 60^{o}C (Al-Neama & Farkas 2018). Since the moisture content levels vary between various agricultural materials as reported by Kumar *et al*. (2016), the control of the process parameters such as air temperature, relative humidity, drying time of product and airspeed are critical (Al-Neama and Farkas, 2016).

Due to the ever-increasing energy demand and limited reserves with the much dependency on fossil fuels for fulfilment of energy needs, there is a wide scope and motivation for new, renewable and alternative energy sources in post-harvest management of agricultural products such as grain (Maia *et al*.,2009). Solar energy is abundant and freely available as a renewable energy source. Concentrated photovoltaic (CPV) systems, which utilize highly efficient PV cells under concentrated solar radiation, are solutions for reduction of the solar electricity cost. The main purpose of CPVs is the utilization of low-cost concentrating optical components that dramatically reduce the required cell area (Steiner *et al*., 2016; Johan, 2005). Solar conversion technology can be classified as solar photovoltaic and solar thermal technologies (Ankit & Dilip, 2014).

According to studies by Timsina *et al.* (2014) one percent increase in moisture reduced the longevity of the seed by half while five degrees increase in temperature also reduced seed longevity by half. It is therefore recommended to dry using desiccants to keep both the temperature and moisture content low and maintain high seed viability and vigour especially during adverse weather conditions. This would benefit both the seed and grain industry. Studies by Osodo *et al.* (2018) found that exhaust air from grain dryers though moist was at significant

high temperatures than ambient and invited recommendations that can utilise the waste heat energy.

A hybrid system comprising of various solar collector configurations to trap solar energy for air heating as well as use of a desiccant to dehumidify warm exhaust from the drying chamber for regeneration into the dryer can be explored. This can improve grain handling, remove drudgery in removal and return of the grain to the stores, reduce the effects of adverse unpredictable weather conditions during drying, improve hygiene and prevent aflatoxin contamination. Therefore, the aim of the study was to optimize performance of an existing dryer into an efficient solar desiccant maize grain dryer.

1.2 Problem statement

Post-harvest handling of maize grain in developing countries particularly in Kenya starts by at harvesting grain at a moisture content of between 19% and 25% and subsequent dying operations to about 13-14% (Tonui *et al*., 2014).As such these high moisture levels are prerequisites for aflatoxin development and the grain is susceptible to mycotoxin contamination. The conventional method used for maize grain drying by small scale farmers that form 90% of the population and produce 75% of the staple food crop is the direct open – air- sun drying. This system is associated with unpredictable and variable weather patterns as well as sporadic atmospheric conditions such as showers and low solar radiation intensities that often coincide with harvest season. Further, open sun drying is time and labour intensive due to drudgery of turning the spread-out grain or unshelled cobs, removal and return of grain into the stores at sunset, covering at night, and protection from attack by rodents and domestic animals. Moreover, direct exposure to solar radiation leads quality degradation due to uneven drying, over-drying, cracking of grain kernels, and losses in tonnage.

When threshed or un-threshed grain is spread on mats or bare ground to dry, formation of dew at deep layers overnight and unanticipated precipitant in the recent weather variability catalyse the hygroscopic characteristic of maize kernels. This facilitates adsorption causing undesired drying and rewetting pattern that leads to cracks in grain kernels which affect processing at later stages. In addition to the large areas required for spreading the grain, predators, rodents, dirt, dust, debris and foreign matter contamination is a major concern. Open sun drying (OSD) exposes the grain to insect and pest infestation that harbour and cause growth of microorganisms due to non-uniform drying (Tiwari, 2016). This exacerbates losses through discoloured grain, as well as rotting and growth of mold on maize kernels.

Spreading maize grain on bare ground as shown in plate1-1is unhygienic and exacerbates aflatoxin contamination when the produce comes into direct contact with bare ground, soil and debris which harbour *Aspergillus flavus* (IFPRI, 2010). Similarly, the practice of field-drying exposes the grain to pest, birds, rodents as well as wetness by occasional rain showers.

Plate 1-1: Illustration of challenges associated with open sun drying of maize grain

Mechanised technologies, electricity and fossil fuelled dryers for maize grain drying are expensive and are thus inaccessible to most small-scale farmers particularly in rural areas. Due to this challenge the farmers sell their maize produce immediately after harvest to middlemen at a loss. Lack of financial capacity and economies of scale, to own and operate mechanized dryers has rendered subsistence farmers who form majority of the population in developing countries vulnerable to harvest losses and food insecurity as witnessed by relief maize importation especially in Kenya. This creates the need for alternative low cost and effective maize drying and storage systems particularly for small scale farmers in the rural areas.

Although it is common for Kenyan maize farmers to be turned back by grain marketers for delivering grain of unacceptable high moisture content, the disadvantages of conventional dryers include over drying grain and loss in mass resulting in loss of income. Rapid drying at high temperatures in conventional dryers create internal tension, sudden shrinkage and internal cracks that lead to undesired rapture of grain despite consuming enormous amounts of energy. Alternatives dryers that harness and utilize solar energy are preferred since it is abundant and freely available, inexhaustible and non-polluting (Lingayat *et al*., 2017).

From the foregoing it is evident that there is need for developing efficient low-cost grain drying systems to provide a solution to resource poor farmers. An attempt to this endeavor is an existing granary bin dryer but does not perform optimally. The area of the solar collector was small and collected a limited amount of solar energy resulting to low drying temperatures.

Further the exhaust from the drying chamber was at higher temperatures than ambient but was exhausted to the environment. In this study a low-cost solar grain drying system is developed and performance optimized through integration of various solar collector configurations, heat transfer techniques and utilization of desiccants to precondition inlet air, dehumidify and regenerate exhaust air for grain drying during adverse climatic conditions.

1.3 Justification

Food security is currently a global concern particularly in developing countries where the need for modern post-harvest management techniques are presently on a rising demand in mitigating and taming heavy losses especially for staple food crops. Maize grain drying is such an important post-harvest operation for the staple food crop in Kenya where small-scale maize farmers rely on the ineffective and unpredictable open air-sun drying despite the numerous challenges in the current times of unpredictable climatic conditions during harvest, posing a threat to food security.

To alleviate these problems there is a need to develop affordable and efficient drying methods that are useful and meet the demands of farmers and people living in remote areas in developing countries. As such as a low cost, effective and affordable hybrid grain drying system that utilises renewable solar (green) energy can be developed to promote food security. An efficient solar grain drying system can be developed through integration of various solar collector configurations, heat transfer techniques and development of new techniques and mechanisms for solar dryers for effectively harnessing radiation in a solar collector.

Because the application of solar energy is completely dependent on solar radiation and sporadic atmosphere, it is important to condition the drying air by improving heat transfer air using various solar collector configurations during high and low intensity radiation hours. The air can in turn be utilized together with desiccants such as superabsorbent polymer (SAP) in a hybrid system to achieve homogeneous drying process which cause less cracks and breakages of grain compared to intermittent direct sun drying. Further, the use of solar thermal collectors causes no greenhouse gas emissions compared to conventional dryers and it is an environmentally friendly way of producing energy for space heating. Further the energy source is practically inexhaustible. This research will yield a more effective drying system incorporating renewable solar energy and a desiccant (superabsorbent polymer) material to effectively lower the cost of drying grain for small scale farmers. The dryer operations do not

operate on electricity or fuel energy during the day and night; thus, it is more economical to small scale farmers who do not afford electricity and other fuels for grain drying during adverse weather conditions at harvest.

The presented hybrid dryer provides low-cost, efficient and enclosed drying system to improve hygiene in post-harvest grain handling, remove drudgery in moving the grain in and out of store and reduce the effects of unpredictable adverse climatic conditions (especially during harvest). The enclosed dryer will prevent grain rot, cracks, breakages and discolouration grain as compared to unhygienic direct open - sun drying. The operation mechanism of desiccant in the dryer prevents adsorption resulting from hygroscopic nature of maize kernels such as at night when solar radiation is unavailable or during periods of low radiation (Figure 1.1).

The developed dryer will enable farmers dry the grain despite the adverse weather conditions during harvest and take advantage of better market opportunities as well as promote food security. It will significantly lower the risk of *Aspergillus flavus* growth and aflatoxin contamination by maintaining low relative humidity conditions of the air and prevent adsorption effects of maize kernels as well as maintain desired temperatures above ambient within the drying chamber during adverse weather conditions. The study builds on yielding a low-cost, portable and efficient hybrid solar-desiccant dryer to benefit both the seed and the grain industry. It will be destined to promote hygiene in grain drying for sustainable food security.

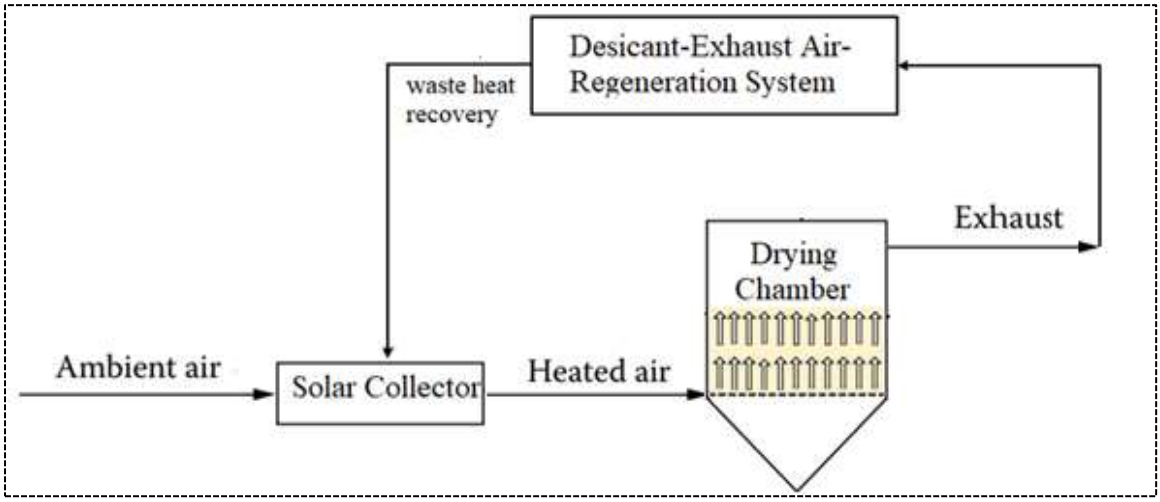

Figure 1-1: Schematic diagram of the optimized hybrid solar-desiccant dryer

1.4 Objectives

1.4.1 Overall objective

The overall objective of the study was to optimize the performance of a hybrid solar desiccant dryer.

1.4.2 Specific objectives

The specific objectives were to;

a) Establish the effect of radiation concentration lenses, longitudinal finned elements and exhaust air regeneration on the efficiency of the solar collector.
b) Design develop and test prototype to optimize solar collector dryer.
c) Test and evaluate thermal performance of solar air-heat collection and maize grain drying.

1.5 Research questions

a) Can the efficiency of existing solar collectors be improved for grain drying?
b) What is the effect of radiation concentration lenses, extended surfaces, desiccant material and exit air recirculation on the performance of solar-desiccant dryer?
c) Is an optimized hybrid solar- desiccant dryer effective for grain drying?

1.6 Scope

This research was focussed on studying an existing granary bin dryer and improving its performance for solar air-heat collection and grain drying in a developed and fabricated hybrid solar collector desiccant dryer. The hybrid solar dryer was fabricated, and experiments aimed at preconditioning the air for grain drying were performed. Additionally, grain drying experiments were performed in the dryer prototype and drying compared to open sun drying as practised by farmers.

Detailed statistical analysis was done to inform the level of significance of the experimental findings and results so obtained. More specifically the aim of this research was to study and investigate the effect of radiation concentration lenses, exhaust air recirculation and regeneration through conduits lined with superabsorbent polymer and methods of increasing heat transfer through finned elements surfaces. The effective application of the dryer was found by conducting grain drying experiments and compared with natural sun drying as commonly practised by small scale farmers.

CHAPTER TWO: LITERATURE REVIEW

This chapter presents a review of past research efforts related to this study. It includes a review of solar collectors, grain drying systems, solar grain dryers and their performance optimization techniques and technologies. Further the effects of these techniques on efficiency improvement for solar grain dryers are reviewed.

2.1 Grain drying

Cereal grain constitutes about 55% of the African food basket (Rembold *et al*.,2011). Post-harvest loss has been considered an important aspect in seeking improvements to cereal grain supply and major donors have focused on loss reduction strategies (FAO/AfDB, 2009; World Bank, 2010; Zorya *et al*., 2011). A significant percentage of these losses is related to improper and or untimely drying of foodstuffs such as maize grain (Osodo, 2018).

Recent estimates put post-harvest losses in maize at 14% to 36% of the total production (Tefera, 2012). According to Kumar & Kalita (2017) post-harvest losses of grain in developing countries accounts for about 19%. For instance, postharvest loss of maize in Kenya in 2007 was 21.1% (Hodges, 2009). Grain drying and appropriate storage systems are important post-harvest operations especially in developing countries such as Kenya where maize is an important staple food crop (Kumar & Kalita, 2017). In these countries, grain losses can rise as high as 80% under very adverse conditions (Osodo, 2018; Bolaji and Olalusi, 2008). Besides there is need to reduce these losses, especially at the post-harvest and storage stages which could lead to total grain loss and all the inputs used during the production process as a result of aflatoxin contamination.

Small-scale farmers in developing countries do not afford the fossil fuelled or electric dryers and only 16% of the rural population has access to electricity in Africa (Kaygusuz, 2011). Additionally, large economies of scale are necessary to operate electric dryers. There have been extensive studies on the barriers of the adoption of improved agricultural systems by small-scale farmers. In one of the studies involving solar dryers, Kumar *et al*.(2014) highlights the high initial and running costs of fuel-powered drying systems as is one of the barriers for adoption by small-scale farmers. Moreover Kumar & Kalita (2017) cited lack of technical know-how and information, inadequate technology as well as poor postharvest handling infrastructure as common problems. For this reason, the farmers utilise open air-sun drying in spite of serious challenges when the rainy season coincides with the harvest period especially

in recent times of climate change. In addition, the nature of solar energy is such that it is only available and effective for 6 - 8 hours a day as well presented by Punlek *et al.* (2009). Moreover, this method involves a considerable daily labour input and drudgery in removal and return of the bulk grain into the stores.

Due to hygroscopic nature of maize grain and during the hours when solar energy is unavailable, such as during the night, there is need to find alternative drying methods. Incorporating solar collector in an existing desiccant dryer can be explored to prevent these challenges and prevent aflatoxin contamination. Solar radiation can be harnessed in a solar drying system to create a greenhouse effect within the drying system and attain temperatures as high as 70°C (Kokate *et al*.,2014).

Solar energy depends on availability of radiation from the sun and can be harnessed by use of a solar collector. Low intensity radiation can be optimized and utilized to increase the heating effects of the drying air by varying collector configurations. This air can in turn be utilized together with superabsorbent polymer in a hybrid system to effect a constant enthalpy drying process that causes less cracks and breakages to the grain and maintain high seed viability and vigour for the benefit of grain and seed industries.

Grain drying is an important post-harvest operation in the handling, preservation, storage and processing of maize grain. According to Saeed *et al*. (2008) grain drying ensures a decrease in water activity of the grain thus inhibiting microbial infestation as well as fungal attack and deterioration. Drying increases storability, reduces haulage costs, prevents aflatoxin contamination, improves subsequent processing operations and maintains the nutritional value of the grain. Besides, Soponronnarit (2017) notes that grain spoilage and losses are a significant setback to farmers in developing countries where they usually sell the grain soon after harvesting due to lack of appropriate grain drying and storage systems thus losing the advantages of market opportunities. According to Prakash & Kumar (2017), grain drying lowers post-harvest losses, facilitates long-term storage without deterioration, provides high quality seed and grain products, secures higher prices, facilitates planning of early harvests and maintains of seed viability.

OSD is achieved by placing grain on polythene mats outdoors to be heated by direct solar insolation and loose moisture to the hot low relatively humid air (Jain &Tiwari 2003). Kumar *et al*. (2014) notes that OSD proceeds at slow rates, intermittently and unpredictable and the

grain is sometimes overdried or, more often under dried. Apart from large area required for spreading the grain it is susceptible to mould growth and rotting due to contact with ambient conditions and unpredictable rain showers and dew at night. Other drying methods such as wind integrated with radiation from the sun have only made an attempt of improving drying conditions of OSD (Belessiotis and Delyannis, 2011). Fudholi *et al.* (2010) reported direct sun drying as a method that requires large open areas, limited by availability of sun radiation and is prone to contaminants from foreign materials such as dust, soil and waste from birds, insect and rodents.

On the other hand, solar dryers are more rapid, faster and provide a controlled drying environment into which hot air is passed and enables higher crop throughput. It utilises much less drying area, saves energy and time compared to open sun drying (Kumar *et al*., 2016). Additionally, solar dryers protect the grain from dust, windblown debris, insects, birds and rodents and domestic animals. Umogbai and Iorter (2013) explored the comparison of OSD method with solar dryers and concluded that the later were more efficient and effective due to uniformly higher drying temperatures and homogeneity of the final grain moisture content. Solar dryers reduced grain cracking and discolouration than in the case of open sun drying (Umogbai and Iorter (2013).

The efficient use of solar technology for grain drying involves well designed contrivances for solar radiation trapping, heating of the air and achieve maximum thermal efficiency in grain dying. Prakash & Kumar (2017) illustrated that correctly designed solar heated grain dryers have numerous merits over OSD method. They resulted in higher drying rates due to heating of the drying air medium by 10 to 30°C from ambient conditions and reduction of relative humidity as well as quick movement of the air throughout the dryer (Prakash & Kumar, 2017). Alqadhi *et al*. (2017) notes that solar drying systems save energy, utilize less space, consume less time, enhance the product quality, increase the overall efficiency of the drying process and have no deleterious impacts on the environment.

2.1.1 Factors affecting grain drying

Numerous researchers have reported similar factors that are pertinent and significant in grain drying. According to Soponronnarit (2017), the factors that would affect grain drying included;

a) Air temperature
b) Relative humidity of the air

c) Type of grain
d) Moisture content of the grain, and
e) Airflow rate
f) Grain layer thickness

These factors are combined in the prediction of grain moisture content during drying to improve drying efficiency. However, the time required in achieving equilibrium is dependent on the difference between grain moisture content and the EMC with air (Mrema *et al*., 2011). The drying temperature is the main factor that controls the drying process. Moreover, the mass flow rate of drying air has some remarkable effect on the overall dryer performance (Aissa *et al*., 2014).

2.1.2 Post-harvest losses

Major grain losses have been reported as postharvest losses in developing countries due to lack of knowledge, inadequate drying technology and poor grain storage infrastructure that often result to aflatoxin contamination (Kumar & Kalita, 2017). Post-harvest losses would mean loss of investment such as seed, fertilizer, herbicide, pesticide, irrigation water, labor, machine time, energy and health concerns in local societies (Ngindu *et al.,* 1982; Okoth & Kola, 2012 and Mrema *et al.,* 2011). The main cause of aflatoxin contamination are high temperatures, humidity and high grain moisture content. Aflatoxin contamination is common in developing countries where small-scale farmers in the rural areas use open-air sun drying systems. When the rains coincide with harvest, the grain kernels maintain a high moisture content for a longer time period which exacerbates aflatoxin contamination.

The indigenous drying and storage structures used by small scale farmers in developing countries are made of locally sourced materials such as grass, wood and mud. The peasant farmers lack scientific designs and thus cannot guarantee harvest protection from pests and contamination for a long-time storage (Kumar & Kalita, 2017). According to Costa (2014) maize grain losses were as high as 59.48% after drying and storing for 90 days in the traditional storage structures (Granary/Polypropylene bags). In conventional drying and storage structures, proper control of temperature, relative humidity and moisture content is easily achieved using electric or fossil fuel power heaters, dehumidifiers, air conditioners and air circulation fans. However, lack of adequate and efficient drying infrastructure makes it impossible to dry grain in good time to effectively forestall aflatoxin contamination (Mrema *et al*., 2012).

2.2 Review of solar grain drying

The most straightforward option for crop drying is open sun drying. No initial costs or expertise are required. This method of drying is also the most adopted by small-scale farmers (Sahdev and Dhingra 2016). Solar drying has widely been adopted at all levels of farming. Spreading maize over mats is the preferred method of open sun drying in tropical and subtropical regions. However, regulating drying rate is a challenge since the energy source cannot be controlled and is dependent on ambient air temperature, radiation from the sun. It is also dependent on ambient relative humidity, wind velocity and the soil temperature below the mat (Jain and Tiwari, 2003). Apart from intensive labour, contamination occurs due to exposure to foreign matter, soil and bare ground which could cause aflatoxin contamination (IFPRI, 2010).

Researchers such as Sharma *et al*., (2009) and Ekechukwu & Norton (1999) noted that, open sun drying methods, are widely practiced by small-scale farmers in large parts of Africa and Asia. However, the conditions of climatic manifest a significant influence on deterioration, losses and the extent of associated crop damage during OSD. For instance, Ekechukwu and Norton (1999) observed that open sun drying has inherent limitations including inadequate drying, possibilities of fungal attacks, insect attacks, birds and rodents, and withering effects. Similar observations were reported by Mulokozi & Svanberg (2003) regarding the loss of nutritional value of crops, and Sadeghi, *et al*.(2012) on contamination of crops by foreign materials and debris.OSD methods are have been reported as cheap alternatives in compariosn with solar drying systems. However, grain quality and value of other dried products so obtained are significantly compromised. In a further contrast Kumar (2016) has presented solar dryers as successful devices of trouble free operations with low investment costs. Other researchers such as Pirasteh *et al*. (2014) stipulated the effective and feasibility of utilizing solar insolation in grain dryers given the amount of energy consumed and taking into consideration the unlimited nature of solar radiation. Moreover solar insolation is available in most parts of the world at an average value of 200–500 W/m^2 (Pirasteh *et al*.,2014).

Prakash and Kumar (2017) have established that solar dryers give desirable and quality product quality without deleterious environmental bang whilst providing a cost-effective drying operation for agricultural produce. On the other hand, Vijaya Venkata Raman *et al.* (2012) have presented three key drawbacks against increased use of solar dryers by small scale farmers, viz. lack of consciousness on cost-effectiveness of drying methods and systems, inadequate scientific knowledge and realistic application practices.

Zarezade and Mostafaeipour (2016) suggested creation of awareness on solar grain drying technologies as well as their effectiveness to encourage utilization. As such, Adelaja *et al.* (2009) developed a forced convection solar dryer powered by a solar photovoltaic module. Further Adelaja *et al*. (2009), found that that a PV powered solar dryer offers a good solution to problems encountered by farmers in the rural communities. Moreover, Bennamoun (2013) suggested that electrical energy from PV panels can be stored by using batteries and used during low solar radiation hours. This made the drying systems self-sufficient and independent of any other external energy sources such as direct radiation.

Bala *et al*. (2009) compared the effect of dying mushrooms using open sun drying and an improved dryer consisting of solar powered fans to circulate air. The investigations noted a significant reduction in moisture content of mushrooms (89.41% to 6.14%) in the improved dryer compared to the OSD method (89.41% to 15%). Benefits of improved air circulation through forced convection technique and the effect of preheating feed air have so far been widely established. In fact, a review by Seshachalam *et al.* (2017) extensively reported varying efficiencies from forced convention systems compared to open sun drying methods.

The foregoing reasons have contributed to an increasing consensus that open-solar drying is unattractive and largely uneconomical even to the small-scale farmers (Ekechukwu and Norton, 1999). Research conducted by Umogbai and Iorter (2013) reported savings in drying time compared to OSD since it took three days to reduce the maize cobs moisture content from 13.3% to 30.3% using a passive solar dryer. On the other hand, it took six days to dry the cobs to 13.4 % under ambient atmospheric conditions of open sun drying.

Perhaps in an effort to increase the feasibility of solar dryer designs for the small-scale farmers, some researchers have made them multipurpose to cater for a range of crops. For instance, the solar tunnel dryer, as illustrated by Singh and Kumar (2012) was designed for drying a wide range of commodities ranging from fruits, vegetables and even grains.

2.3 Classification of solar dryers

Considerable and significant effort is presented by various researchers in systematic classification of solar dryers. Fudholi *et al*. (2010), Belessiotis & Delyannis (2011) and Toshniwal & Karale (2013) have classified solar dryers based on mode of air flow, direction of air flow, products dried and type of assembly insulation. Alqadhi *et al*. (2017) categorised solar dryers into three distinct classes that included mixed mode, indirect and direct dryers in accordance to the passive mode of drying process.

Developed solar dryers are classified by considering the mode of drying as direct, indirect or mixed mode. Mixed mode solar dryers utilize both radiation and heat conduction via transparent glazing with convection of the heat from the air heat collector.
The researchers have generally alienated the solar dryers into three categories, namely: direct, indirect and hybrid solar dryers, (Belessiotis & Delyannis, 2011; Fudholi *et al*. 2010; Toshniwal & Karale, 2013 and Alqadhi *et al*. 2017).

2.4 Performance optimization technologies for solar collectors

Various techniques, designs, configurations and methods have been adopted to optimize performance and utilize solar collectors effectively. Recent optimization trends and methods are focused on increasing thermal performance of solar dryers.

As reported earlier, it is possible to note the need to exercise control of the drying parameters beyond ambient conditions which may adversely extend to extreme conditions. As such, optimization techniques and methods have focused on controlling air circulation parameters within the dryers (Yeh ,2014; Banout *et al*., 2011 and Bala *et al*., 2009). Typical cases involve the use of blowers or fans to control the circulations of air (Aravindh and Sreekumar, 2014,), the use of solar concentrators to raise the temperature of the circulated air above the ambient temperature (Aravindh and Sreekumar, 2014, ; Bagheri, 2015), the use fins to maximise heat transfer rates and hence the drying temperature of feed air flow (Bhattacharyya, 2017) as well as the use of different desiccants to control the absolute humidity of the feed air flow (Padmanaban *et al.*, 2017). However, alternative research has indicated that specific amount of heat is optimal depending on the product being dried as it may affect the quality of the product (Armel *et al.*,2015; Misha *et al*., 2014).

One of the notable improvements to conventional flat plate solar collectors is the incorporation of fins (Bhattacharyya *et al*., 2017). Kurtbas and Turgut (2006) reported that using fins located on the collector absorber increased heat transfer and pressure drop. Further research by Kurtbas and Turgut (2006) reported that fixed fins embedded on the collector plate were more effective than free fin collectors. Optimization and analysis studies for indirect solar cabinet dryers by Sami *et al*. (2014) reported that increasing the surface area of collectors with small surface areas (< 2.5 m^2), raised the air temperatures from the collectors. Further, Sami *et al*. (2014) conducted optimisation studies using energy storage materials under the absorber plate of the collector and experimental results indicated significant reduction on the cost ratio of the dryer

per drying batch. Experimental investigations by Chabane *et al*. (2013) using longitudinal fins embedded on the bottom of the collector plate; increased the heat exchange and rendered air flow in the channel uniform with substantial improvement in thermal efficiency of up to 40%.

Several investigations on optimizing heat transfer have focused on establishing the best configuration and number of fins in solar collector hybrids. Elsafi & Gandhidasan (2015) for example, assessed heat transfer augmentation using various parameters such as the number of fins, air flow rate, length of fins and duct depth. Similar experiments were conducted by Seshachalam *et al.*(2017), Other reserchers such as Yeh (2014) investigated the efficiency of double pass solar collectors with internal fins while Naphon (2005) analysed the entropy generation and performance in a similar design, double pass, but using longitudinal fins on both sides of the absorber plate (Bhattacharyya *et al*.,2017).

A consensus derived from the mentioned studies reflected an existing optimism number and size of fins. Most of these studies, however, were based on controlling various parameters and the outlet air temperature levels used in determining the performance. Comparatively, the studies highlighted the potential benefits of incorporating fins in a solar collector. However, as reported in the study by Bhattacharyya *et al.*(2017), an optimal number of fins exist beyond which the performance starts to deteriorate.

Similarly, review of different collector configurations and the use of fins by Bhattacharyya *et al*. (2017), it was evident that solar collectors displayed varying contributions to the overall drying efficiency. Further analysis, including varying the configuration of the fins to either increase or reduce the feed air flow rate provided significant results (Aravindh and Sreekumar, 2014). For instance, researchers have established significant effects of mass flow rates on performance of heating system and various types of solar collector configurations (Ibrahim *et al*.,2009; Alobaid *et al*.,2018; Bake *et al*.,2019; Zelzouli *et al*.,2012 and Abdullah *et al*., 2019). Some investigations have also highlighted the effects of controlling characteristics and condition of the ambient air in assessing the performance of solar dryers. Effectively, some researchers such as Padmanaban *et al.* (2017) and Chramsa-ard *et al.* (2013) have gone ahead to explore different desiccants to control the absolute humidity of the feed air flow. In assessing the performance of solar dryers, Chramsa-ard *et al.(*2013) reported that mass flow rate, temperature and humidity homogeneity of feed airflow were the most important parameters that determined the quality of the dried product. Effectively, some of the recent innovations have focused on improving feed rate using forced convection, development of more efficient

collector designs, and mitigating the effects of humidity using desiccant dehumidification such as desiccant wheels (Law, 2013).

Studies on the use desiccant assisted drying techniques have been explored by Padmanaban *et al.*(2017) where the time of drying was reduced significantly compared to conventional passive dryers. Shanmugam and Natarajan (2007) built an indirect desiccant-integrated forced convection solar dryer and tested the system in the mode of sunlight and sunlight absence hours. Besides, Shanmugam and Natarajan (2007) conducted drying experiments with and without the integration of the desiccant. Results showed a faster removal of moisture when using desiccants. More experiments on the integration of desiccants with solar dryers were conducted by Shanmugam and Natarajan (2006) where they designed an indirect forced convection and desiccant integrated solar dryer to study its performance under hot and humid climatic conditions in India. In other drying studies, a desiccant unit of silica gel integrated with a forced convective solar crop dryer with similar connection to solar air collector reduced the time of drying by 44 hours (Hodali & Bougard, 2001). Experimental studies by Badgujar (2012) investigated solar dryers with regenerative desiccant materials for multicrops and made comparison when using solar energy alone and when radiation focusing mirrors were incorporated. Misha *et al.* (2016) conducted drying performance of a solid desiccant dryer and found that the desiccant wheel improved drying air latent and sensible efficiencies by 67% and 74% respectively.

Other notable optimization studies on forced and natural convection drying systems have been performed by various researchers (Mc Doom *et al*., 1999; Smitabhindu *et al*.,2008; Sami *et al*., 2014 and Sámano *et al*.,2013). McDoom *et al*. (1999) optimized a scaled–down dryer by recirculation of the hot air, altering the degree of venting and increased the energy saving up to 29 to 31%. Optimization of geometry and operational parameters such as optimum values of useful collector area and air recycle factors for optimal design model of a solar-assisted drying system were studied by Smitabhindu *et al*. (2008) to minimise drying cost per unit of dried product.

Sami *et al*. (2014) performed optimization studies on the effects of solar collector length, solar collector surface area, mass flux of air, and initial moisture content of solid. Appropriate cost ratio and the optimum range of these parameters were obtained for design purposes (Sami *et al*.,2014). Research by Sámano *et al*. (2013) optimized energy efficiency in an improved small-scale solar dryer by varying radiation optical concentration angles from 45° to 20° and

increased the feasibility of the dehydration of food products for individual and local market usage and storage. Related studies by Chabane *et al*. (2013) optimized efficiency and achieved highest air temperatures and collector efficiency with longitudinal fins on the back of the absorber plate at 45°. Effectively, experiments by Chabane *et al*. (2013) have reported solar air collector thermal efficiencies of 40.02% and 34.92% with and without fins respectively.

From the foregoing, it is evident that there are significant efforts among researchers to understand performance optimization and efficiency parameters in solar collectors. Many researchers have proposed techniques ranging from solar dryer designs, lining materials, optimal air circulation and effective solar collection and heat transfer configurations. There has been a notable consensus surrounding the importance of mass flow rate and solar radiation as key parameters in determining the performance of collectors (Aravindh and Sreekumar., 2014). Moreover, there has been overwhelming evidence on the significant contribution of various solar collector designs on the efficiency of grain drying. While much focus has concentrated on the fundamental objective of solar dryers- moisture removal and fastest and easiest ways to achieve the desired grain moisture content; an almost equal effort has been directed towards assessing the quality of such methods. Some of the evident studies have gone ahead to focus on the effect of drying methods on the nutritional value of crops (Bala *et al.*,2009).

2.4.1 Efficiency enhancement and appraisal of solar collectors

Development of efficient solar collectors constitutes new technologies that can be promoted to reduce the use of fossil fuelled dryers to mitigate global warming. Solar collectors are in use widely and their efficiency enhancement are necessary to decrease the effect of environmental pollutants released from conventional methods (Tsoutsos *et al*.2005). Despite the increase in energy consumption, climate change has lately become a significant issue globally due utilization of conventional energy resources. As a response to these concerns many researchers are focussed on improving existing solar technologies, developing environmentally friendly energy devices and components and finding effective energy production methods with new energy efficient measures (Jradi, 2012). The intermittent and inconsistent nature of the solar energy with the significant seasonal variations of radiation intensity has informed research on development of concentrating solar systems with advanced tracking devices to maximize the amount of solar energy produced and improve the overall efficiency (Jradi,2012).

Numerous researchers have focused on increasing the convective heat transfer to the working fluid usually air from the absorber surface while at the same time minimizing the overall heat losses from the system (Kalogirou,2007).

Chabane *et al*. (2013) sought to increase solar collector thermal efficiency using a single pass counterflow with longitudinal fins and obtained substantial enhancement in thermal efficiency as high as 40.02% and 34.92% with and without fins respectively for an air mass flow rate of 0.012 kg/s. Similar efficiency improvement studies have explored the effect of increased surface area of the collector, including the use of fins and number of passes. Yeh (2014) assessed the effect of pass number on collector efficiency where he observed a considerable increase in the collector efficiency when the number of passes was increased. Studies by Mahboub *et al*. (2016) found that the flow vortices that formed in the cross sectional of the curved duct solar collector enhanced heat transfer between the absorber surface and the air. Researchers and experts of solar drying have argued that efficiency depends on the design. As such the efficiency may vary between a downward-type and an upward type even for the same number of passes. Delgado *et al.* (2013) optimized the performance of an existing solar dryer model and identified gaps by characterizing temperature profiles and drying kinetics and built a new model that improved efficiency by 43.75%.

Hossain *et al.* (2008) tested and performed experiments on a hybrid solar drying system and reported substantial high temperatures (60°C) at the outage of the collector unit with daytime temperature change of 30°C. However, Hossain *et al.* (2008) found that night-time air temperatures were low (<20°C). During this period drying was uncertain and irregular and not suitable for the solar dryer. This notes the need for alternative mechanisms of maintaining higher temperatures in the night than ambient.

In a different study, Hossain *et al.* (2008) analysed collector efficiencies for collectors with a solar reflection unit and the one without the reflector. The collector with reflector enhancement collector efficiency by approximately 10% where it increased to 43.78% from 34.02% without the reflector. Prasad *et al*. (2006) improved solar biomass (hybrid) dryer and achieved average temperature of drying air of 60°C with dryer efficiency of 18%. Gulandaz *et al.* (2015) evaluated a modified hybrid solar dryer for paddy seed where the highest efficiency at mid-noon was 36% but varied from 20% to 36% at a collector temperature of 49.9 ºC with 29 ºC ambient temperature. El-Sebaii *et al*. (2002), provides 45.5 and 55.5°C as the optimal temperature range for drying most agricultural products.

Studies on efficiency enhancement by various collector designs, including lining materials (Aravindh and Sreekumar, 2014), the use of longitudinal fins (Bhattacharyya *et al*. 2017) number of the pass (Yeh, 2014) among other designs have illustrated varying efficiencies and solar dryer performance. The studies have overwhelmingly reported the contribution of the various parameters on the overall efficiency of both the collector and the dryer. The effect of lining materials have produced significant results using porous collectors (Sharma *et al*., 2009). For instance, wire mesh, steel wool among other materials. A study by Aravindh and Sreekumar (2014) comparing the increase of efficiency found steel wool having a higher increase (26%) compared to glass wool (10%). However, efficiency increased with increased mass flow rate for different materials.

Several hybrid technologies have been developed to increase the efficiency of solar dryers. In a recent study by Misha *et al*. (2016) on a solar-assisted solid desiccant dryer the drying efficiency was found to be 19%, at full capacity although 65% of the energy used was solar energy. Omofunmi & Alli (2016) developed a solar dryer and conducted performance evaluation and drying characteristics of sliced plantain and maize. Results showed that the collector outlet, storage unit and drying chamber temperatures ranged from 37°C– 47°C, 36°C– 46°C, and 33°C– 45°C, respectively (Omofunmi & Alli, 2016). Further, Omofunmi & Alli (2016) found out that about 70.1% of moisture was evaporated using solar dryers compared to 45% using open sun drying. Gill *et al*. (2012) has reported 54.0% average drying efficiency for a developed batch natural circulation solar dryer.

Experiments performed by Singh *et al*. (2006) on a natural convection solar dryer developed by Punjab Agricultural University, India reported maximum temperatures of about 75 °C at maximum solar radiation of 750 W/m^2 and ambient temperatures of 30 °C. Amer *et al*. (2010) reported 65% efficiency for a developed and tested hybrid solar dryer utilizing direct solar radiation and heat exchangers. Examination of various active type solar air collectors for drying different biological products was done by Henriksson and Gustafsson (1986). It was found that there were benefits when the collectors were integrated, and the dryers had the potential to compete economically with oil as a source of heat. Tiwari *et al*. (1994) have forwarded a significant efficiency and reduction in the drying time of a solar crop dryer due to increased thermal energy as a result of a reflector placed over the chimney wall. Hematian and Bakhtiari (2015) reported that operating a solar dryer with natural convection resulted in higher efficiencies compared to solar collector with the forced convection. Badgujar (2012) reported

drying efficiency of 60% during an experimental study on investigation of solar dryer utilizing regenerative desiccants compared to 43% when using solar energy alone. Similarly, there was a 53% improvement in efficiency when optical radiation concentration mirrors were incorporated.

Effectively there is need for continued research on performance improvement and attempts to fill the knowledge gaps of solar drying technologies. Moreover, researchers have argued that progressive use of alternative, low cost and robust locally available materials for fabrication and construction of solar drying units, without affecting their performance should be an ongoing and progressive endeavour (Sharma *et al*., 1994).

2.4.2 Solar concentrators for air heating

Solar concentration technology was introduced for air heating particularly in unglazed transpired collectors (Leon and Kumar, 2006). According to Belessiotis *et al.* (2016), solar concentrators are key components of active solar air heating systems. They transmit heat to a fluid usually air or water by gathering, concentrating suns radiation, focussing and transforming it to heat energy. Solar collector designs utilize flat plate collectors with transparent glazing and concentrating collectors that use mirrors or lenses to focus the sunlight into a small absorber (Shemelin & Matuska, 2017). As such in concentrating collectors, solar energy is optically concentrated before being transferred into heat (Belessiotis *et al*., 2016). Solar collectors use lenses and mirrors to concentrate and focus solar radiation and sunlight onto a thermal receiver. The receiver absorbs and converts sunlight into heat (Poole, 2001).

Concentrated solar power systems provide environmentally friendly energy and virtually produce no emissions, since they utilize sunlight and consume no fuel (Poole, 2001). The three main types of solar power concentration systems include parabolic troughs, dish and central receivers. Trough parabolic solar collectors employ mirrored troughs that can focus the energy from the sun onto a fluid-carrying receiver tube. Poole, (2001) suggests that the tube location is at the focal point of the parabolically curved trough reflector (see Figure 2-1). Dish-shaped parabolic mirrors are employed in dish systems as reflectors for concentrating and focussing the sun's rays onto a receiver, mounted above the dish centres.

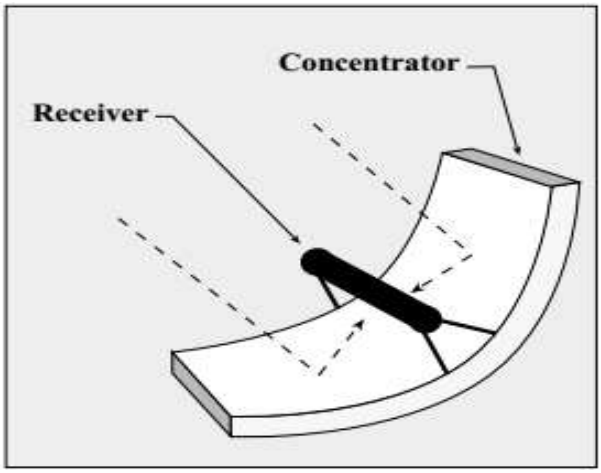

Figure 2-1(a): Parabolic solar collector (Poole, 2001)

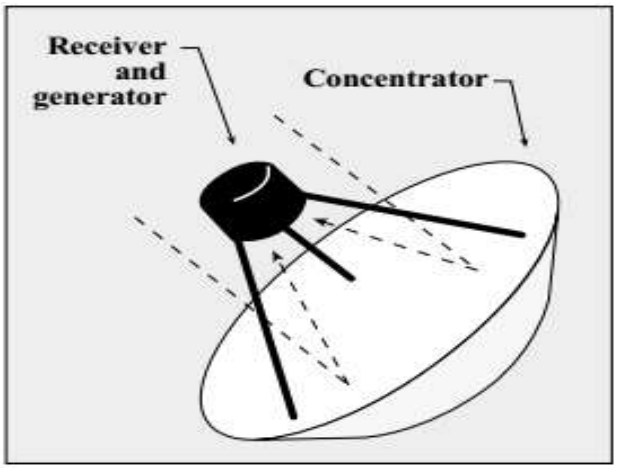

Figure 2-1(b): Dish type solar collector (Poole, 2001)

According to Poole (2001), researchers are developing high-efficient low-cost solar concentrators. The goal is to further develop this technology and increase acceptance of the systems for penetration of the locally growing and international energy demands. Advancement in the technology and the use of low-cost thermal storage can allow future concentrating solar power plants to operate for longer hours during the day and shift solar power generation to evening hours. Prasad *et al.* (2006) compared the results of flat plate collector with and without solar tracking and reported a gain in collector efficiency by 5-7% by using tracking mechanism.

According to Ong (2013), solar concentrator converges together the sunlight that strikes a wide area and directs it to a smaller area. Unlike solar trackers, which move solar panels such that the sun strikes at the best angle, solar concentrators are stationary. Poole, (2001) reported that solar concentrators are one of the major avenues of research that will lead to lowering global energy costs, and there are several approaches currently being followed.

2.4.3 Magnifying glass and radiation concentration

When a beam of light is focused by a magnifying glass onto a piece of paper the diameter of the light beam becomes smaller and the concentrated light is a lot warmer than the ambient surrounding air. Unlike solar trackers which move the solar panels so that the sun strikes at the best angle solar concentrators such as magnifying glass are stationary. Magnifying glass can concentrate and focus radiation from the sun to a small area and achieves high temperatures. Naveen Kumar *et al*. (2016) reported a gradual increase in temperature when convex lens was used as a concentrating medium in a solar water heater even without using an insulating water chamber. They concluded that convex lenses attained maximum efficiency when combined

with transparent flat glass compared to conventional flat plate collectors. Plate 2-1 illustrates the effectiveness of lenses in solar concentration and heating. Increasing the air temperature in grain drying, which may be achieved through solar concentration using mirrors and lenses has been associated with improvement in the drying rates (Misha, *et al*., 2014).

Plate 2-1: Heating by magnifying glass *(Image source https://www.scienceabc.com)*

2.4.4 Solar drying psychrometry

Psychrometric variables are helpful in improving the post-harvest solar drying of agro-products. It gives the idea about the changes in properties of air and efficiency of dryer during heating and drying. Prakash and Kumar (2017) presented solar drying as an induced solar energy mass transfer mechanism that results in loss of water through evaporation during conventional solar drying and as a natural process for OSD. Studies by Munira *et al.* (2013) noted that the process of drying occurs at a temperature level between the temperatures of the grain bed inlet and the dryer outlet. Munira *et al.* (2013) as well as Prakash and Kumar (2017) have forwarded that successful solar drying system requires;

a) Sufficient solar heat energy to withdraw moisture,
b) Sufficiently dried low humid air to absorb the released grain moisture,
c) Adequate circulation of air to remove moisture and
d) Controlled solar heat gains to avoid grain cooking or over drying.

Drying phenomenon and mechanisms as studied by scholars have also reviewed that the moisture removal rate from a drying product is pro rata to the difference of the average moisture content and the equilibrium moisture content (Srikiatden & Roberts, 2007). Heat and mass transfer take place from wet solid through moist air and the changes in thermodynamic

properties of air ought to be evaluated before and after drying to measure the effectiveness of drying process (Maheshwari, 2014).

Researchers such as Munira *et al.* (2013) and Norton (2017) have summarised the drying process in a solar collector using psychrometry as shown in Figure 2-3. For instance, Munira *et al*. (2013) considered that air is heated from A to B at constant humidity ratio to dry grain iso-enthalpically from point B to point C in the solar dryer.

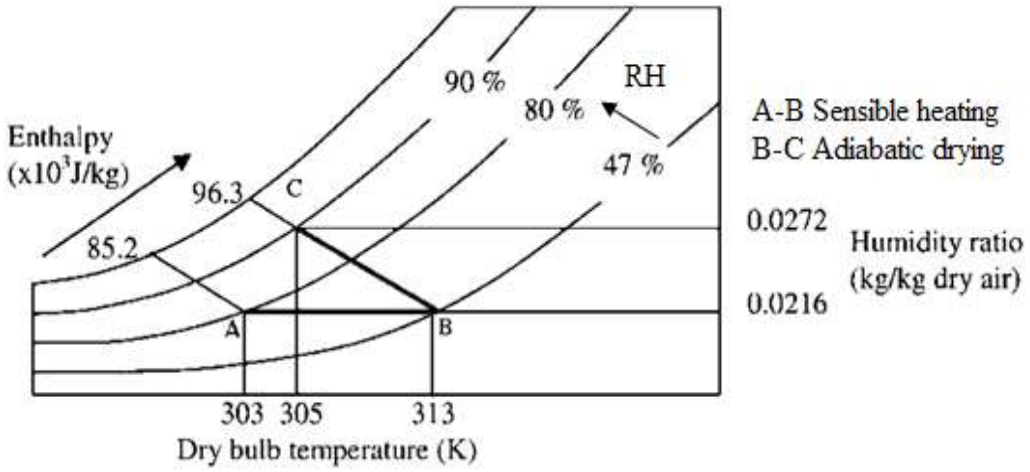

Figure 2-2: Psychrometric illustration of solar grain drying process (Munira et al., 2013)

Figure 2-3 shows that the effect of sensible heating in a solar collector increases in the capacity of the air to absorb moisture. During drying the air regains the moisture through a constant enthalpy process (Norton, 2017).

2.4.5 Psychrometry of desiccant drying

A large volume of water is absorbed by a desiccant material such as superabsorbent polymers. When water vapour is adsorbed into the desiccant surface it undergoes a phase change from vapor to an adsorbed quasi-liquid (Gluesenkamp and Radermacher 2011). Generally, an adsorbed substance has internal energy somewhat between its solid and liquid forms at the given temperature. Dessicant holds a lot of moisture about 40% of their own weights the desiccant fabric can be regenerated using solar energy once saturated. (Chen *et al*., 2015 and chen *et al.,* 2016).

According to Gluesenkamp and Radermacher (2011) the release of this latent heat raises the process air temperature, and in practice this sensible heat gain is roughly equal to the latent energy removed from the process stream. In this sense a desiccant wheel is a constant enthalpy

device that exchanges latent energy for sensible energy and simultaneously dehumidifies and heats the process airstream (Gluesenkamp and Radermacher, 2011). As such desiccant adsorbents have attracted much attention in air dehumidification and enthalpy recovery (Zhang, 2013). Agricultural and biological food materials such as grain cannot be dried at very high temperatures due to the possibility of affecting the product quality and cellular damage (Alqadhi *et al*., 2017). Therefore, suitable desiccant materials can be used in the drying process to dehumidify the drying air and provide appropriate drying conditions. Experiments by Badgujar (2012) found that desiccant dryers can be utilized in drying agricultural food materials with significant reduction in drying time and improvement dried product quality.

A moisture removal process produces not just dried air, but a rise in thermal rates, because of the isothermal operation. Studies by Hii *et al*. (2009), noted that at low thermal operations of dryers or during the off-sunshine hours especially at night, the drying process was achieved by utilizing desiccant. According to Alqadhi *et al*. (2017) utilization of desiccants is regarded as renewable energy, desiccant regeneration can be achieved by renewable or non- renewable energy processes.

Attempts have been made by several researchers on suitability and integration of desiccant materials in dryers (Román *et al.,* 2019). The dehumidification capability of desiccants presents the most promising research area in mechanisms of solar thermal drying and storage (Hodali and Bougard, 2001). Chramsa-ard *et al.* (2013) reported that temperature and humidity ratio of the air the affected the desiccant rate of desiccant moisture adsorption. However, variation in air mass flow from 0.08 to 0.15 kg/s did not have any effect on adsorption rate of silica gel and the air temperature was inversely proportional to the rate of adsorption. Further Chramsa-ard *et al.* (2013) found that humidity ratio had a direct relationship with adsorption rate. Effectively studies by Chramsa-ard *et al.* (2013) have reported a reduction in drying time by 20.83% for a dryer with desiccant dehumidification system compared to the one without. Drying efficiencies of 42.1 % and 39.6 % with and without desiccants respectively were reported by Chramsa-ard *et al.* (2013). It was observed that silica gel could be regenerated using solar radiation. Further investigation by Badgujar (2012) reported that the desiccant materials were stable even after continuous use for more than a year and could be dried and degenerated using heat energy from solar collectors.

Studies have shown that lowering the relative humidity by SAP is a constant enthalpy process that results in loss of moisture with about 20% humidity decrease and slight gain in heat of dry air (Mbuge *et al*., 2016).

Amongst the available desiccants, superabsorbent polymer (SAP) has been found to have the highest moisture adsorption efficiency by previous researchers. Román *et al.* (2019) reported that the SAP material increased the rate of grain drying substantially, especially in the upper bulk zone of grain where drying air flow reaching it was dehumidified the most. Researchers concluded that SAP materials could significantly assist in rapid maize grain drying and other crops. Saps can as well be utilized during storage to avoid rewetting of the crops during periods of high relative humidity (Román *et al.*, 2019). Studies have shown that high moisture absorption capability of desiccants can be adopted for drying during adverse climatic conditions to prevent rewetting and avert aflatoxin contamination (Mbuge *et al*., 2016; Román *et al.*, 2019).

2.5 Equilibrium moisture content

Equilibrium moisture content (EMC) of grain is the moisture content at which the material is neither gaining nor losing moisture to the surrounding air (ASABE, 2009). It provides important insight in drying and dehumidification processes, grain storage and microorganism's growth conditions that cause material deterioration.

Food materials and all seeds are classified as either hydrophilic or hygroscopic and they lose moisture in the bound water region or water-sorption region (Srikiatden and Roberts, 2007; Probert, 2003). Establishment of a water potential gradient between the seed surface and its internal tissues would cause the water to diffuse along the gradient. Thus, maize grain is considered hygroscopic and loses or gains moisture to attain equilibrium with adjacent air (Jaruk & John, 2007). Drying occurs through evaporation of water from the surface of the grain kernel. Evaporation of water from the surface of the seed depends on moisture gradient between the surrounding air and the seed. As grain moisture content levels attain equilibrium with the surrounding air, drying rate slows down exponentially (Probert, 2003). Further, moisture transfer during drying with falling rate period of drying has been described by a diffusion model of Fick's second law (Guan *et al*., 2013).

Equilibrium moisture content is dependent on the relative humidity and the temperature of the air. The Equilibrium moisture in drying of agricultural materials can be used to estimate the

required parameters of the drying air medium. ASABE standards (2008) provides standards for temperature, relative humidity and final equilibrium moisture content of dried product. The equilibrium moisture content (EMC) of grain is determined by the storage condition of temperature of the air and relative humidity. Commercial systems are capable of measuring relative humidity (RH) and temperature (T) of the air as well as grain moisture content during storage using sensors and equilibrium EMC models (Armstrong *et al*., 2017).

In every combination of temperature /relative humidity of air there is a specific EMC, a point at which the moisture in the air and the grain material have reached a steady state equilibrium. At this point air will not take or release moisture to the grain and the grain material can be stored, usually at 12-13% MC for maize grain. In an example that requires 12% EMC, dried from say 20% initial moisture content, the required drying air parameters would be 60% RH, at 30°C air temperature (See Figure 2-5).

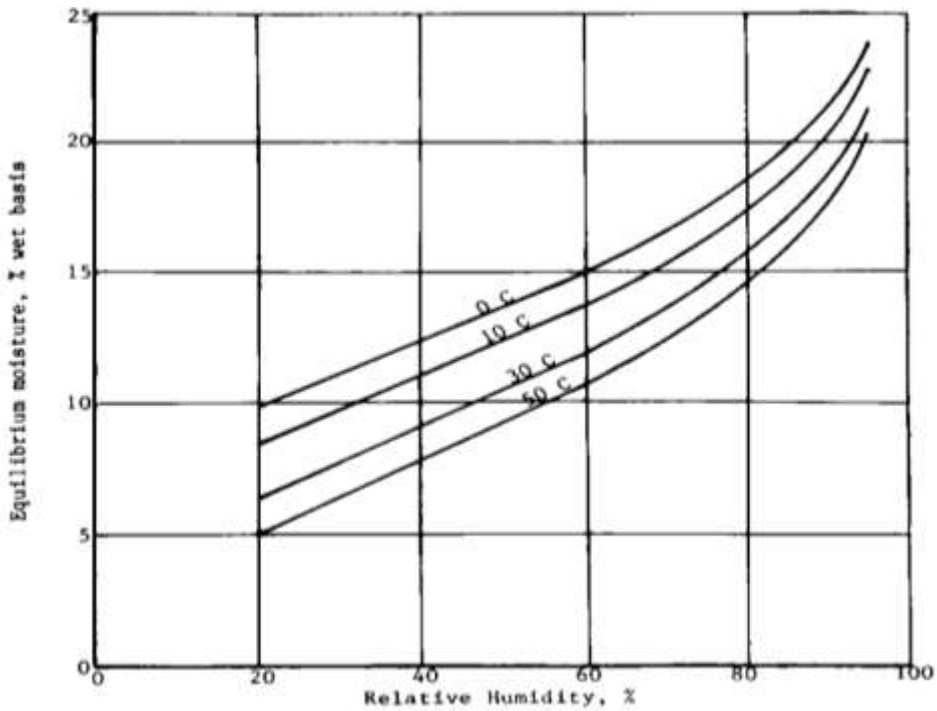

Figure 2-3: Equilibrium moisture content, yellow dent corn (ASABE Standards, 2008)

2.6 Summary of reviewed literature

Past studies have shown the importance of using solar collectors in preconditioning the drying air for use in enclosed solar dryers compared to open sun drying. Further, literature has shown that solar collectors operated with natural convection had high efficiency compared to solar collector with the forced convection. It was necessary to allow natural convection at the inlet

and into the solar collector to realise results for various configurations under undisturbed influences on heat transfer. Numerous performance optimization techniques and technologies utilized in solar collectors and solar grain dryers have been reviewed. The efficiency and the desired high collector outlet temperature from solar collectors have been found to be a function of mass flow rate. Therefore, the fan suction mass flow rate should be kept constant during the experiment such that a uniform fan and air speed influence on the data collected is maintained.

Fins have been reported to influence increased turbulence, pressure drop, thermal contact and friction with the absorber surface for improve useful heat gain and heat transfer to the air. Moreover, the literature has forwarded that fins located on the absorber increased heat transfer and desired pressure drop. Furthermore, fixed fin collectors were more effective than free fin collectors. In this study it was hypothesized that welding finned elements beneath the collector plate would optimize heat transfer as well as pressure drop by incoming convection. Experiments investigated such effect on drying air temperatures and relative humidity.

Reviewed literature has shown that the exhaust air from dryers though moist is at higher temperatures way above ambient conditions. Moreover, desiccant materials have been reported to dehumidify air with reduction in relative humidity associated with slight rise in temperature in a constant enthalpy process. Thus, desiccation in constant enthalpy is a more effective drying mechanism for biological food materials susceptible to thermal damage compared constant moisture reduction process using costly conventional energy dryers. The proposed dryer uses super absorbent polymer (SAP) commonly known as Luquafleece® in exhaust regeneration conduits to lower the relative humidity of the air before it is passed through grain. Thus, conduits lined with Superabsorbent polymer were used to test its effect in preconditioning the exhaust air whose regeneration into the collector and waste heat recovery effects were studied.

Literature suggests that solar dryers can be powered by photovoltaic modules as well as use of batteries to store energy for use during low solar radiation periods. This research considered the use of the PV cells to provide electrical energy to the sensors, fans as well as storing electrical energy using a battery for use during low solar radiation hours to maintain homogeneous circulation of drying air through the desiccant. During the experiments the drying systems was self-sufficient and independent of any external source of energy devoid of interrupted power supply.

Reviewed literature has shown significant heat loss effects by wind flow crosses at higher velocity on the solar receiver plate. It was hypothesised that the sensors ought to collect data at uniform meteorological parameters for all the collector setups. Transparent plexiglass glazing was used to prevent convection and long-wave radiation heat losses and protect the absorber plate against occasional cooling and dust. Solar radiation concentrators achieve maximum radiation concentration at right angles with the incoming radiation and should be positioned to receive radiation throughout the daylight. It was necessary to configure the lenses along the curvature of the glazing to receive radiation at right angles with East-West radiation trajectory of the sun throughout the day.

The foregoing literature has presented numerous efficiency optimization techniques and their significance in optimizing air drying conditions such as temperature and relative humidity. Moreover, researchers have argued that progressive research on performance improvement of solar collectors ought to be continuous endeavour. Evidently, evaluating the question in this study regarding the contribution of solar collectors in grain drying, it is possible to hypothesize an existing effect. The effect, according to the reviewed literature, and considering the definition of trying to include both performance optimization, dryer efficiency, moisture removal and the quality of the product, it is possible to report a range of findings. Firstly, an overall effect of solar collector performance improvement has been overwhelmingly established in the foregoing literature. Secondly, such an effect has been associated with a range of efficiency enhancement techniques. Effectively, it is possible to argue of a multifaceted influence of solar collector configuration on performance optimization regarding both the thermal efficiency and grain drying effectiveness

From the foregoing review it is evident that the need for highly efficient low-cost solar grain drying systems can be developed through integration of various solar collector configurations, heat transfer techniques or development of new techniques and mechanisms for solar dryers. From the foregoing review, various collector designs have shown significant reductions in drying periods, but some were fixed dryers. It was thus necessary to design a compart solar collector for an enclosed static grain drying bin of a portable dryer.

Generally, finned elements have been applied by previous researchers to increase the effectiveness of heat transfer. However, the incorporation of RCL, and DEARS and their combined effect with finned elements has not been reported. Therefore, the study was carried out to provide more knowledge into this effect.

CHAPTER THREE: THEORETICAL FRAMEWORK

This chapter presents the fundamentals, principles, equations and models that explain and describe the performance of solar collectors and solar grain drying technologies. Theories pertinent to undertake the study are described.

3.1 Pertinent parameters in solar air drying

Solar drying is a natural or an intentional technique of solar energy-induced mass transfer. The process utilizes incident radiation and converts it into thermal energy required for drying through removal of water by evaporation. Successful solar drying requires (a) Solar heat to withdraw moisture, (b) dry air to absorb released moisture, (c) appropriate control of solar heat gain to avoid cooking the crop and (d) adequate air circulation to remove the moisture.

3.2 Thermal performance and useful energy gain of a solar collector

For typical solar collector with solar radiation intensity I (W/m^2) on a collector of area A (m^2), Struckmann (2008) states that the amount of heat energy, Q_i (W) at the collector is found by

$$Q_i = I.A \tag{3.1}$$

Part of the radiation is however reflected into the sky while the glazing absorbs some more as the rest is transmitted to the absorber plate. Thus, the percentage of the solar rays that penetrate transparent cover is indicated by a conversion factor as the product of cover transmission rate and absorption rate of the absorber (Struckmann, 2008).

$$Q_i = I\,(\tau\alpha).\,A \tag{3.2}$$

Where;

τ= Transmission coefficient of glazing, dimensionless

α =Absorption coefficient of plate, dimensionless

However, as the collector absorbs heat energy the temperatures get higher than the surrounding and heat losses occur through convection and radiation depending on collector heat loss coefficient and temperature as described in Equation 3.3 (Struckmann, 2008).

$$Q_o = U_L A(T_c - T_a) \tag{3.3}$$

Where;

Q_o= Rate of heat losses ($W/m^2.K$)

U_L= Overall heat transfer coefficient of the collector (W/m^2)

T_c = Collector temperature (°C)

T_a= Ambient air temperature (°C)

The useful heat energy extraction rate by solar collector Q_u under steady conditions is proportional to the difference between the rate of useful energy absorbed and the amount lost to the surrounding. This is presented as (Struckmann, 2008).

$$Q_u=Q_i-Q_o=I\,(\tau\alpha).\,A-U_LA(T_c-T_a) \quad (3.4)$$

Where;

Q_u = useful heat energy (W)

Q_i =collector heat input (W)

Q_o= heat loss (W)

Since Equation 3.4 can inconvenience due to the difficulty of obtaining collector average temperature, heat removal factor can be used in relating the actual useful energy gain into the whole collector surface were at the fluid inlet temperature (Struckmann, 2008). Thus

$$F_R= m_{cp}\,(T_o-T_i)/\,(I\,(\tau\alpha).\,A-U_LA(T_c-T_a)) \quad (3.5)$$

Since the highest possible useful energy gain would occur when the whole collector reaches inlet fluid temperature, the useful energy gain Q_u is found by product of collector heat removal factor F_R by the highest possible useful heat energy gain.

$$Q_u=F_RA[I\tau\alpha-U_L(T_i-T_a)] \quad (3.6)$$

Where;

Q_u = Useful heat energy (W)

F_R = Collector heat removal factor

A = collector area, (m^2)

I = intensity of solar radiation (W/m^2)

U_L= Collector overall heat loss coefficient (W/m^2)

T_i = inlet temperature (°C)

T_o= outlet temperature (°C)

τ = Transmission coefficient of glazing

α = Absorption coefficient of plate

3.2.1 Thermal efficiency of solar collectors

Solar collector performance can be estimated by the collector efficiency (η) defined as the ratio of the useful heat energy gain to solar insolation incident at the collector plate over a time period. Duffie and Beckman, (2013) presented a basic method of measuring performance of solar collectors by exposing the operating collector to solar radiation and measuring inlet and outlet fluid temperatures. The rate of heat extraction (useful heat gain) from a collector is given

by the amount of heat energy carried away by the air that passed the collector (Duffie and Beckman, 2013).

$$\dot{Q_u} = \dot{m}.C_P(T_c - T_o) \quad (3.7)$$

Where;

Q_u = Useful heat energy, W

Tc = Collector inlet temperature, °C

To = Collector outlet temperature, °C

ṁ = Mass flow rate (kg/s)

C_p = Specific heat of air, kJ/kg.K

The air mass flow rate ṁ is found by multiplying the density of air and the volumetric air flow rate. The volumetric flow rate is found by the product of area of air flow duct (collector inlet) and the air speed. Al-Neama and Farkas (2016) suggested Equation (3.8) for finding the air mass flow rate. Therefore,

$$\dot{m} = \rho * v * A_{duct} \quad (3.8)$$

Where;

ṁ = Mass flow rate (kg/s)

ρ = Density of air (kg/m^3)

A_{duct} = Collector inlet (m^2)

v= Air speed (m/s)

The efficiencies of the various solar collector configurations were determined from equation 3.9 which is a ratio of useful energy gain by the air to the product of solar insolation and the solar collector plate area. Similar relation was used by other researchers (Weiss and Buchinger, 2012; Allan *et al*., 2015; Kareem *et al*., 2013; Kareem *et al*., 2017; Kumar *et al*., 2016; Al-Neama and Farkas, 2018; Ramani *et al*., 2010; Shemelin and Matuska, 2017).

The efficiency of a flat plate solar collector is given by:

$$\eta = \frac{Q_u}{G*A_c} \quad (3.9)$$

Where;

η = Collector efficiency

Q_u = Useful heat energy, (W)

A_c = Collector area, (m^2)

G = Global radiation intensity (W/m^2)

For a flat plate solar collector, the efficiency is the ratio of useful energy gain to the solar energy incident over a particular time period.

Equation (3.11) can be used in determination of instantaneous efficiencies during tests with a range of solar collector temperature conditions (Weiss and Buchinger, 2012).

$$\eta = \dot{m}C_p\,(Tc - Ta)/A_cG_T \quad (3.10)$$

Where;

$\dot{m}$ = Mass flow rate (kg/s)

C_p = Specific heat of air, kJ/kg.K

Tc = Temperature of the solar collector (°C)

Ta = Ambient air temperature (°C)

G_T = Solar irradiance (W/m^2)

Hottel and Whillier (1954) developed the following equations for efficiency of solar collectors:

$$\eta = FrA(\tau\alpha)\text{-}U_LA(\frac{T_c\dot{-}T_a}{AI}) \quad (3.11a)$$

$$\eta = Fr(\tau\alpha)\text{-}FrU_L\,(\frac{T_c\dot{-}T_a}{I}) \quad (3.11b)$$

Where;

$F_r(\tau\alpha)$ and (F_rU_L) are coefficients of heat losses

$F_r(\tau\alpha)$ and (F_rU_L) represent coefficients of y-intercept and slope of the curve that can characterize performance estimates of many solar heating systems (Duffie and Beckman, 2013; Al-Neama and Farkas, 2018). Similarly, Duffie and Beckman, (2013) presented equation (3.12a) stipulated that the performance of a solar collector can be presented with a curve showing the relationship between thermal efficiency and the term $(T_c\text{-}T_a)/I$ by a linear model formula given by;

$$\eta = a\frac{T_c - T_a}{I} + b \quad (3.12a)$$

Moreover, Al-Neama and Farkas (2018) developed linear mathematical that can be applied for single and double pass solar collectors presented as;

$$\eta = a\frac{T_{avs} - T_a}{I} + b \quad (3.12b)$$

3.3 Moisture ratio

Moisture ratio equation of drying is defined by Equation (3.13) (Erenturk *et al.*,2004 & Mewa *et al.*,2019)

$$MR = \frac{M_i - M_e}{M_o - M_e} \quad (3.13)$$

Where;

M_i =Moisture content at drying time t, (% dry basis)

M_e = Equilibrium moisture content (% dry basis),

M_o = Initial moisture content at time t= 0, (% dry basis)

3.3.1 Moisture removal rate

Drying rate of grain from initial moisture content to a final moisture content is expressed in Equation 3.14 (Querikiol *et al*., 2018).

$$R_D = \frac{M_{(t+\Delta t)} - M_t}{Dt} \quad (3.14)$$

Where,

R_D is the rate of drying (kg/hr)

M_t moisture content at time t, (% w.b)

$M_{(t+\Delta t)}$ moisture content at time t + Δt, (% w.b)

D_t is the drying time interval (hrs.)

According to Bola *et al.* (2013) the moisture removed (M_R) during a drying process can be calculated as;

$$M_R = C\left[\frac{M_1 - M_2}{1 - M_2}\right] \quad (3.15)$$

Where;

M_R = Moisture removed

C = Dryer capacity per batch (kg),

M_1 = Initial moisture content of the maize to be dried (%)

M_2 = Maximum desired final moisture content (%)

3.3.2 Drying air quantity

The drying air mass necessary to effect drying can be calculated from (Bola *et al*, 2013):

$$Q_g = \left[\frac{M_R}{RH_2 - RH_1}\right] \quad (3.16)$$

Where;

Q_g= Amount of air required (kg)

M_R = Moisture removed (kg)

RH_1= Initial humidity ratio (kg/kg dry air)

RH_2 = Final humidity ratios (kg/kg dry air)

3.4 Grain drying models

Drying kinetics and simulation of grain drying by moisture removal process is important in drying systems performance evaluation, design, equipment development and performance optimization studies (Corrêa, *et al*., 2011; Rajkumar *et al.*,2007). Various drying models are used to simulate drying of agricultural materials. As such the drying of maize grain can be evaluated using proposed mathematical models as shown in Table 3.1.

Table 3.1: Drying models

No.	Model name	Model equation	References
1.	Newton	MR=exp(-*kt*)	Fudholi *et al*. (2011)
2.	Page	MR=exp(-kt^n)	Doymaz, (2004)
3.	Modified page	$MR = \exp[-(K t)^n]$	Vega *et al*. (2007)
4.	Henderson and Pabis	MR=*a*.exp(-*kt*)	Meisami-asl *et al*. (2010)
5.	Modified Henderson and Pabis	MR=a.exp(-*kt*) +*b*.exp(-*gt*) +*c*.exp(-*ht*)	Zenoozian *et al.* (2008)
6.	Logarithmic	MR=*a*.exp(-*kt*) +*c*	Rayaguru &Routray (201 Kaur &Singh (2014)
7.	Midilli	$MR = a.\exp(-kt) + bt$	Midilli *et al.* (2002); Darvishi &Hazbavi (2012 Ayadi *et al.* (2014)
8.	Modified Midilli	$MR = a.\exp(-kt) + b$	Gan & Poh (2014)
9.	Two-Term	MR=a.exp(-$k_o t$) +b.exp(-$k_1 t$)	Henderson (1974) & Chayjan *et al.* (2011)
10.	Two- term exponential model	MR=a.exp(-$k_o t$) + (1-a) exp(-$k_1 at$)	Dash *et al.*2013
11.	Wang and Singh	MR=1+at+bt^2	Omolola *et al*. (2014)
12.	Diffusion approach	MR=a.exp(-*kt*) +(*1-a*) exp(-*kbt*)	Yald´yz & Ertek´yn (2007
13.	Verma *et al*	MR=a.exp(-*kt*) +(*1-a*) exp(-*gt*)	Akpinar (2006)
14.	Peleg model	$MR = 1 - t/(a + bt)$	Da Silva *et al*. (2015)
15.	Two term and Page	MR = a.exp (-$K t^n$) + b.exp (-ht^n)	Kumar *et al.* (2012)
16.	Hii *et al*	MR = a.exp [-($K_1 t^n$] + bexp [- ($K_2 t^n$]	Kumar *et al.* (2012)
17.	Singh et al model	MR=exp(-*kt*) - *akt*	Diamante *et al.* (2010)
18.	Silva *et al* model	$MR = \exp(-at - b\sqrt{t})$	*Pereira et al*. (2014)
19.	Demir *et al* model	$a.exp(-Kt)^n + b$	Demir *et al.* (2007)
20.	Diamante *et al*	Ln(-lnMR) =a+b(lnt)+c(lnt)^2	Diamante *et al.* (2010)

where: t = drying time (s); k = drying constant (s^{-1}); a, b, c, g, h, n = model's parameters specific to individual equations

Most of the models are empirical and have obtained satisfactory results through mathematical analogies based on experimental data and statistical analysis (Midilli *et al.,* 2002 & Corrêa *et al.,* 2011). Studies have shown that understanding of experimental drying models and mathematical considerations of drying kinetics can significantly improve the efficiency of dryers, minimize the cost of production, and improve the quality of the dried grain (Onwude *et al*., 2016).

During analysis of drying kinetics experimental moisture ratios data can be fitted to the drying models and the best fitting model selected by considering statistical parameters such as coefficient of determination (R^2), chi-square (χ^2), root mean square error (RMSE) and sum of square error (SSE). The parameters are expressed as; (Iwe *et al*., 2019; Aregbesola *et al*., 2015).

$$R^2 = \frac{\sum_{i=1}^{N}(MR_{exp,i}-MR_{pre,i})^2}{\sqrt{\left[\sum_{i=1}^{N}(MR_{exp,i}-MR_{pre,i})\right]^2 * \left[\sum_{i=1}^{N}(MR_{exp,i}-MR_{pre,i})\right]^2}} \quad (3.17)$$

$$RMSE = \left[\frac{1}{N}\sum_{i=1}^{N}\left(MR_{pre,i} - MR_{exp,i}\right)^2\right]^{\frac{1}{2}} \quad (3.18)$$

$$\chi^2 = \frac{\sum_{i=1}^{N}(MR_{exp,i}-MR_{pre,i})^2}{N-n} \quad (3.19)$$

$$SSE = \frac{\sum_{i=1}^{N}(MR_{exp,i}-MR_{pre,i})^2}{N} \quad (3.20)$$

Where $MR_{exp,i}$ and $MR_{pre,i}$ are the experimental and predicted moisture rations respectively, N is the total number of observations and n is the number of model constants.

A good fit is described by having R^2 close to 1 and RMSE, χ^2 and SSE close to zero (Fernando & Amarasinghe 2016; Erenturk *et al*. 2004; Demir *et al*. 2004; Goyal *et al*. 2007).

CHAPTER FOUR: MATERIALS AND METHODS

This chapter describes the procedures, materials and methods adopted in meeting the objectives of the study. Data collection procedures are outlined, and various instruments and equipment utilised described.

4.1 Introduction

A hybrid solar desiccant dryer (HSDD) was fabricated, and experiments aimed at preconditioning the air for grain drying were performed. They included solar collector with; (a) High density longitudinal finned elements (LFES) for enhanced efficiency of heat transfer, (b) Radiation concentration lenses (RCL) for increased solar radiation intensity, (c) desiccant exhaust air regeneration conduits (DEARS) to enhance exhaust dehumidification and waste heat recovery and (d) Combined solar collector (CSC) of the three configurations. Maize grain drying experiments were performed in the most efficient configuration dryer and results compared with open sun drying method. Detailed statistical analysis was done to test statistical significance of the experimental data. Drying curve models from experimental data were analysed to determine the correlation with existing drying models developed by numerous researchers.

4.2 Conceptual dryer design considerations, material selection and fabrication

The solar dryer consisted of a fabricated solar collector unit and the grain drying compartment of 1120 mm height with a base and top diameter of 390 mm (Approx. 0.14m^3). The area of the solar collector was limited by the existing dryer bin top surface and collected a limited amount of solar energy. Since it was necessary to produce a compact drying system, four solar collector configurations were studied to optimize grain drying performance inside the dryer compartment. As shown in conceptual design operation Figure 4.1 the heated air from the collector is sucked by the D.C fan down to the plenum where it forced up the grain layers to cause drying. This is due to high temperatures and differences in relative humidity. The exhaust hot but humid air was passed through exhaust air desiccant regeneration system for possible potential waste heat recovery and recirculation into the solar collector (see Figures 4-3 and 4-5).

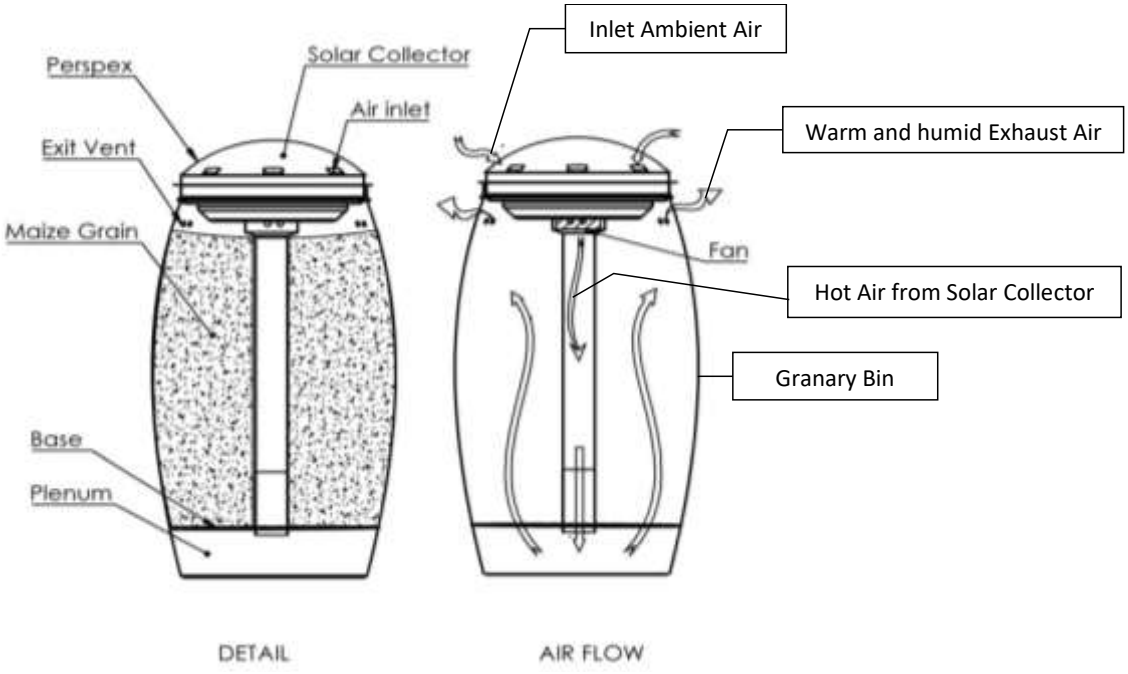

Figure 4-1: Conceptual design operation of the dryer

The solar collector is composed of a flat plate of maximum area of $0.5m^2$ made from galvanised steel sheet gauge 24. It was painted black for maximum absorption of radiant heat energy as well as reduction of the tendency to corrode. The solar concentrator glazing was moulded in a glass annealing oven using a clear 2 mm acrylic material selected based on high infrared transmittivity (90 %), UV light stability and good shatter resistance.

The collector glazing design had a depth of 250 mm onto which 20 radiation concentrating lenses of 50 mm diameter and variable focal lengths (200mm and 250mm) were embedded. The lenses were fixed along the curvature of the glazing based on the length of their radiation concentration focal points at the collector flat surface and the suns day-arc trajectory. The collector was glazed by a dome shaped acrylic material to allow infrared wavelength that is responsible for heating to penetrate and facilitate build-up and accumulation of heat energy in the system. Additionally, the glazing served to prevent loss of heat from the solar collector and maintain collector plate temperature and increase heat collection efficiency by the drying air.

Radiation concentration lenses were embedded on the glazing to further increase the concentration of heat energy on the collector plate. Cutting, shaping, riveting and welding machining processes were used in fabrication of the solar collector as shown in conceptual fabrication methodology in Appendix F. Description of other dryer material components is

tabulated in Table 4.1 while the dimensions of the grain drying bin are as shown in Appendix A. The drying chamber had the capacity to hold a one standard bag (90kg) of maize grain. Other components and design considerations included;

a) 12 volts dc power storage battery

The backup battery was utilized to ensure uniform power supply to the fan for purposes of nighttime drying by forced convection through superabsorbent polymer air recirculation conduits.

b) Solar photovoltaic panel

This design considered the use of the PV cells to provide electrical energy to the sensors and the fan. Moreover, it supplied stored electrical energy in the 12v D.C battery for use during low solar radiation hours and at night to maintain a uniform circulation of drying air through the desiccant. During the experiments the drying systems was self-sufficient and independent of any external source of energy thus devoid of interrupted power supply. Therefore, the design is a hybrid all weather drying during the daylight by high temperature from the concentrated solar radiation and off and night-time or off sunshine hours by the exhaust desiccant dehumidifier.

c) Acrylic glazing

Acrylic glazing was molded in a glass annealing oven into a dome shape with a radius of 0.2m corresponding to the focal length of the radiation concentration lenses. This was to ensure maximum heating by allowing the radiation rays to be concentrated on the focal point, a distance corresponding with absorber plate from the glazing. Acrylic material was chosen based on its infrared penetration characteristics.

d) Solar collector insulation

The acrylic glazing was completely sealed and made airtight using silicon sealants to eliminate free convective and conductive heat loss from the collector plate.

e) Absorber plate

The collector plate absorber was made from steel sheet metal (galvanized) and the exposed surface painted black chrome to absorb the incoming direct radiation and decrease its reflectivity.

f) Heat exchange zone

The high-density finned elements surface from the backplate formed an enclosed airtight compartment into which air was passed. This created a zone of heat transfer to the drying air. The high-density finned elements surface ensured thermal contact between the absorber and

the air. The heat exchanger zone was specially designed to prevent direct interaction with incoming ambient air and adjacent to the fan. Table 4.1 provides properties of various components and material consideration during fabrication.

Table 4.1: Solar collector components

Material	Dimension /Rating	Material	Dimension /Rating
Acrylic	3 square meters	Flex conduits	0.0762 meter Ø
Lenses	50 mm Ø	Centrifugal fan	12V DC
Galvanised sheet	Square meter 24 gauge	Silicon sealant	500 ml
Photo-voltaic panel	80W	Contact adhesive	200 ml
DC Battery backup	12V-9Ah rechargeable	Wire netting	2 square metre
Paint	1 Litre	Drill bits	1.5-4mm
Sap desiccant fabric	0.8 kg	Drying bin	120 kg empty
Nuts and bolts	1-3.5mm	Pipe conduits	5 m - 0.0762 m Ø

4.3 Solar collector configurations

4.3.1 Finned elements surfaces

The back plate of the collector plate surface was fabricated into an extended surface using finned elements. A high density 80 mm longitudinal finned elements totalling 1568 fins were embedded and welded inferior to the surface of the absorber plate resulting to an extended gross heat transfer surface of 1.0046 m^2 (Figure 4-2). Fins enhanced heat transfer to the drying air by increasing thermal interaction surface area. The heat generated by the direct, focussed and concentrated radiation was transferred to the extended finned elements and onto the air.

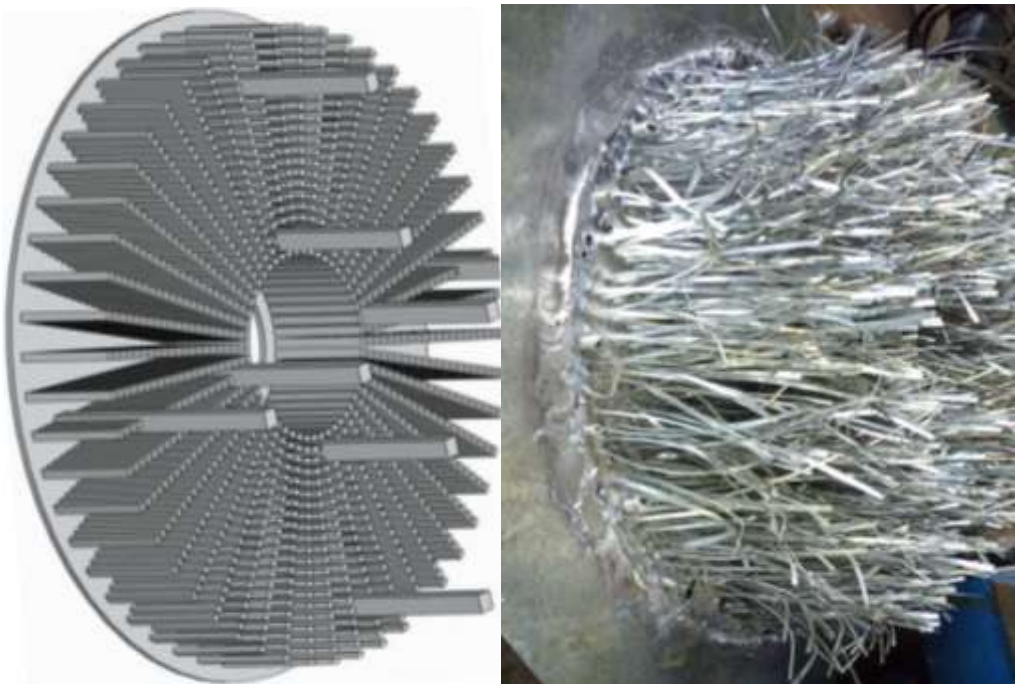

Figure 4-2: Finned element surfaces

Further, the hot finned elements improved interaction with air by increased pressure drop beneath the collector plate and decelerated movement and speed of airflow within the collector thus increasing the collectors useful heat transfer to the air per unit temperature rise.

4.3.2 Desiccant exhaust air regeneration system (DEARS)

As shown in Figure 4-3 the exhaust regeneration conduits integrated with superabsorbent polymer was incorporated in the solar dryer. Four desiccant lined exhaust recirculation conduits of 50mm diameter were used to provide equivalent outflow into the inlet area to regenerate exhaust air for maximum waste heat recovery into the finned elements heat transfer chamber and the radiation concentrator plate heat sink.

During loaded dryer testing experiments the moist, hot exhaust air was regenerated through these conduits as shown in schematic experimental set up Figure 4-10. Superabsorbent polymer desiccant fabric was used due to its high moisture sorption capacity and workability. Once saturated the desiccant can always be regenerated using solar heat energy as reviewed in literature.

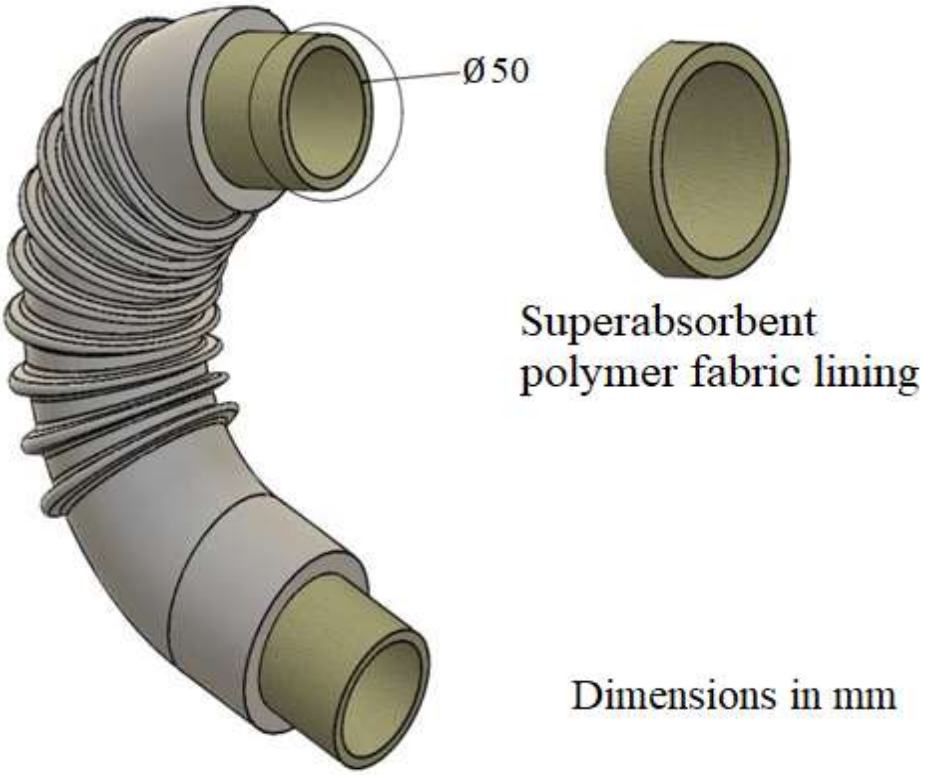

Figure 4-3: Desiccant exhaust air regeneration system (DEARS)

4.3.3 Radiation concentration lenses (RCL)

Figure 4-4 shows the incorporation of radiation concentration lenses embedded on the acrylic glazing. Concentration of solar radiation on the collector plate was achieved by 20 lenses of 50 mm diameter. Radiation concentration -refractive lenses with 0.2m focal length were used to concentrate solar radiation onto the collector plate. These lenses were embedded onto the dome shaped glazing to form a solar radiation tracking mechanism with the apparent diurnal motion of the sun. Apart from the direct radiation absorbed by the flat plate these lenses focused radiation rays onto smaller area and increased the intensity of solar radiation heating. The desired effect was to concentrate solar radiation and increase temperatures of the collector plate to effect high air temperatures.

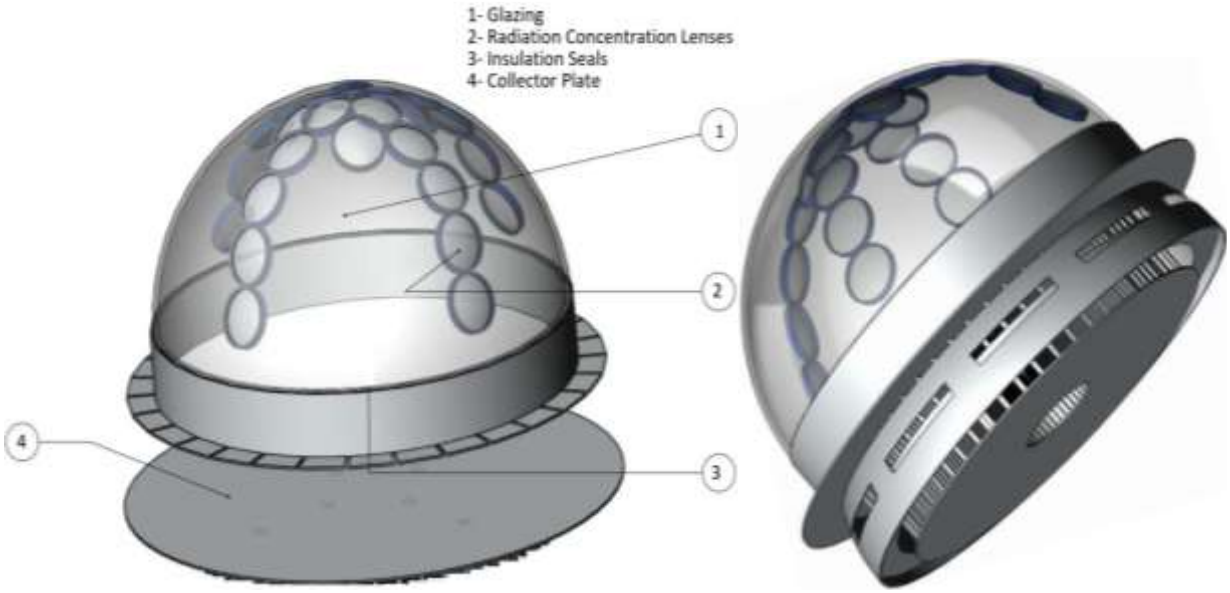

Figure 4-4: Radiation concentration lenses

4.3.4 Combined soar collector

The combined solar collector configuration utilised RCL to achieve high temperatures, LFES to increase heat transfer rates to the drying air and DEARS to enhance exhaust dehumidification. This was desired to effect waste heat recovery from the exhaust of the drying chamber. This was in turn recirculated into the solar collector for further reheating and utilisation into the grain drying compartment as shown in Figure 4-5. The combined radiation concentration lenses, finned elements and the exhaust regeneration configuration is shown in Figure 4-5

Figure 4-5: Combined solar collector

4.4 Components of the hybrid solar desiccant dryer

The solar collector components of the combined configuration were incorporated into the drying granary compartment as shown in Figure 4-7. These include the radiation concentration lenses, High density longitudinal finned elements surfaces and a system of exhaust air desiccant regeneration conduits. The D.C power backup that is recharged by a P.V panel during the day to run the fan is shown. The complete HSDD is shown in Appendix O.

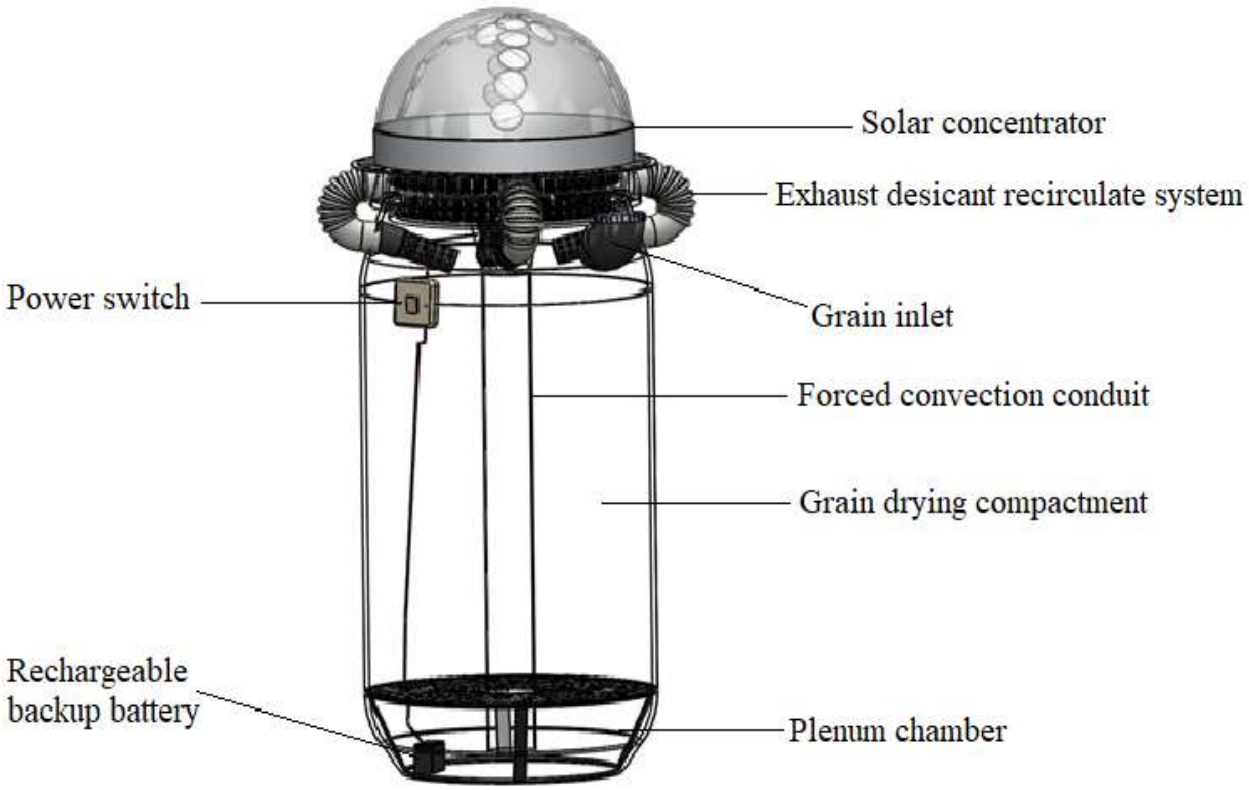

Figure 4-6: Interior components of the hybrid solar desiccant dryer

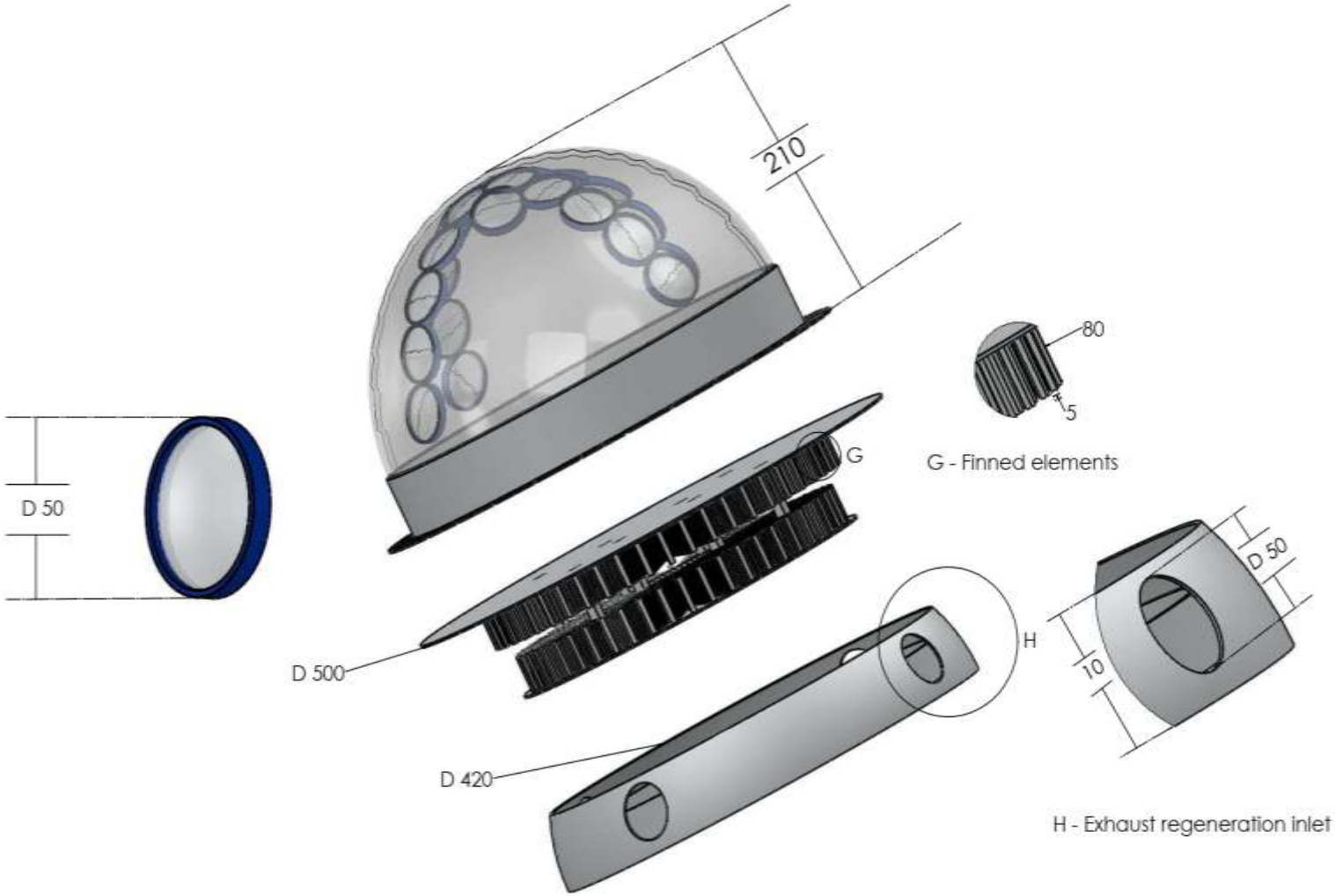

Figure 4-7: Solar collector showing exhaust drying air inlets, radiation concentration lenses and fins

4.5 Experimental set up

4.5.1 Study location

The study was carried out in the Department of Environmental and Biosystems Engineering at the Food and Process workshop in Kabete, Nairobi, Kenya (1º 15.111'S, 36º43.951'E) at an elevation of 1863 meters above sea level. Figure 4-8 and 4-9 shows the experiments location. The area experiences annual average temperature range of 18°C-24°C. It is a zone of moderate to high solar energy potential with average daily global solar insolation of 4.9 – 6.2 kWh.m^{-2}. The amount of available solar energy is season dependent, with months of September, October, January and February season receiving the highest amount of insolation and mean daily sunshine hours. During the experimental sessions, insolation ranged between 4.9 – 6.1kwh/m^2 per day that was similar and well comparable with the maize growing zones that fall within the tropics. Drying experiments were carried out on 10-13th October 2018.

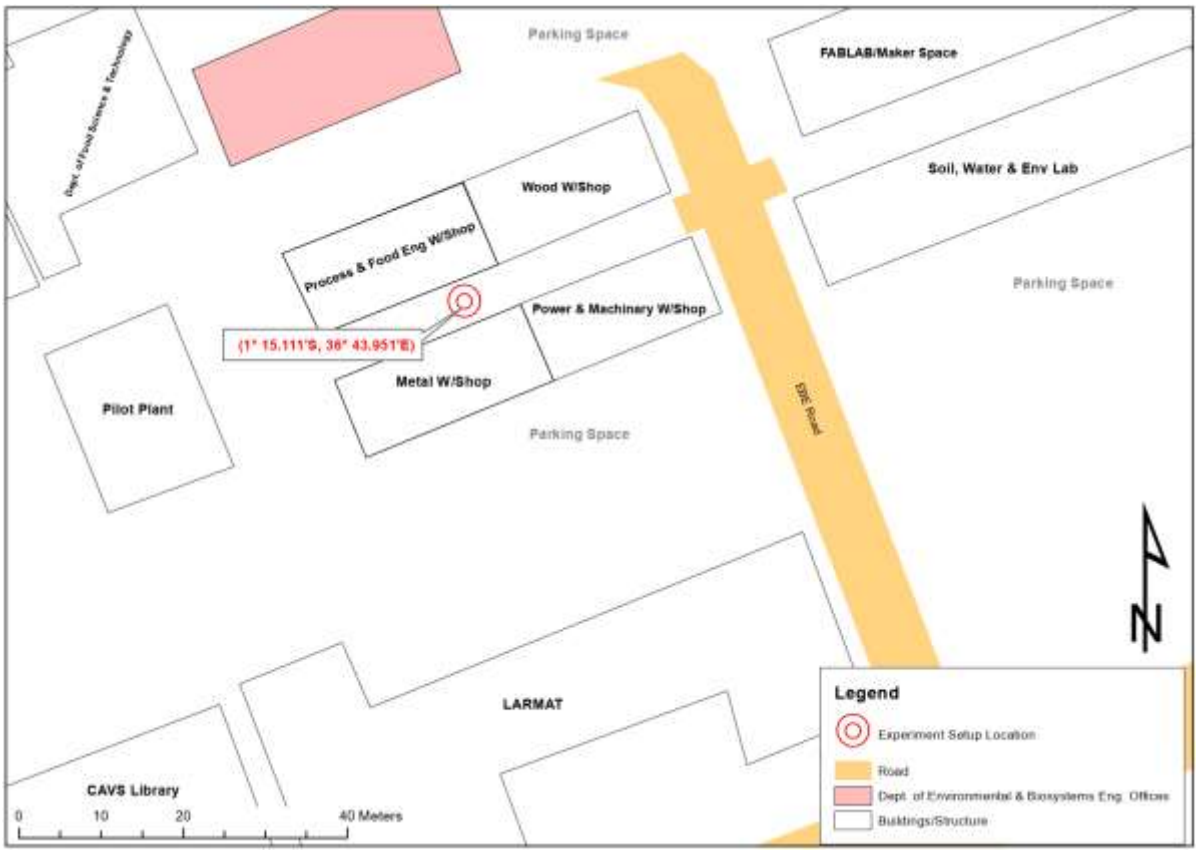

Figure 4-8: Solar collector's experiments location

Figure 4-9: Latitude and longitude of experiments location (Google map, 2018)

4.5.2 Solar collector experiments

Solar collector experiments were carried out to explore the effect of various collector configurations in preconditioning the air for a prototype hybrid grain dryer developed at the Food and Processing workshop. Specifically, the experiments were performed to establish the effect on temperatures and relative humidity parameters of the forced convection flow as well as heat transfer through the solar collector configurations. Ambient air conditions were recorded simultaneously. Temperature and relative humidity were monitored by sensors probes and their values recorded by a digital data logger (Plate 4-1) with a programmed module to record each of these values at time intervals of 2 minutes throughout the experiment.

The datalogger had 10 temperature sensors labelled (T_1-T_{10}) and 10 relative humidity sensors (H_1-H_{10}). Plate 4-1 shows the sensors with datalogger. Temperature and relative humidity of the air inside the various solar collector configurations studied as well as ambient values were recorded and instantaneously for every 2 minutes interval for the collector test period of 10 hours. Anemometer probe (Plate 4-2) was simultaneously used to record, compare and verify the recorded values. 30 data points were recorded for each parameter within an hour and about

300 data points for every parameter throughout the experimental duration of 10 hours. The output data from the datalogger was read from a laptop in the form of excel spreadsheet. Air velocity readings was measured by Testo-445 instrument. The experimental set up consisted of an indirect forced convection solar dryer with four solar collector configurations. The configurations studied included solar collector with;

a) High density longitudinal finned elements
b) Solar radiation concentration lenses
c) Exhaust air recirculation via superabsorbent polymer desiccant conduits
d) Combined lenses and finned elements integrated with desiccant exhaust recirculation.

4.5.3 Measuring instruments and equipment

a) Sensor probe data logger

This was used to measure and record drying air parameters which include temperature, humidity and moisture levels within the dryer. The specific sensor components of the data logger included;

i) Temperature digital sensors

These were used to monitor and record temperature of the drying air at various points, at the inlet-ambient temperature, system temperatures in the solar collector, Outlet to Solar Collector, Inlet of the fan, at the plenum, Outlet of the dryer, and recirculated air temperature.

ii) Humidity sensors

These were used to measure humidity of the air from with a range of 0 to 100% RH of the drying air.

iii) Digital moisture sensors

These sensors were used to record the moisture levels within the system at similar points with the temperature sensors.

iv) Digital time sensors

These sensors were incorporated within the data logger programmed module as shown in Plate 4-4 to record the corresponding time when data on (i) to (iv) above was captured within a range of 2 minutes interval. The output data in the form of Microsoft Excel spreadsheet was read from a laptop.

b) Testo-445 multifunctional climate measuring instrument.

Testo-445 instrument was used to record airflow velocity, temperature, absolute humidity, and relative humidity simultaneously.

Plate 4-1: Sensor probe datalogger

Plate 4-2: Testo-445 instrument

c) Digital Temperature and Relative humidity meter

A digital relative humidity meter to verify the ambient data from the dataloggers. The range over which the meter can measure varies from 10% RH to 99% RH with humidity accuracy ±4%. Humidity meter display has a resolution of 1% RH and temperature range of -50 °C-70°C.

Plate 4-3: Digital relative humidity meter

Plate 4-4: Solar collector configurations data collection

4.5.4 Grain drying experiment

Grain drying experiments were conducted to evaluate the effectiveness of the developed hybrid solar dryer for maize grain drying. Shelled maize (ADC600-23A-White) of 24.1% M.C (wet basis) was loaded into the dryer and a similar sample dried using OASD. Drying was commenced and average samples were progressively collected from both drying systems at intervals of 30 minutes. Variations in grain moisture content over the drying time was monitored and measured using Farm-pro moisture analyser equipment shown in plate 4-5. Drying process continued till a steady state of final moisture content was reached. Testo-445 multifunctional climate measuring instrument with air velocity probe was used to measure the speed of drying air.

Plate 4-5: Farm-pro moisture analyzer

Temperature and relative humidity levels at the inlet and outlet of the drying chamber were recorded by a sensor probe data-logger and Testo-445 multifunctional climate measuring instrument as shown in the schematic experimental set up Figure 4-10.

The drying performance of the hybrid solar dryer with desiccant exhaust regeneration system was also compared against the ambient inlet and outlet (single pass dryer) as well as ambient conditions open sun drying (OASD) for maize grain drying during the period of experimentation. The performance of the OASD was highly dependent on the solar insolation and ambient temperatures.

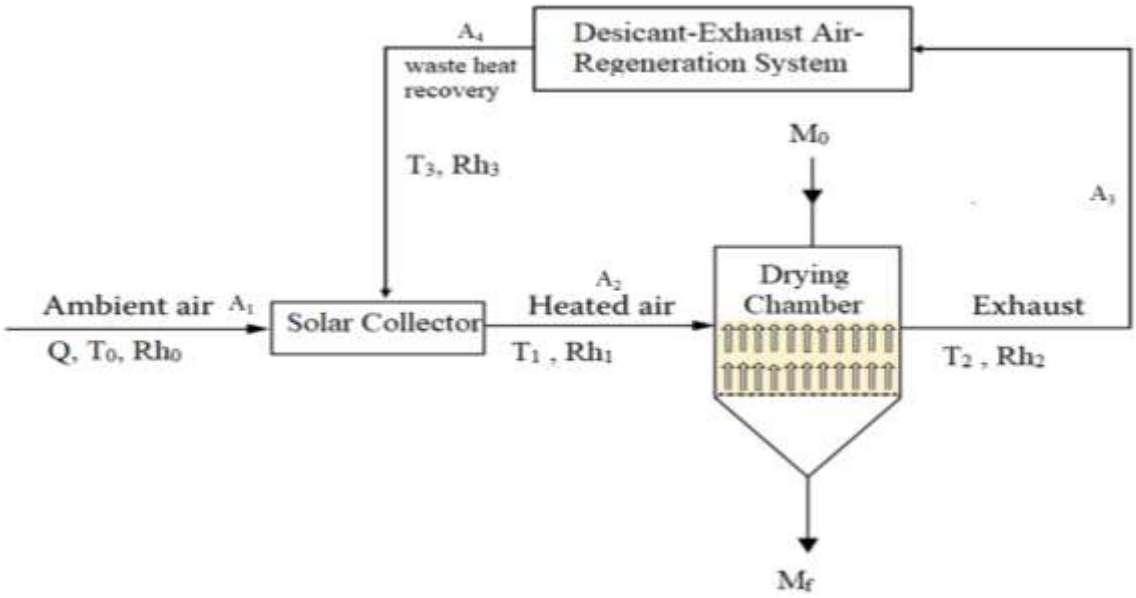

Figure 4-10: Schematic set up of the hybrid solar desiccant dryer grain drying experiment

The types and position of sensors that were used during grain drying experiments are tabulated in Table 4.2 while Plate 4-6 shows the grain drying experimental setup.

Table 4.2: Location of sensors in experimental set up

No	Sensor type	Position of Sensors
1	Air temperature and humidity	A_1
2	Air temperature, humidity, velocity	A_2
3	Air temperature and humidity	A_3
4	Air temperature and humidity	A_4

The instruments that were used to record various parameters are as shown in Table 4-3.

Table 4.3: Characteristics of the measuring instruments

No	Instrument	Parameter	Range	Accuracy
1.	Farm-pro moisture analyzer	Moisture content	5 – 50 %	0.25 % M.C
2.	Pyranometer	Solar radiation	0 - 1250 W/m^2	±3 %
3.	Sensor probe data logger	Temperature	0-100°C	1°C
4.		Relative humidity	0-100 %	1 % RH
5.	Digital relative humidity meter	Relative humidity and temperature	10 % - 99 % -50 °C - +70°C	±4 % RH
6.	Testo-445 instrument	Air velocity	0 - 60 m/s	0.01m/s
		Temperature	-50 - +180°C	0.2°C
		Relative humidity	0 - +100 %	0.1% RH

Plate 4-6: Grain drying experimental setups

4.6 Experimental data analysis

4.6.1 Solar collector data analysis

The drying air mass flow rate in the solar collector was found using Equation 3.8 from the air speed as recorded by the digital Testo-445 anemometer probe. Equation 3.7 was applied to calculate useful heat energy gained by the air from known solar insolation received and the area of the solar collector plate against the measured change in air temperatures as described in Appendix W. Consequently Equation 3.9 was then applied in calculation of the efficiencies of respective solar collector configurations and values tabulated as shown in Table 8.9.

Equations 3.11(a) and 3.11(b) were used in characterisation of collector efficiency with changes in temperature per insolation heat gain for various collector configurations. The instantaneous collector efficiencies calculated from experimental data using Equation 3.11a for various solar collector configurations and was plotted against the respective reduced temperature functions as described by Equations 3.12(a) and 3.12(b).

4.6.2 Grain drying data analysis

The length of time to dry grain from initial moisture content to final moisture content was considered in analysis of drying rate as expressed in Equation 3.14. Moisture content data of the HSDD was used to develop experimental drying curves and grain drying models in the HSDD using moisture ratio Equation 3.13. These were compared with drying mathematical

models and equations listed in Table 3.1 using MATLAB software nonlinear regression analysis.

4.7 Statistical analysis

4.7.1 Statistical significance of solar collector configurations experimental data

The four different solar collector configurations were used to establish their effect in preconditioning the temperature and relative humidity of air for a hybrid grain dryer. The datasets from the solar collectors were analysed and compared for any evidence of statistically significant differences across the means of the datasets.

Statistical analysis of the solar collector configurations drying temperature data was performed using stratigraphic16.1. Multiple range tests were used to test for significant differences between the means of temperatures from the contrasted collector configurations. The change in temperatures and values for the collector configurations were subjected ANOVA single factor to test for statistically significant differences in the changes of temperatures from the various configurations at 95% level of confidence. A t-test was performed to estimate any significant differences between variation of moisture content of grain dried using desiccant exhaust regeneration dryer and the inlet outlet (single pass) dryer.

4.7.2 Drying kinetics analysis of experimental data

Nonlinear regression analysis was performed using MATLAB statistical computer program (Version R2016a) to regress the HSDD grain drying data and select the best fitting drying model amongst 18 commonly used drying models (Table 3.1). The coefficient of determination (R^2) was primarily used as the criterion for selecting the best model to describe the drying curves and account for variation in the drying curves of the dried samples. Moreover, chi-square (χ^2), root mean square error (RMSE) and sum of square error (SSE) were used to estimate the deviations of experimental and predicted model values to determine the goodness of the fit. The higher values of R^2, RMSE and SSE was used as the criterion to select the suitable drying model and the goodness of fit. These parameters were calculated using Equations 3.17, 3.18, 3.19 and 3.20.

CHAPTER FIVE: RESULTS AND DISCUSSION

This chapter presents results and interpretation of the findings from the study. The results of the solar collector testing experiments and the loaded grain dryer experiments are discussed.

5.1 Experimental site solar irradiance

The highest irradiance recorded for experimental site (Kabete, Nairobi (1° 15.111'S, 36°43.951'E) was 850 W/m^2 while the average monthly irradiance was 670 W/m^2. Figure 5-1 shows there was significance variation of irradiance values within the month as depicted by the graph of irradiance against days of the month. The graph shows that during day1 to day 16, high irradiance values were received compared to the rest of the month. This was attributed to changing atmospheric conditions due to cloud cover that intercepted solar radiation.

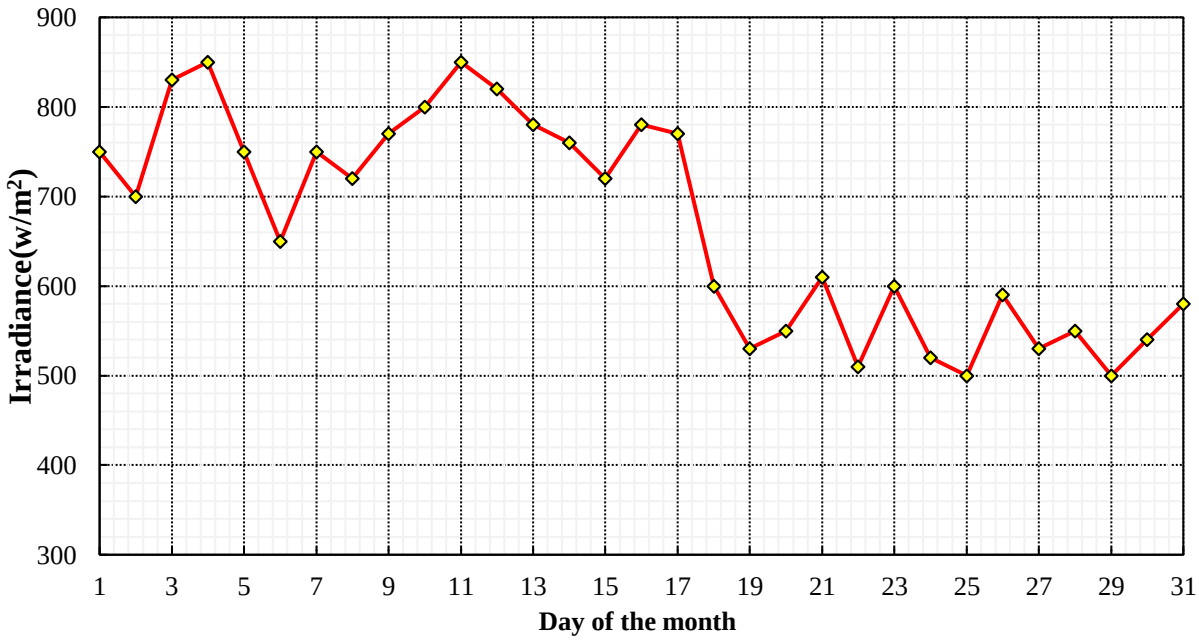

Figure 5-1: Daily solar irradiance for Kabete for the month of October 2018

5.2 Solar collector experiments

The results of the effect of collector configurations described earlier are presented. The data on temperature and relative humidity as well as respective changes in these values from ambient conditions were analysed and solar collector efficiencies evaluated.

5.2.1 Temperature profile of the solar collectors

The instantaneous variation of the recorded air temperatures from the four solar collector configurations are presented in Figure 5-2. The solar collector temperatures increase with the time of test till it reaches the maximum value at maximum ambient temperature, then it

decreases gradually when the values of ambient temperature and solar irradiance decreases. The rise of temperature fluctuated sporadically to reach maximum values at 13:00 hrs with increase in ambient temperature and solar irradiance (Figure 5-2) after which they begin to decrease. The intermittent rise and fall of the values were attributed to radiation blocking by some sporadic clouds, haze and ambient air temperature instability. Experiments by Sencan and Ozdemir, (2007); Yang *et al.* (2012) as well as Al-Neama and Farkas (2018) reported highest temperature values were achieved from solar collectors between 13:00 and 14:00hrs in summer.

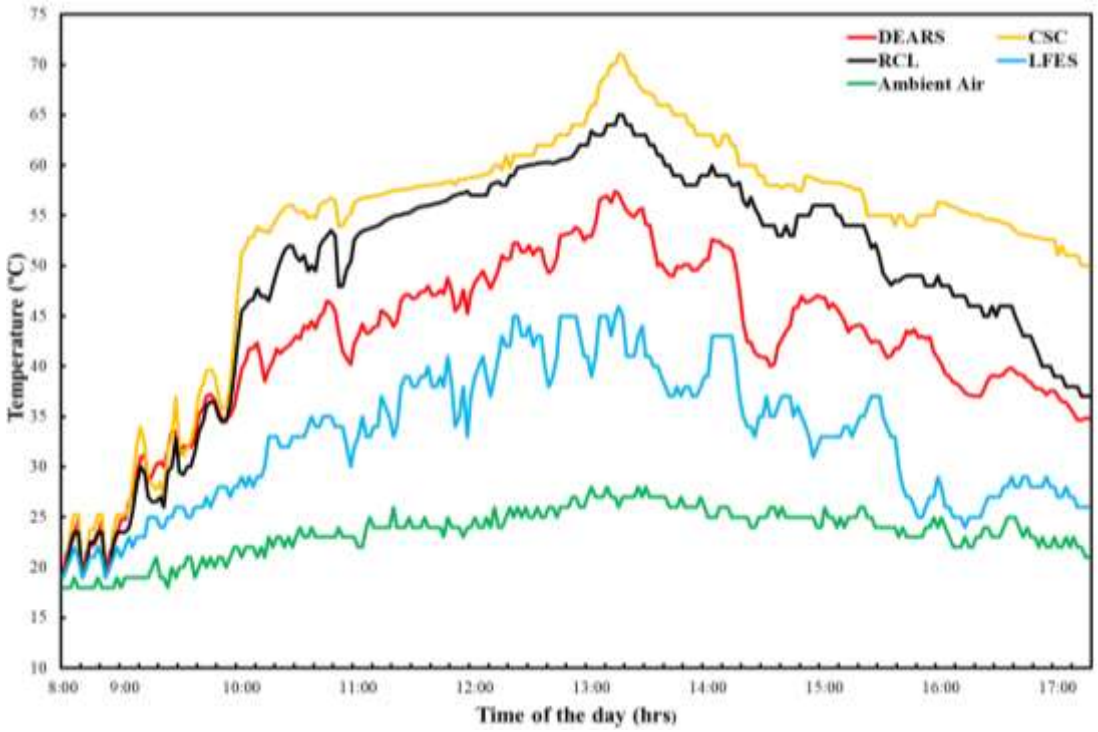

Figure 5-2: Temperature profile of the solar collector

The temperature datasets from every hour were averaged and average hourly solar collector temperatures with time were as shown in Figure 5-3. The solar collector air temperature increases with the time of test till it reaches the maximum value at maximum ambient temperature, then it decreases gradually when the values of ambient temperature and solar irradiance decreases. The collector configuration with longitudinal finned elements surfaces (LFES) had the least temperature values throughout the experiment compared to other configurations. Desiccant exhaust air regeneration (DEARS) presented high temperature values during the start of the experiments compared to the collector with radiation concentration lenses (RCL), however after about $2\frac{1}{2}$ hours RCL recorded higher temperature values as shown in Figure 5-3. This was attributed to increase in solar insolation and the

radiation tracking and concentration effect by the lenses on the collector plate for air and space heating. Similar observation was reported by Emelue *et al.* (2014) and Ohijeagbon *et al.* (2016). Emelue *et al.* (2014) reported higher temperatures in solar collectors with radiation concentration mirrors than in the solar dryers without. However, the temperatures of radiation concentration lenses configuration within the solar collector drop significantly in response to changing radiation from 14.00hrs (Figure 5.3).

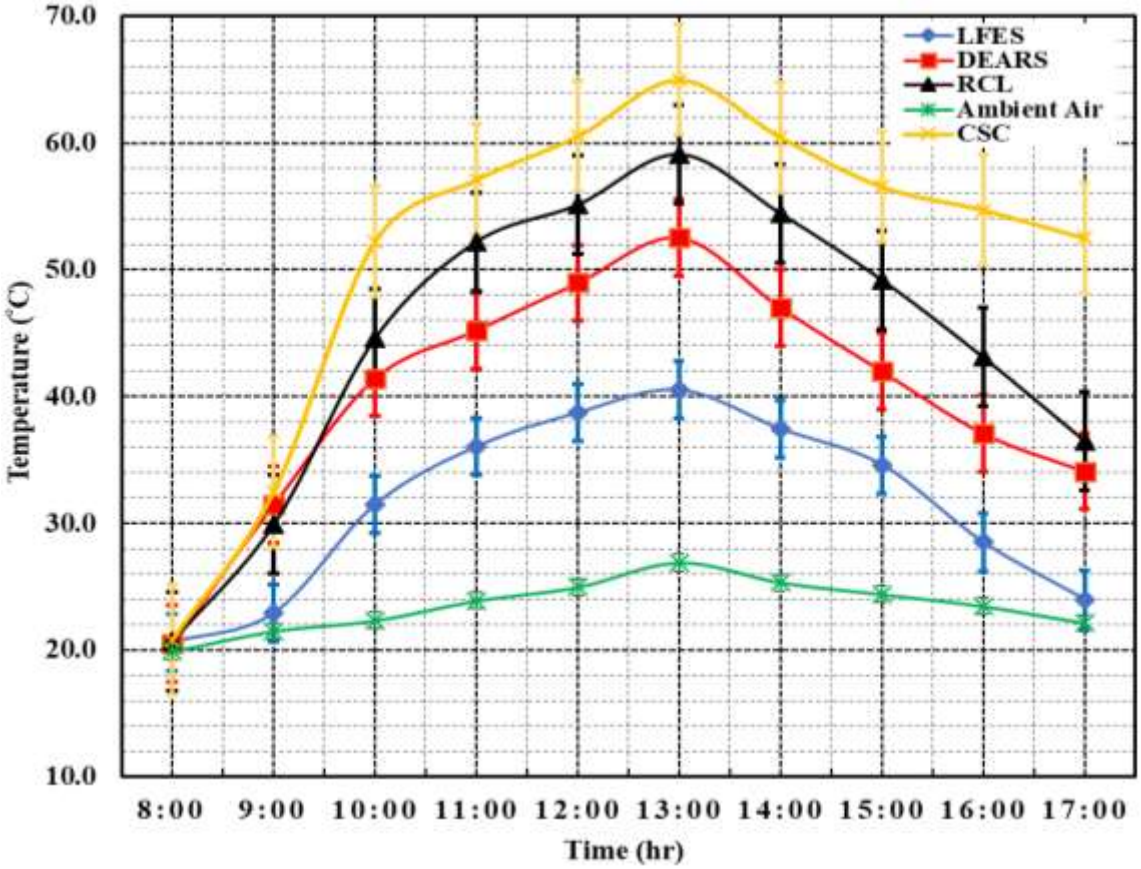

Figure 5-3: Solar collector hourly temperature variation with time

The combined solar collector configuration (CSC) had significant improvement in maintaining higher temperatures within the solar collector as indicated by the combined curve and does not drop significantly after the maximum temperature hour (13.00 hrs.). Higher temperature values can first be attributed to the effect of maintaining the high temperatures achieved by the effect of radiation concentration lenses during maximum solar radiation hours and the recirculation of every pass into the collector chamber. Similar observation was reported by Al-Neama and Farkas (2018) where recirculation solar collector had higher temperatures because of the effect of second pass heat transfer. Secondly, the superabsorbent polymer desiccant in the regeneration conduit dehumidifies and maintains temperatures of the warm exhaust to be reheated into the solar collector.

Figure 5-4 showed that average hourly temperatures increased with increased insolation up to 13:00 hrs. and thereafter decreased. Temperature variation during the solar collector testing experiment in both the data logger sensors as verified by the testo-445 probe had rising values with maximum temperatures at 13.00 hrs. This was the common trend on the effects of RCL, LFES, DEARS, CSC and the ambient values. However, the effect of collector CSC recorded the highest maximum temperature values at the maximum insolation (13:00hrs) of 65°C at which solar insolation was maximum and does not drop significantly thereafter. The corresponding maximum temperatures at 13:00 hrs for collector configurations under lenses, regeneration, fins and ambient conditions were 59.1°C, 52.5°C,40.5°C and 26.9°C respectively. Studies by Bolaji *et al*. (2005) reported maximum temperatures of 57°C inside a designed solar air collector at maximum ambient temperature 33.6°C.

The average temperature for CSC configuration was 51.23°C. The corresponding average temperatures for RCL, DEARS, LFES and Ambient conditions were 44.48°C, 40.03°C, 31.47°C, and 23.48°C respectively.

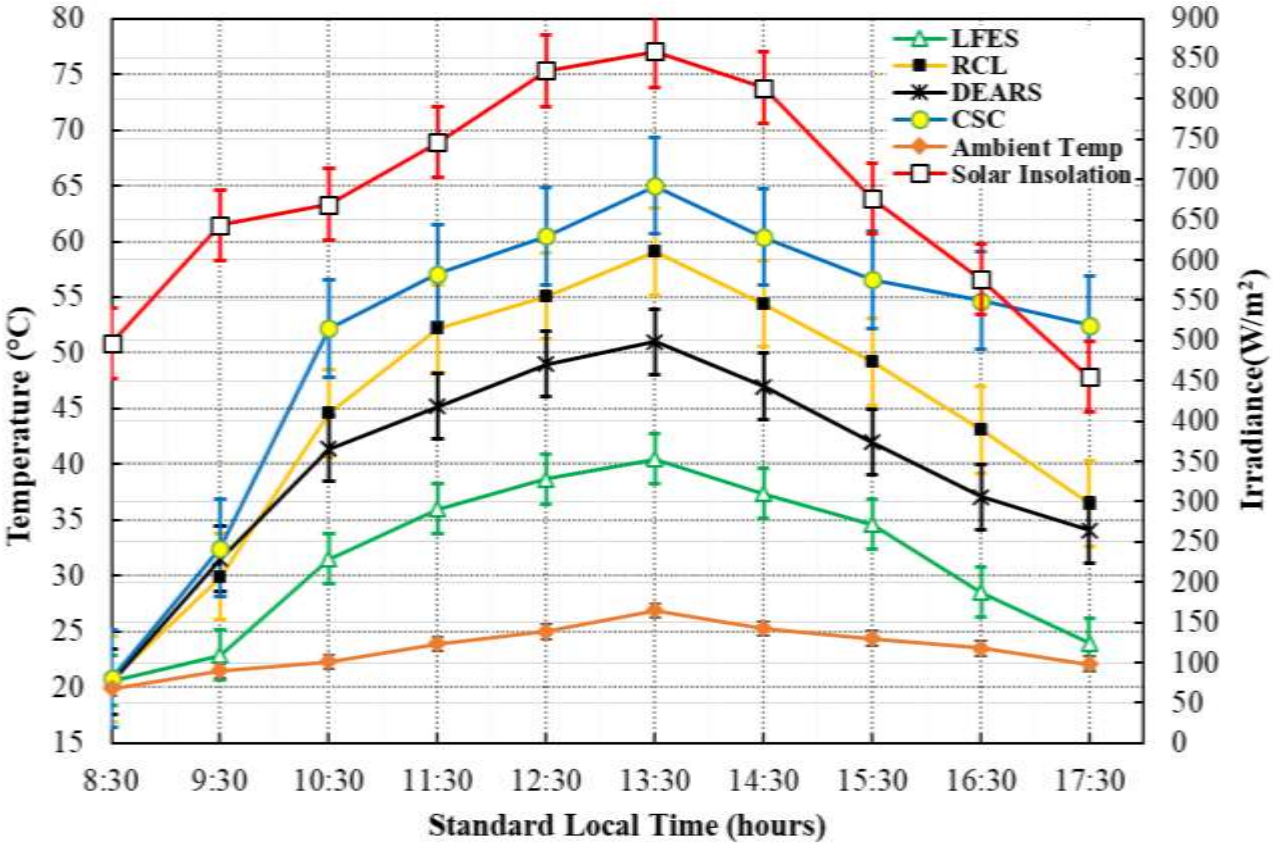

Figure 5-4: Solar collector temperature variation with insolation

Similar work by Hossain *et al*. (2008) tested and performed experiments on hybrid solar drying system and recorded substantial high collector temperatures of 60°C with daytime temperature change of 30°C.

It is very clear that the temperature values of the collectors with regeneration are all initially high than other configurations which was attributed to the effect of second and subsequent pass heat transfer. This scenario is maintained for the combined configuration. However, the temperatures of the configuration with the effect of radiation concentration using lenses rises significantly as solar radiation intensity increases to surpass the configuration that had only exhaust regeneration with no radiation concentration. This observation was maintained during the rest of the experimental time period.

From the hourly average temperatures (Figure 5-4) the CSC configuration maintained significant high temperature and does not drop significantly in response to changing ambient conditions and solar radiation after 14:00 hrs compared to the other setups as observed earlier (Figure 5-4). This was attributed to the effect of recirculation of every pass through the desiccant dehumidifier conduit and reheating of the same air pass. Aravindh and Sreekumar (2014) and Bagheri *et al.* (2015) reported a similar effect on the use of solar concentrators to raise the temperature of the circulated air above the ambient temperature. Desiccant dehumidification was well presented by Padmanaban *et al.* (2017) to control relative humidity of the feed air flow.

5.2.2 Relative humidity profile of the solar collector

The variation of relative humidity with time in the four solar collector configurations is shown in Figure 5-5. During the day the measured relative humidity in the solar collectors decreased with increase in temperature up to 13:00 hrs and thereafter declined. The general trend of relative humidity curves was a drastic decrease from the morning to the noon and rises in the afternoon with some fluctuation due to aspects of variation weather.

As shown in Figure 5-5 the relative humidity differences were very close at the beginning and had a wide range at the end of the experiment. This was due to increasing ambient relative humidity of the incoming air and low absorbing surface temperature due to reduced solar insolation.

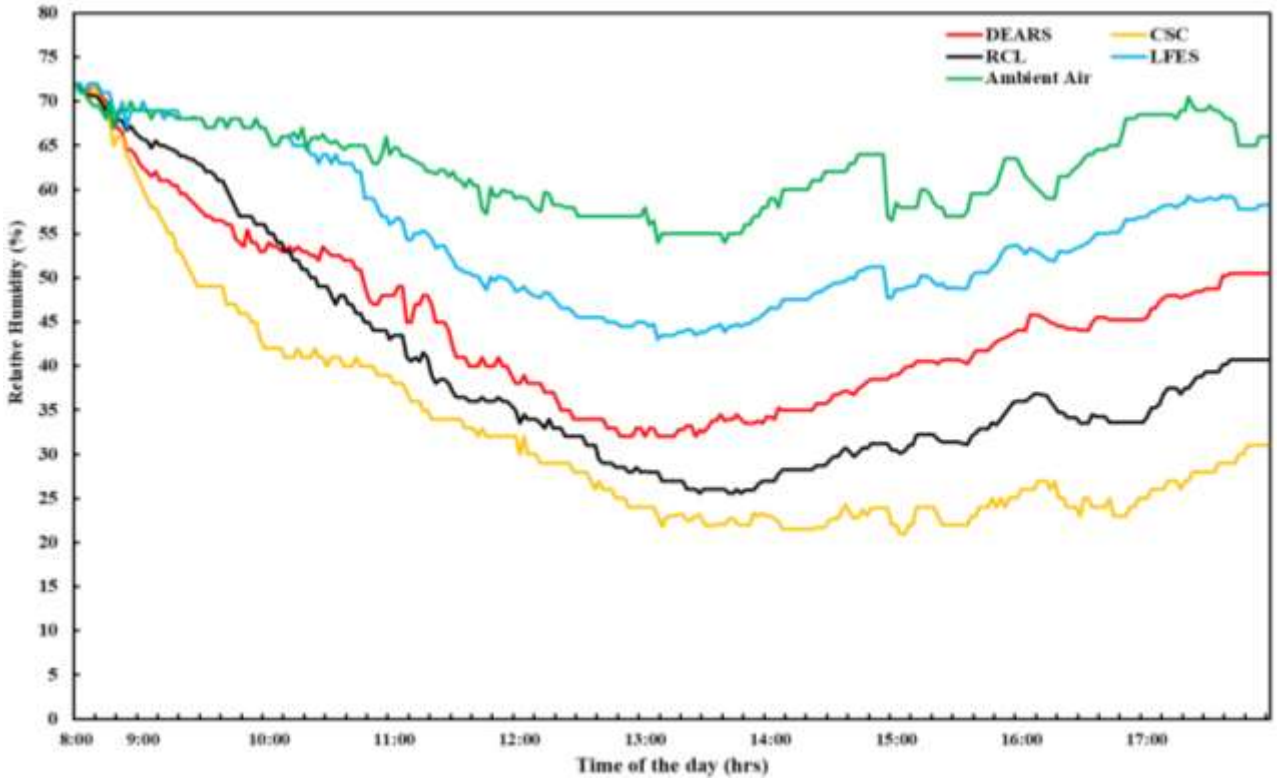

Figure 5-5: Relative humidity profile of the solar collector

The minimum values of relative humidity at 13:00hrs were; 57%, 47%, 32%, 35% and 27% for ambient, LFES, RCL, DEARS and CSC respectively. There was a decrease in relative humidity values to a minimum of 27% for the CSC at the 13:00hrs during which maximum solar radiation was observed earlier. However, these values increased significantly with up to 68% for the ambient control experiment after 14:00 hrs. as shown in Figure 5-6. This was attributed to increased temperature with solar irradiance such that the amount of water vapours that the air could hold increases, so that the relative humidity decreased and vice-versa.

During the day the measured relative humidity decreases inside the solar collectors, as the temperature of air between the absorber and the back plate increased. However, in the afternoon from about 13:30hrs, the absorber plate cools and the relative humidity of the air in gap begin to increase. Similar solar dryer experiments by Shazibuddin *et al.* (2016) reported a decreasing relative humidity with increasing temperature until 14:00hrs and then increase due to addition of moisture in the atmosphere and decrease in temperature.

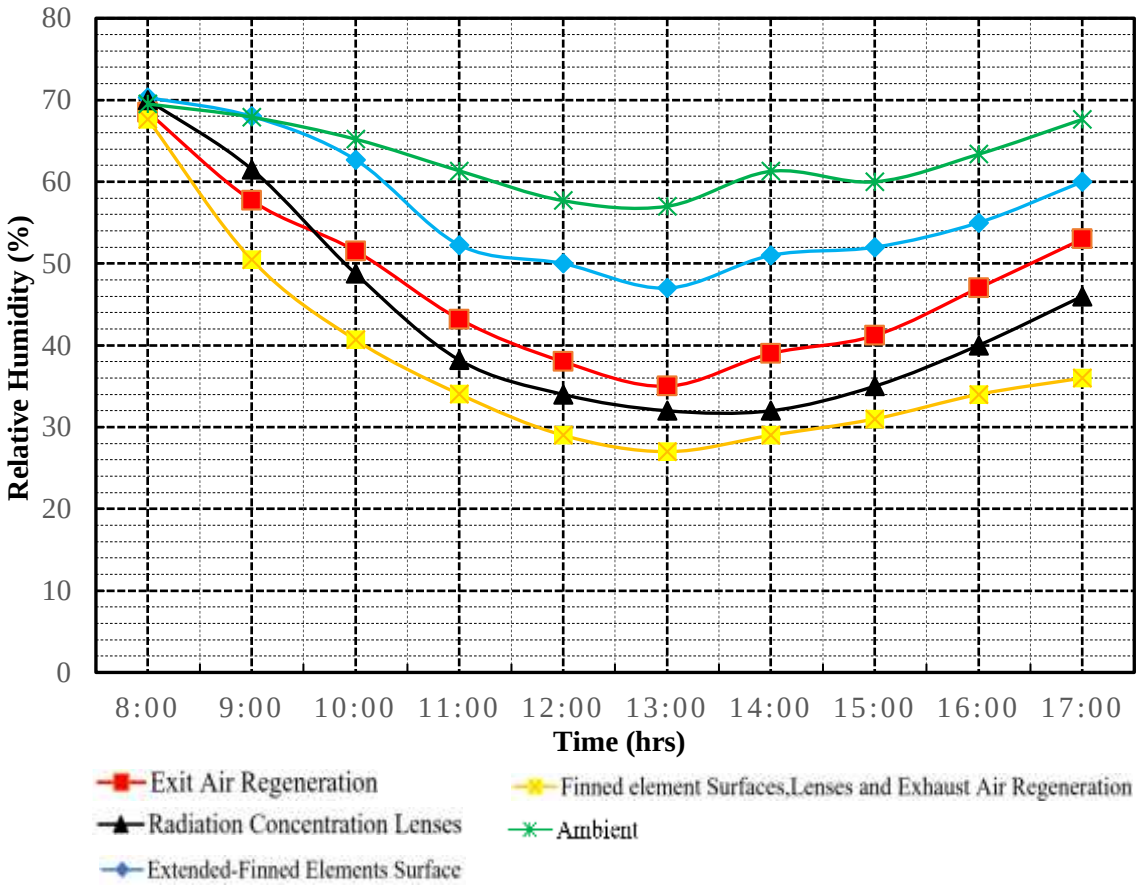

Figure 5-6: Hourly relative humidity variation with time in the solar collector

The set up with combined radiation concentration lenses, finned element surfaces and exhaust regeneration system maintained lower relative humidity values after the maximum solar insolation hour compared to the other setups. This was due to the effect of desiccant dehumidification and high temperatures achieved earlier by radiation lenses.

5.2.3 Temperature and relative humidity variations

Figure 5-7 shows that the maximum average hourly ambient temperature and the corresponding minimum relative humidity were 27 and 58 at 13:00 hrs. respectively. The figure shows a decrease in average hourly relative humidity with a rise in temperature for each of the solar collector configuration. However, this effect was most significant in the collector integration of finned elements, lenses and exhaust regeneration. The moisture holding capacity of air depends on the air's temperature and increases with increase in temperature. As the moisture holding capacity increased the relative humidity decreased, provided no moisture was added to the air. Similar studies by Al-Neama and Farkas (2018) reported trends of decrease in relative humidity with increase in temperature with fluctuations in the afternoon due to sporadic atmospheric conditions that affected the temperature variations of air.

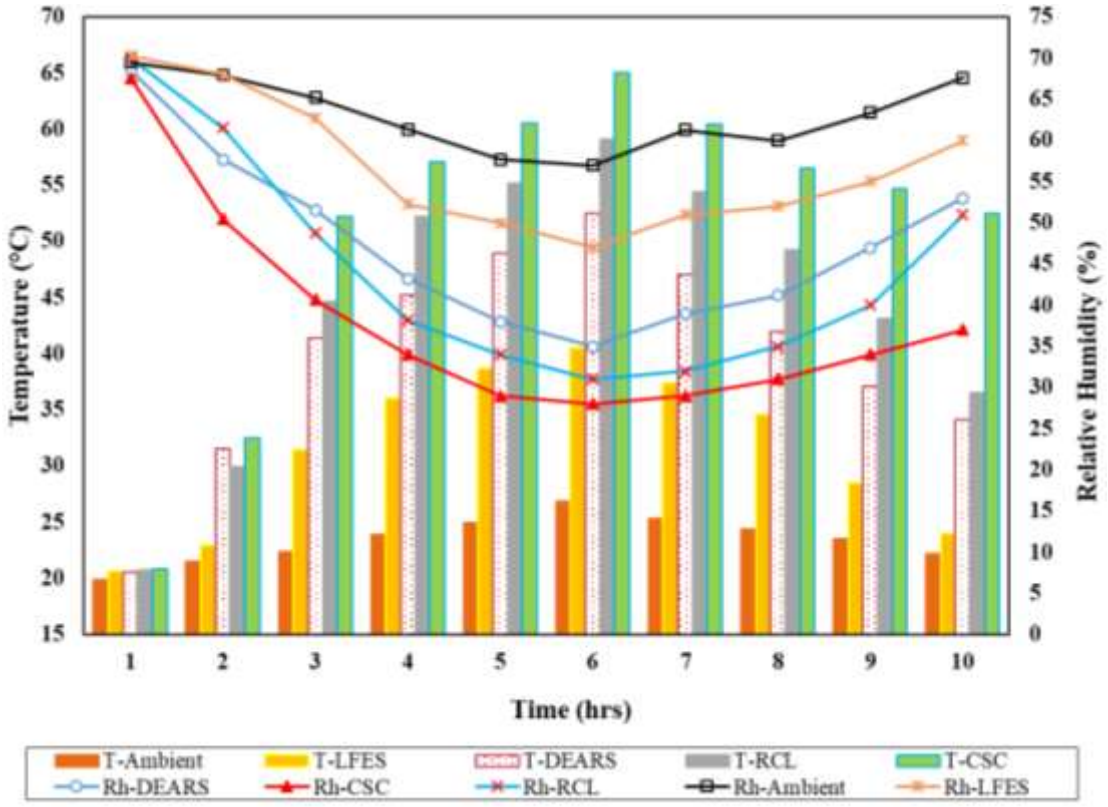

Figure 5-7: Temperature and relative Humidity profiles of the solar collector

While radiation concentration lenses played a significant role in raising the temperatures and lowering the relative humidity values in the solar concentrator at the 6th hour (13:00hrs), the effect of exhaust air regeneration was significant during recession of solar radiation (from 14:00 hours). This relates to low relative humidity values recorded after 13:00hrs for the combined collector configuration. Increase in temperature within the solar collector decreased the relative humidity either due to increase in solar insolation during the early hours before noon and later because of waste heat recovery and exhaust air desiccant drying effect of the superabsorbent polymer.

5.2.4 Temperature change

Figure 5-8 shows the changes in temperature from ambient conditions for various solar collector configurations. The maximum changes in temperatures were at 13:00 hrs. During this time the combined collector set up with finned elements, exhaust air regeneration and radiation concentration lenses recorded the highest values of change in temperature of 38^{o}C from ambient conditions. This collector had the maximum average change in temperature of 28°C for the whole experimental period of 10 hours. The average changes for other collector

configurations were 8°C, 17°C and 21°C for finned elements, exhaust regeneration, and radiation concentration lenses respectively.

Vlachos *et al.* (2002) reported a change of approximately 10-20°C in the air leaving the solar collector during experimental testing of a newly designed solar tray dryer. Hossain *et al.* (2008) reported a change of 30°C while testing a hybrid solar drying system. Moreover, Bolaji (2005) reported a change of 23.4°C heating temperatures inside a dryer from ambient temperature throughout the daylight in a developed solar dryer consisting of solar collector and drying chamber with no desiccant exhaust regeneration conduits.

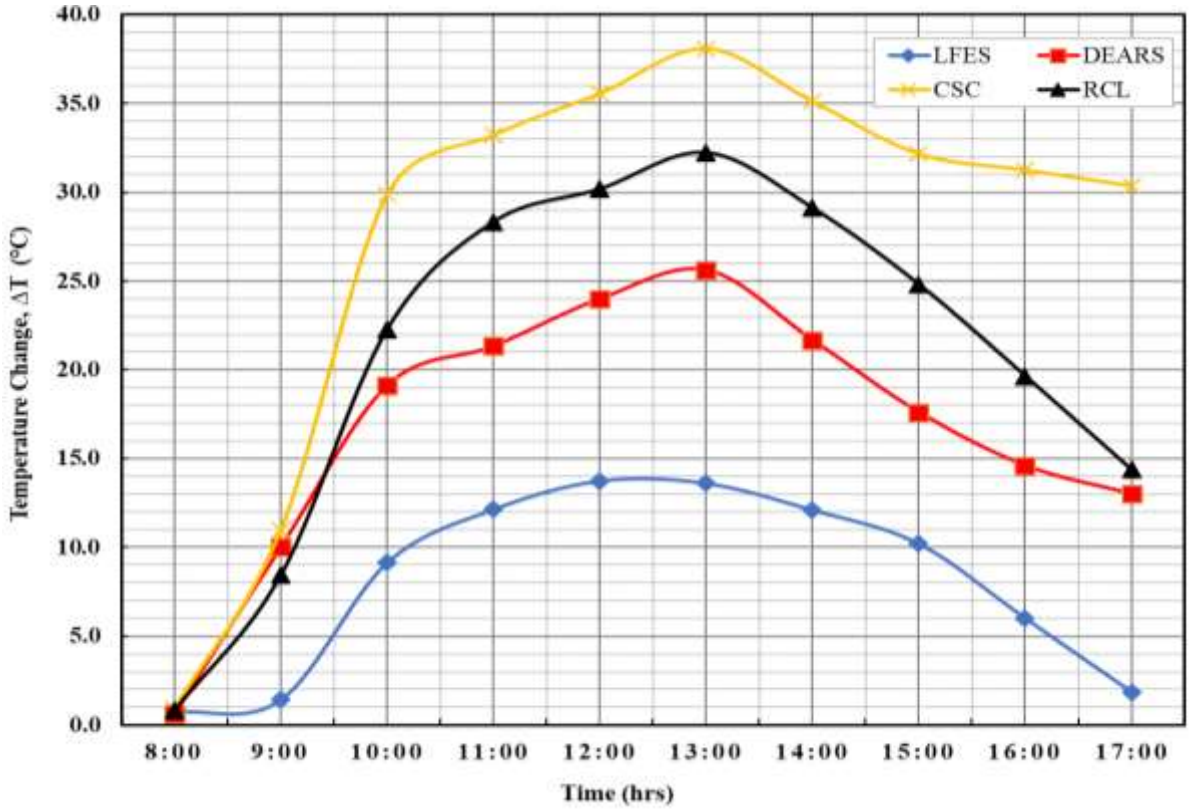

Figure 5-8: Temperature changes from ambient within the solar concentrator

5.2.5 Change in relative humidity

Figure 5-9 shows the changes in relative humidity of drying air for different solar collector configurations from ambient conditions. The magnitude of change in the decreasing relative humidity rises with time up to 13:00hrs after which the magnitude of the changes declines attributed to decline in collector plate temperatures resulting from changing radiation. The change in relative humidity was directly corelated to temperature. A similar observation was reported by Hanif e*t al.* (2014) where changes in relative humidity readings were highest at maximum temperatures in a solar thermal collector assembly. As observed earlier, a rise in

temperature resulted in a decrease in relative humidity since the moisture holding capacity of air is depends on the air temperature. As the moisture holding capacity increased the relative humidity decreased, since no moisture was added to the air.

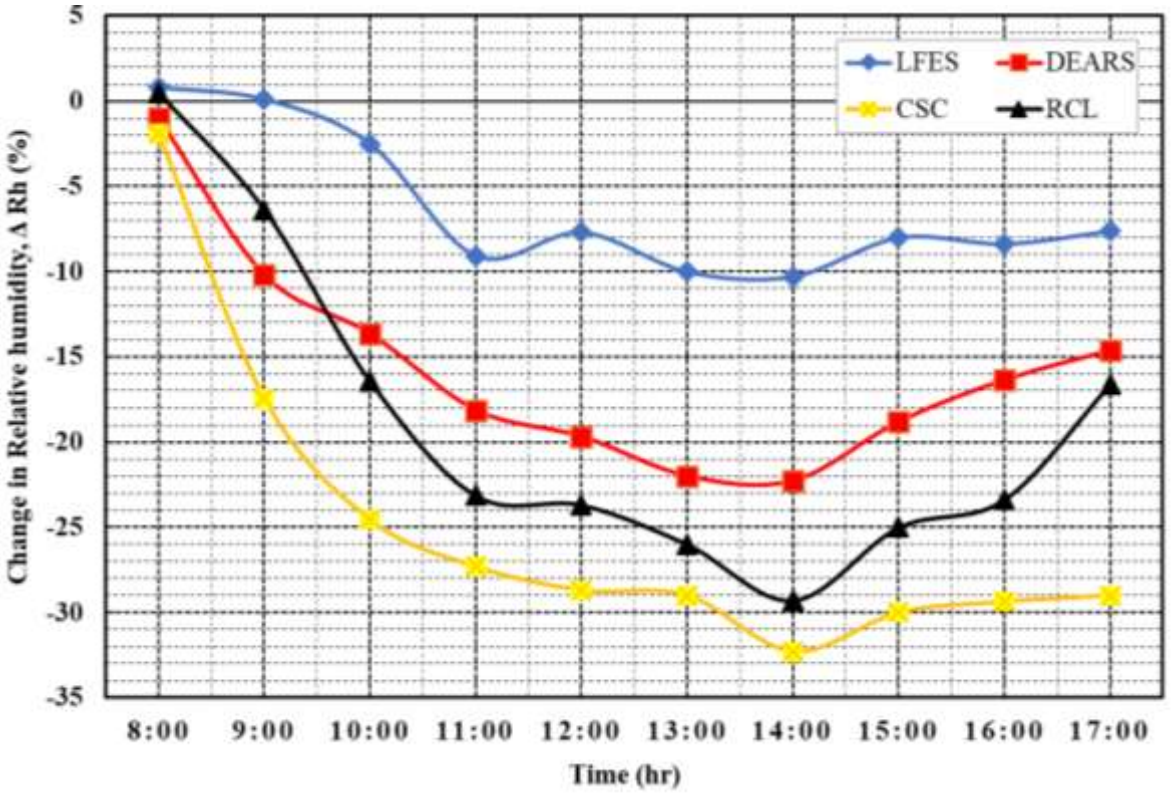

Figure 5-9: Changes in relative humidity values with time

Figure 5-8 and 5-9 showed that increasing air temperature for all the solar collector configurations resulted in a decrease in relative humidity. This relates to the fact that the moisture holding capacity of air depends on temperature. Furthermore, as the moisture holding capacity increased the relative humidity decreased, since no moisture was added to the air. Temp (2011) stipulates that a rise in air temperature results in a decrease in relative humidity, regardless of whether water vapor has been removed. The combined collector achieves the highest values of temperature at lowest values of relative humidity.

Figure 5-10 presents the changes in temperature with corresponding change in relative humidity. The maximum temperature change between the solar collector and ambient air were reached at maximum radiation intensity values of about 859 W/m^2 at 13:30hrs. However, except for the combined collector (CSC) these values fluctuated significantly for the other configurations as a result of ambient air temperature and radiation instability due to sporadic clouds. The temperature difference (ΔT) and change in relative humidity (ΔRh) through solar

collector increased indirectly with the time of day and radiation intensity (Figure 5-13). A similar scenario was reported by El-Sebaii *et al*. (2011), Prasartkaew and Kumar (2014) and Al-Neama and Farkas (2018).

The collector set up with combined finned elements, exit air regeneration and radiation concentration lenses recorded the most significant change in temperature and Relative humidity (38 ^{o}C and 32 %) respectively from ambient conditions at maximum insolation hour. The average changes were highest at 28 °C and 25 % during the experimental test period of 10 hours. This was attributed to the waste heat recovery and the constant enthalpy effect of desiccant polymer in the recirculation conduits.

The maximum change in relative humidity for the combined collector at (14:00 hrs) were not exactly at the same times of maximum temperatures (13:00 hrs). This further indicates that the combined configuration maintained appropriate air-drying conditions after the maximum radiation hour. A similar effect was reported by Al-Neama and Farkas (2018) using double pass solar air collectors.

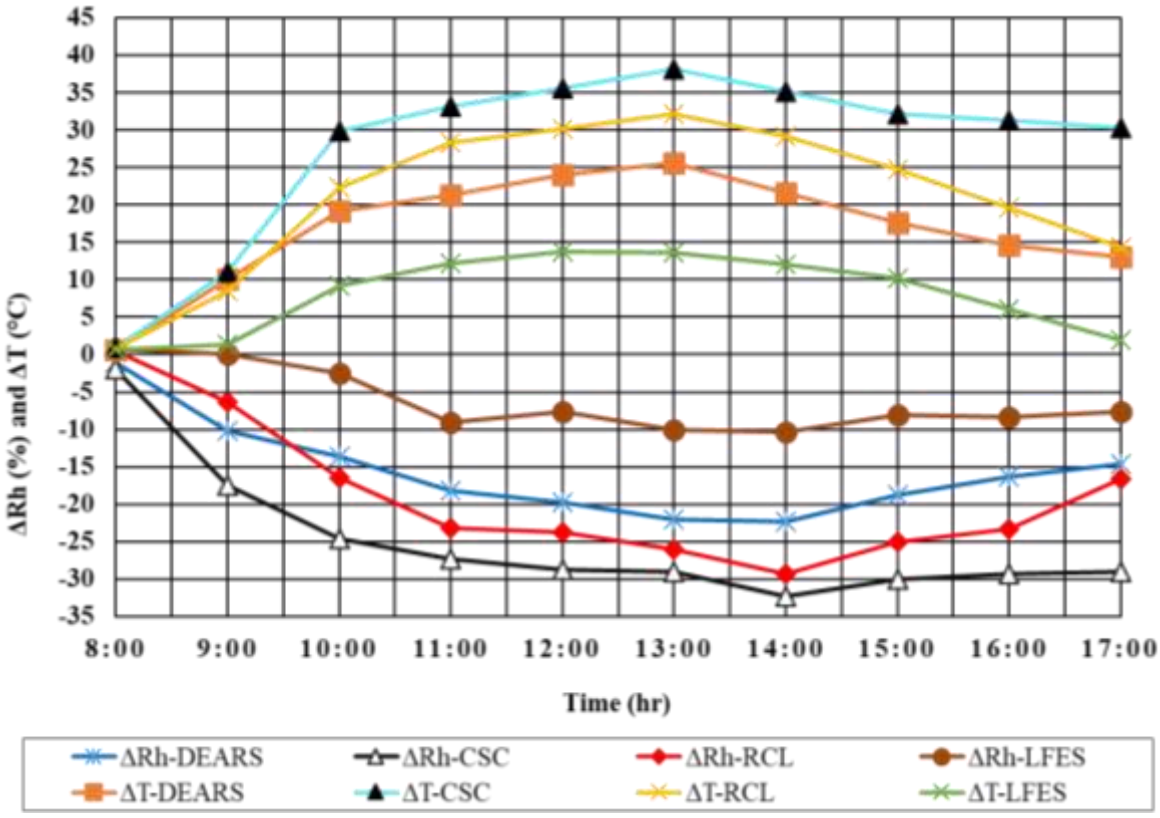

Figure 5-10: Changes in humidity values and temperatures in the solar collector

Figure 5-11 shows a plot of changes in temperature with the magnitude of changes in relative humidity. The slope of the curves indicates the rates of change in temperature differences with

changes in relative humidity. The slope is highest in the radiation concentration lenses configuration (0.8836) due to instantaneous sudden rise and fall of air temperature and relative humidity followed by collectors with exhaust regeneration effect alone (0.8441). This relates to the effect of changes in magnitude of radiation concentration at the collector plate with changing sunshine intensity.

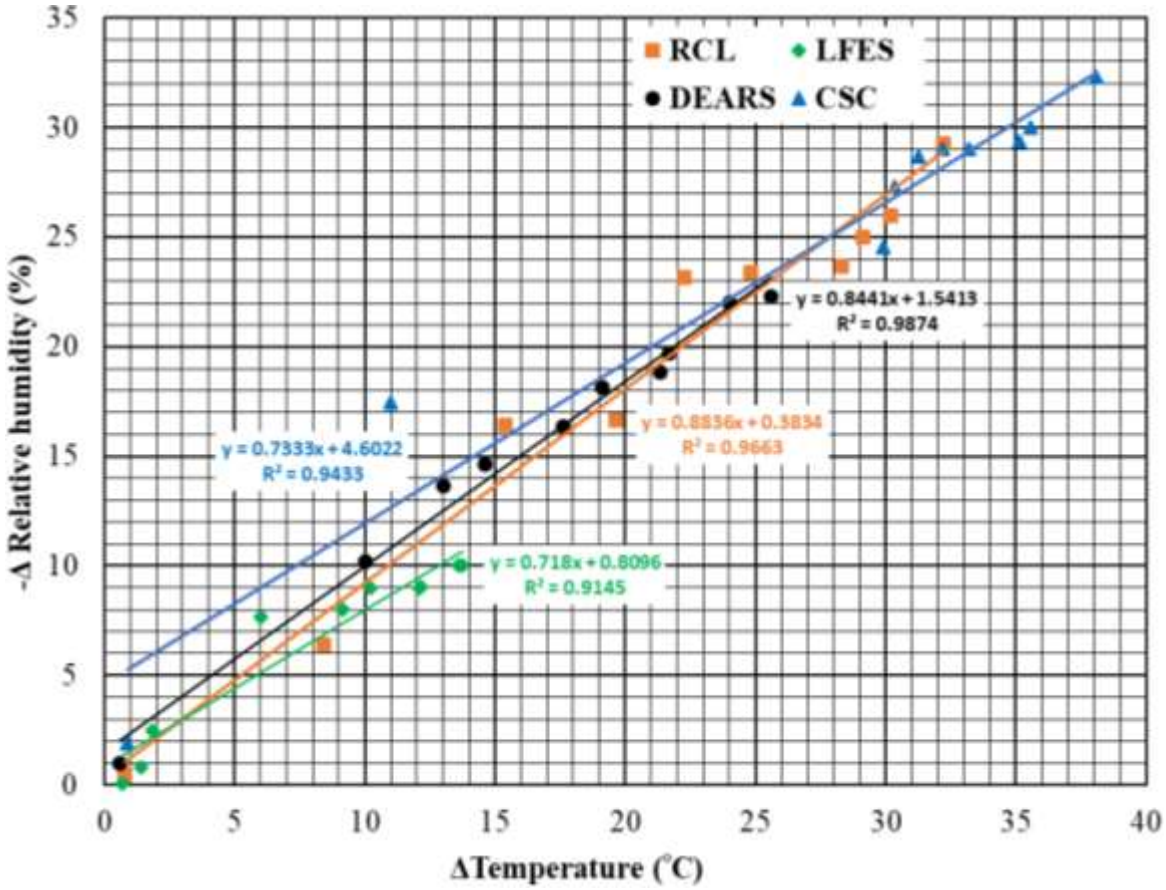

Figure 5-11: Effect of collector configuration on temperature and magnitude of relative humidity changes

Finned elements configuration had the lowest rate of change in temperature differences and relative humidity (0.718). This shows that increased surface area by the effect of dense finned elements maintained uniform conditions without drastic changes to air temperature and relative humidity although at undesirable lower values. Under these constraints Figure 5-11 shows that the combined collector with fins, regeneration and lenses achieved highest performance by maintaining high values of changes in temperatures and relative humidity under similar experimental conditions and at a lower rate of change of condition of heated air with sudden changes in external conditions (0.7333). Thus, the combined collector configuration improved on performance by maintaining high values of change in temperature and relative humidity

without undesirable interruption and sudden changes with changing insolation and other external conditions. This collector maintained the drying conditions as reported earlier without drastic changes after the maximum insolation hour.

5.3 Solar collector performance analysis

The changes in temperatures drying air from various solar collector configurations were used to analyse useful heat gained by the air as well as solar collector efficiencies. Detailed thermal performance equations, efficiency formulas and calculations done are explained and outlined in Appendix W and the results tabulated in Tables 8-8 to 8-12.

5.3.1 Solar insolation and collector temperature changes

Figure 5-12. represent the changes in solar collector temperatures with insolation for various collector configurations. Temperature difference (ΔT) through solar air collector increased with increase in solar insolation. Similar observation was reported by Kareem *et al.*, (2016), Al-Neama and Farkas, (2018) and Yang *et al.*, (2012).

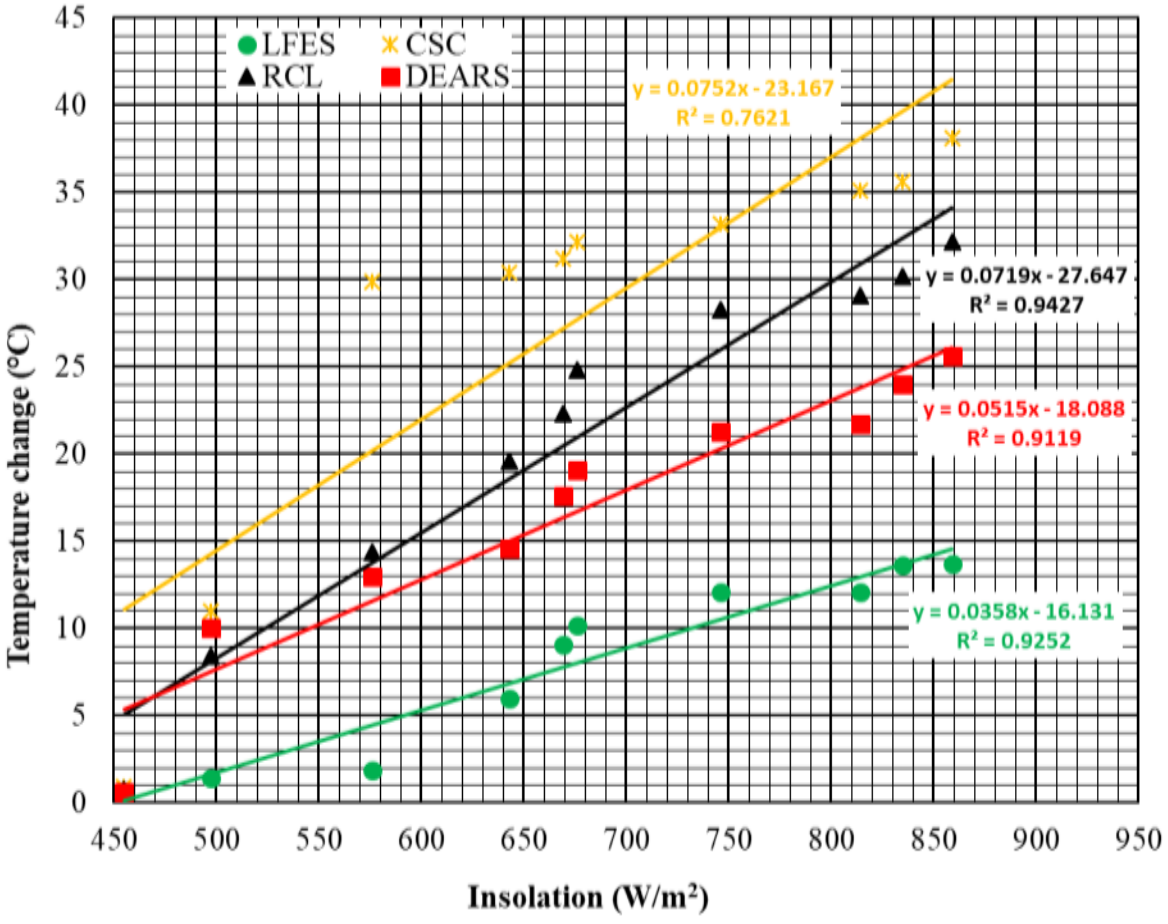

Figure 5-12: Insolation versus temperature changes for various collector configurations

The slope of the curves from figure 5-12 shows that the rate of change of temperature differences with insolation was maximum in the combined setup with lenses, fins and exhaust air regeneration (0.0752) compared to 0.0358 for finned elements setup alone.

This showed that the temperature differences in the combined solar air collector were more significant than the other solar collectors at the equal insolation values. The curves behaviour agreed with the results of many studies (El-Sebaii *et al*., 2011; Prasartkaew and Kumar, 2014).

5.3.2 Solar collector useful heat gain

The useful heat energy had different values for the various solar collector configurations as a result of differences in irradiance as shown in Table 5.1. The collector's useful energy gain increased with the time of the day till it reaches the maximum value at 13:00hrs (maximum insolation hour), then it declines when the values of solar irradiance decreases. However, the combined collector useful heat does not drop drastically after the maximum radiation hour as compared to other configurations as shown in Figure 5.13. The highest levels of useful heat gained was between 1230hrs and 1330 hrs because of the high solar radiation intensity and solar collector changes in temperatures as reported earlier.

Table 5.1: Solar collector useful energy with irradiance

Time (hrs.)	**Solar irradiance (W/m^2)**	**Useful energy absorbed, MCpΔt (kJs)**							
		LFES		**DEARS**		**RCL**		**CSC**	
		ΔT	MCP ΔT	ΔT	MCP ΔT	ΔT	MCP ΔT	ΔT	MCP ΔT
8:00	497	0.7	0.005	0.6	0.005	0.8	0.006	0.9	0.007
9:00	643	1.4	0.011	10	0.076	8.4	0.064	11	0.083
10:00	669	9.1	0.069	19.1	0.145	22.3	0.169	29.9	0.227
11:00	746	12.1	0.092	21.3	0.162	28.3	0.215	33.2	0.252
12:00	835	13.7	0.104	24	0.182	30.2	0.229	35.6	0.270
13:00	859	13.6	0.103	25.6	0.194	32.2	0.244	38.1	0.289
14:00	814	12.1	0.092	21.7	0.165	29.1	0.221	35.1	0.266
15:00	676	10.2	0.077	17.6	0.134	24.8	0.188	32.2	0.244
16:00	576	6	0.046	14.6	0.111	19.6	0.149	31.2	0.237
17:00	455	1.9	0.014	13	0.099	14.4	0.109	30.4	0.231
Average	677	8.1	0.061	16.8	0.127	21.0	0.159	27.8	0.211

Figure 5-13 shows plot of useful energy with time of the day. The maximum value of useful heat gained was 0.103kJs, 0.194kJs, 0.244kJs, and 0.289kJs respectively for fins, regeneration, lenses and the combined collector respectively at the 13:00hrs. Similar trend was reported by Al-Neama and Farkas (2018) where they reported highest useful heat of 0.328kJs (328 W/m^2) at solar insolation of 1017 W/m^2 and highest levels of solar collector temperature differences at the highest insolation hour of 12:00 hrs-13.00 hrs for a solar air collector. Proszak-Miąsik

and Rabczak (2017) stated that the most favourable conditions for solar collectors to receive solar energy are at Noon -13:00 hrs when the sun is at its zenith and when the sky is cloudless for sunrays to reach the collector without any obstacles and haze.

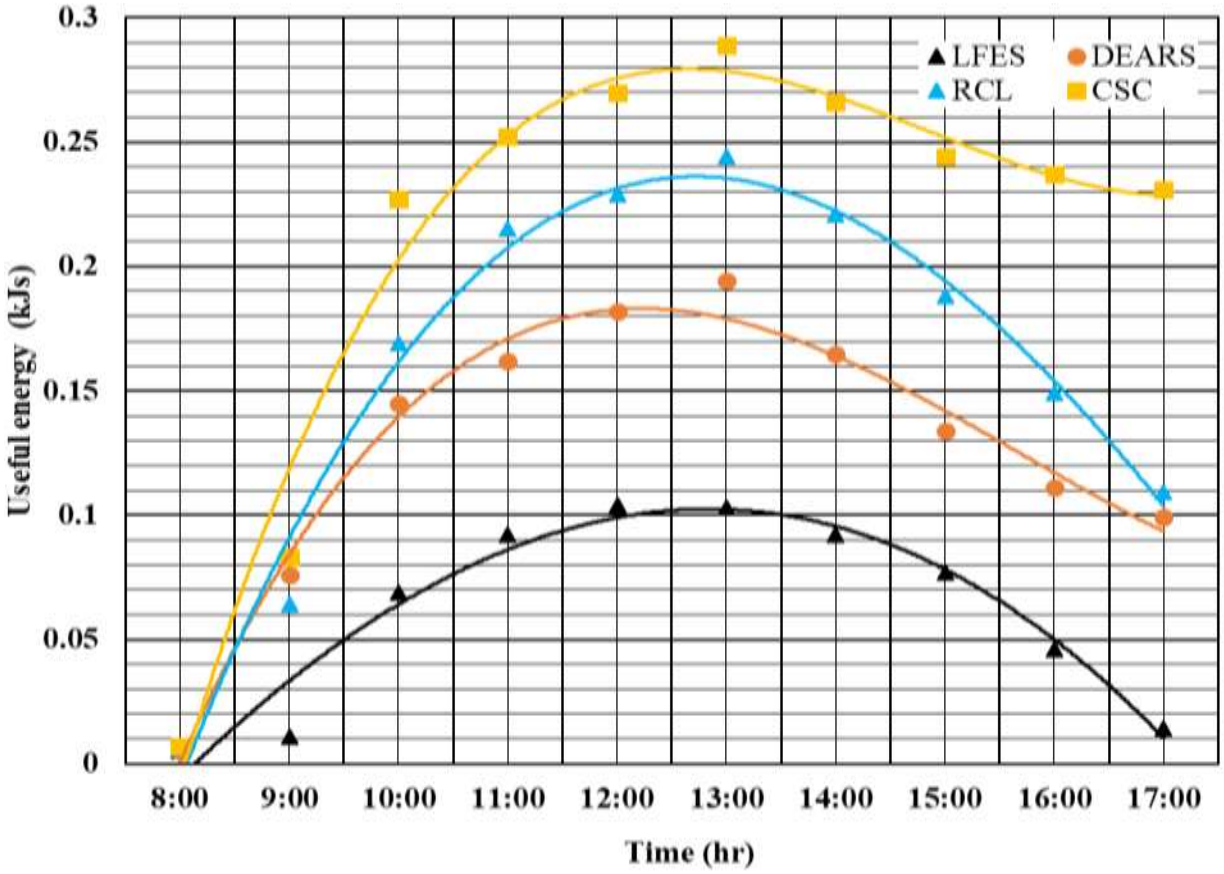

Figure 5-13: Useful heat gain with time for various solar collector configurations

5.3.3 Collector useful heat gain and insolation

Figure 5-14 shows that the useful heat obtained from the solar air collector was directly proportional to the values of solar insolation which were related and proportional to temperature changes through the collector as reported earlier. It seems that the behaviour of the useful heat gain with insolation was similar to the behaviour of change in temperature with insolation curves as reported earlier.

The results showed that the useful heat energy increased with the amount of solar insolation while the gradient of the curve of the combined collector with integration of lenses, fins and desiccant exhaust air regeneration had the highest rate of gaining useful heat energy with increase in solar irradiance as shown in Figure 5-14.

The useful heat increased to reach the maximum value of 0.289 kJs,0.244 kJs,0.19 kJs and 0.104 kJs for CSC, RCL, DEARS and LFES configurations respectively. This was the time of

maximum solar insolation (859W/m^2) and maximum temperature differences at 13:00 hour as reported earlier. A similar scenario was reported by Al-Neama and Farkas (2018) where two solar collectors studied reached maximum heat gain values of 0.1665kJs and 0.1122kJs at maximum insolation hour.

From Figure 5-14 the slope of the linear relations indicates that the rate of useful heat gain with respect to insolation values was highest in the combined collector (0.006) which had the effect of mult-pass recirculation of high temperature air and lowest for the finned elements surfaces configuration alone (0.0003). Studies by Al-Neama and Farkas (2018) reported that the useful heat gained by using double pass recirculation solar collector was significantly higher than the useful heat gained by using single-pass solar air collector.

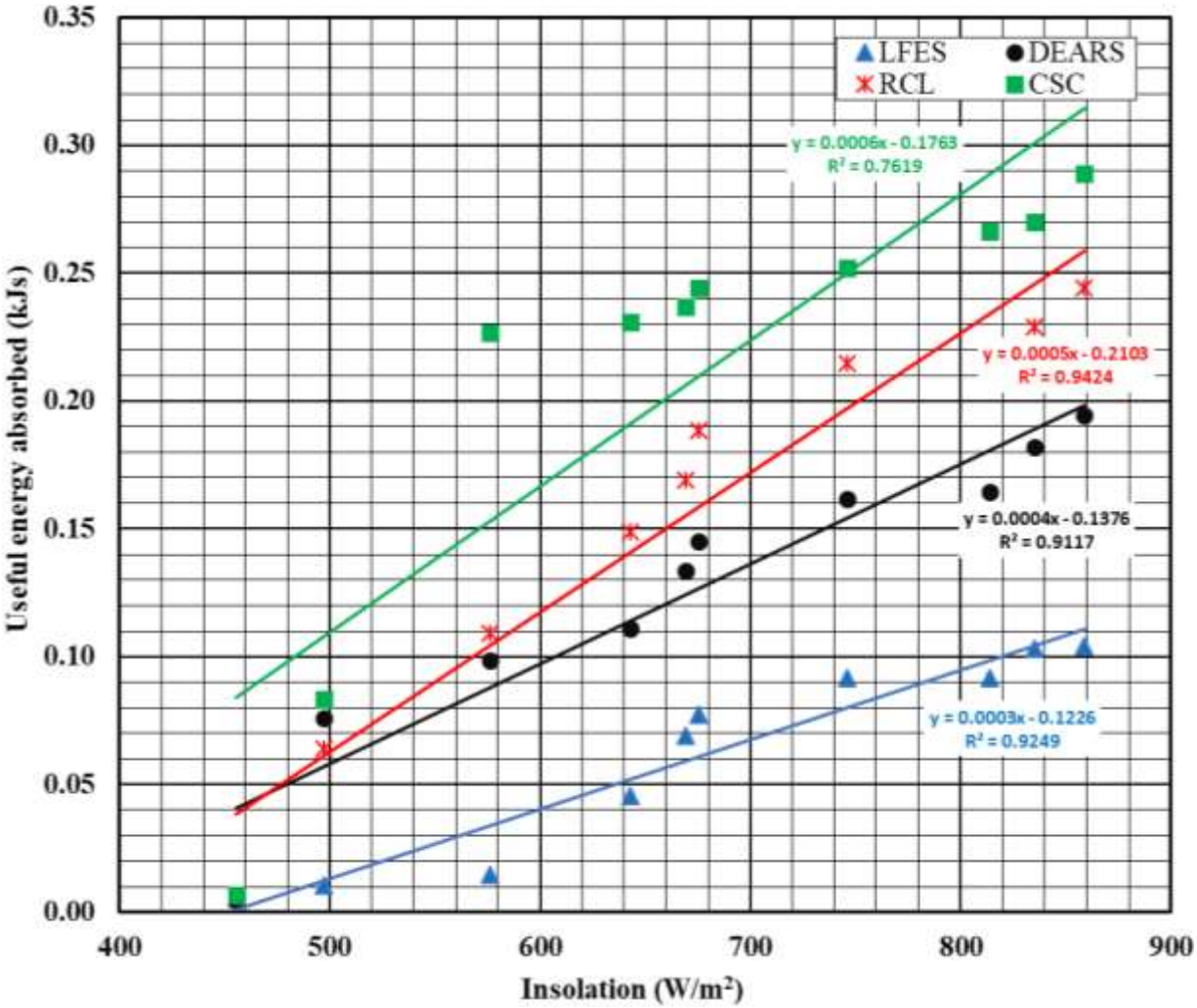

Figure 5-14: Variation of useful heat gain with solar irradiance.

Figure 5-14 showed that the useful heat gains were directly proportional to the solar insolation intensity which relates to proportional temperature changes through the collector various

collector configurations as reported earlier. Similar observation was reported by Al-Neama and Farkas (2018) and Nyariki *et al*. (2016). The combined collector configuration had highest values of useful heat increases to attain maximum values at the time of maximum temperature change in the collector.

In general, the useful heat obtained from the solar air collector configurations was directly proportional to solar insolation values with maximum values at 13:00-14:00 hrs, the time of maximum solar insolation and temperature changes from the solar collectors. Similar observation was reported by Al-Neama and Farkas (2018). Figure 5-14 showed that the useful heat increases to reach the maximum value 0.289kJs (289 W/m^2) at maximum solar insolation of 859 W/m^2 at the same time of maximum temperature differences for the combined collector.

5.3.4 Thermal efficiency of the solar collectors

Results indicated variability in solar collector efficiency values with time, amount of solar insolation, changes in heat gain as a result of temperature change and the type of solar collector configuration. Table 5.2 shows the averaged solar collector efficiency values for various configurations.

Table 5.2: Average efficiencies for various collector configurations

Solar Collector Configuration	Average Solar Collector Efficiency (Decimal)	Average Solar Collector Efficiency (%)
Longitudinal finned elements surfaces	0.167	17
Desiccant exhaust air regeneration	0.363	36
Radiation concentration lenses	0.452	45
Combined solar collector	0.608	61

The average efficiency was 17% for the finned elements collector configuration while lenses and regeneration had 45% and 36% respectively. The maximum average efficiency of 61% was obtained with the collector configuration with integrated fins, lenses and exhaust air desiccants regeneration conduits (EADRC). This was due to high temperatures and multi-pass recirculation of every pass into the solar collector for subsequent reheating.

Al-Neama and Farkas (2018) reported that using double pass (recirculation effect) solar air collector the efficiency was significantly higher than using single-pass solar air collector due to heat recovery. Similar observation was reported by Ramani *et al.* (2010) where thermal efficiency of double pass regeneration collector was found to be 10 % - 25 % higher than that of single pass solar collectors.

The superabsorbent polymer desiccant in the exhaust regeneration conduits provided a further mechanism of dehumidifying the exhaust air and further recirculation into the collector inlet. Investigations by Akpinar and Koçyiğit (2010) on the flat-plate solar air heater reported that efficiency varied between 20 % and 82 % with the highest efficiency for the solar air heater with an absorbent plate in the flow channel duct for all operating conditions.

As noted, the effect of regeneration has been found to have a significant positive effect on the efficiency due to recirculation of every pass which encouraged waste heat recovery as further reported by Al-Neama and Farkas (2018). The combined collector improved efficiency by a margin of 44%, 25% and 16% from the finned elements configuration, exhaust recirculation alone and radiation concentration lenses alone respectively.

Similar solar collector investigations reported that the double-action of air pass increased the daily thermal efficiency of solar air collector from 38.25 % to 45.56 % due to heat recovery from previous pass (Al-Neama and Farkas, 2018). Studies by Ahn *et al*. (2015) on the performance of photovoltaic/thermal (PV/T) solar air collectors coupled with heat recovery ventilation reported an overall efficiency of 38 %. Also, Ahn *et al.* (2015) reported improved heat transfer efficiency from heat recovery ventilation by about 20 % with pre-heat air from PV/T collector. Bolaji (2005) obtained maximum efficiency of about 60 % using box-type absorber solar air collector while those of flat plate absorber and fin type absorber were 21 % and 36 % respectively.

5.3.5 Solar collector efficiency and insolation

The efficiency of various solar collector configurations with the variation of solar insolation changes are as shown in Table 5-3. The efficiency curves fluctuation with solar insolation formed a similar trend with useful heat gain curve fluctuation against solar insolation as reported earlier. This shows the dependence of collector thermal efficiency on insolation and useful heat gained by solar collectors. The linear relations are of the form $y = mx + c$ and the slope of the indicated that the combined collector configuration had the highest rate of increase in efficiency with change in solar insolation.

Table 5.3: Irradiance and solar collector efficiency

Solar Irradiance (W/m^2)	**Efficiency**			
	LFES	**DEARS**	**RCL**	**CSC**
497	0.021	0.018	0.024	0.027
643	0.033	0.236	0.198	0.260
669	0.206	0.433	0.506	0.678

746	0.246	0.433	0.576	0.676
835	0.249	0.436	0.549	0.647
859	0.240	0.452	0.569	0.673
814	0.226	0.405	0.543	0.655
676	0.229	0.395	0.557	0.723
576	0.158	0.384	0.516	0.822
455	0.063	0.433	0.480	0.923

Figure 5-15 shows that the changes of radiation intensity influenced the efficiencies of various solar collector configurations. The efficiency increased linearly with solar insolation with the combined collector with the highest rate of change in efficiency with insolation as shown by the slope of the curves. Past research, experimental investigations and published results by researchers showed that solar collector efficiency increases with increasing solar radiation intensity (Aldabbagha *et al*., 2010; Ibrahim *et al*., 2013; Chabane *et al*., 2013; Umayorupagam *et al*., 2017; Sharma & Saha, 2017).

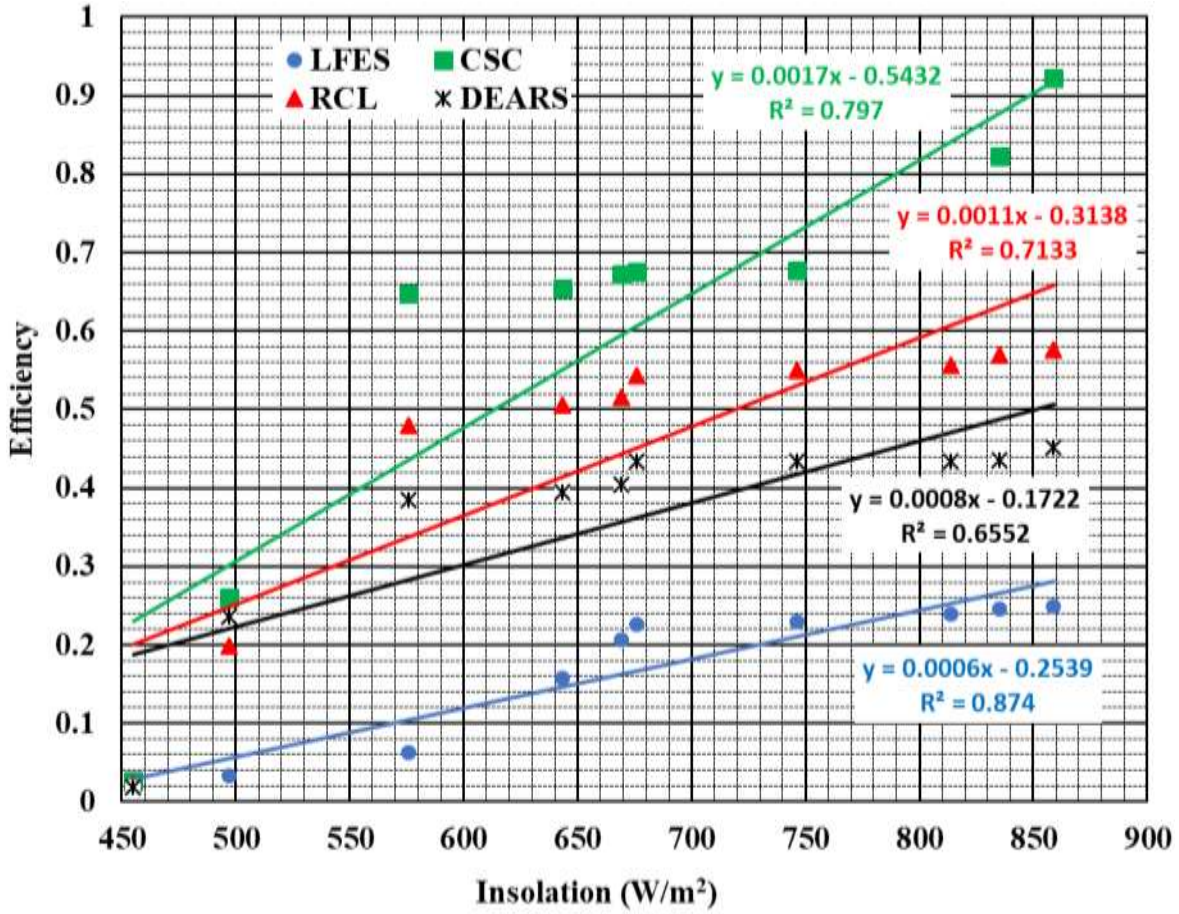

Figure 5-15: Effect of solar insolation on various collector configuration efficiencies

The effectiveness in air heating increased drastically with solar irradiance for the CSC collector (slope 0.0017) as shown in Figure 5-15. The rate of increase in efficiency was lowest in the

LFES collector (0.0006), RCL had 0.0011 while DEARS alone had a rate of efficiency gain with insolation of 0.0008. The rate of change in efficiencies with insolation increased with solar irradiance at the collector plate due to increased changes in temperature values from the ambient conditions.

Kareem *et al*. (2017) stipulated that the changes in insolation intensity have a significant influence on the efficiency of the collector installed in the system in question. Similar observation was reported by Akpinar and Koçyiğit (2010) in an experimental investigation of a designed flat-plate solar air heat collector where the efficiency was found to be dependent on solar insolation.

Al-Neama and Farkas (2018) reported increased efficiency as a result of improved useful heat gain by a solar collector as a consequence of increased temperature difference across the collector due to increased solar insolation intensity. As shown in Figure 5-15, the efficiencies increased with solar insolation at the collector plate which resulted from increase in changes of temperature values from the ambient conditions for all the collector configurations

5.3.6 Collector efficiencies and temperature changes

Figure 5-16 shows the instantaneous collector efficiencies as a function of change in temperature resulting from changing insolation for various collector configurations during the experiment. Efficiencies of the combined collector were higher compared to other solar collector setups due to high temperature changes. The gradient of the lines represents the rates of efficiency gain with change in temperature and are highest for combined collector (0.0218) and lowest for regeneration alone (0.0161).

Despite having low efficiency values the finned elements collector has high rate of efficiency gain per unit change in temperature (0.0175) compared to finned elements and radiation concentration lenses. This was attributed to interaction of air with increased heat transfer area by integrated high density of longitudinal finned elements. Moreover, the fins decelerated the movement of air in the collector due to turbulence and friction forces between flowing air and surface of fins which resulted to increased rate of heat transfer. This shows that integration of fins has a significant effect in increasing the rate of heat transfer to the air in solar collectors.

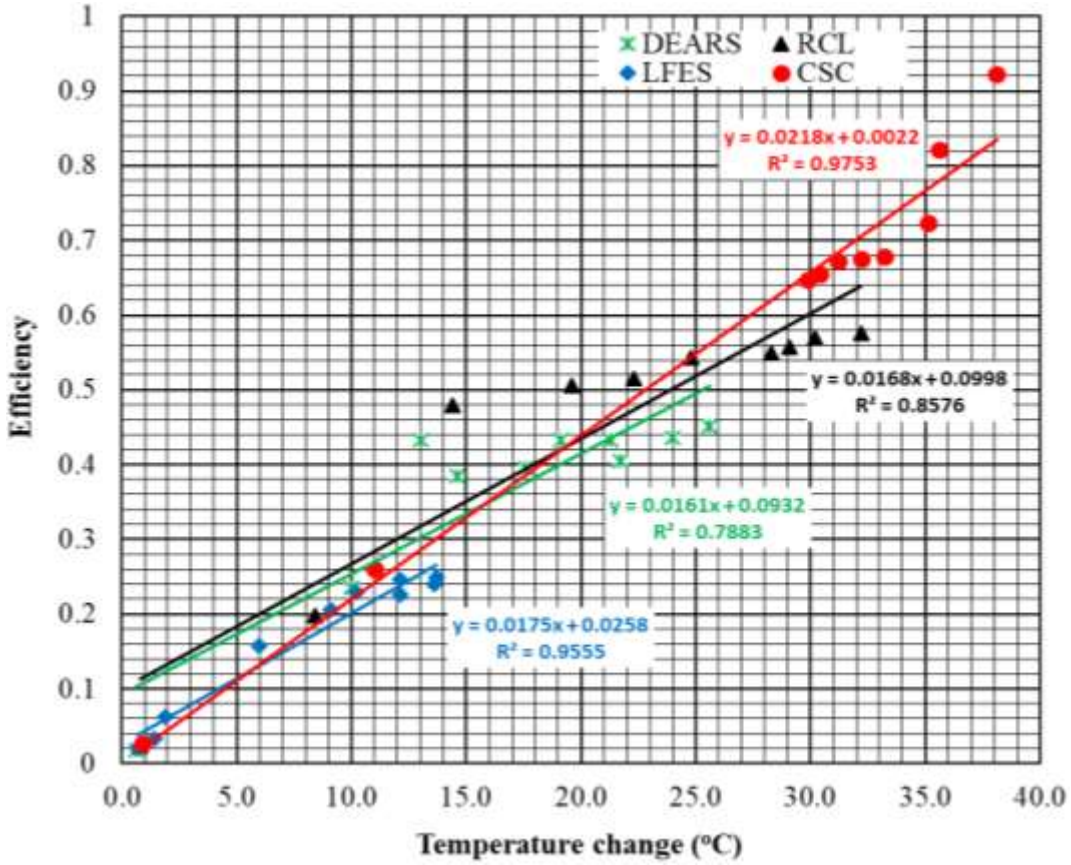

Figure 5-16: Effect of temperature changes on solar collector efficiency

Studies by Al-Neama and Farkas (2018) reported that the percentages of thermal efficiency of finned plate collectors were higher than flat plate collector without fins. Furthermore, the efficiency changes with temperature change values from finned collector configuration had a steady behaviour with a correlation coefficient of 0.9555, higher than regeneration (0.7883) and lenses (0.8576) while the combined collector had 0.9753 (Figure 5-16). Al-Neama and Farkas (2018) found that horizontal fins incorporated in a double-pass solar air heat collector had more steady behaviour in temperature changes than a flat plate double-pass solar heat collector without fins.

5.3.7 Collector efficiency and useful heat gain

Solar collector efficiencies were plotted as a function of the useful heat gain for various collector configurations during the experiment. Figure 5-17 shows that instantaneous efficiency of solar air collector fluctuated and varied linearly due to useful heat gain as a result of temperature variations reported earlier.

The efficiencies were higher for combined collector values because of the higher useful heat gains by the drying air. The thermal efficiency depends mainly on useful heat gained from

absorbing surface according to Equation 3.9 which as a result, depends on collector temperature rise drawn from subsequent increase in solar insolation as reported earlier. Studies by Al-Neama & Farkas (2018) forwarded a similar observation.

From Figure 5-17, the lowest value of efficiency (0.02) occurred at the lowest value of useful heat gain (0.005kJs) both for finned elements and recirculation and 0.06 kJs and 0.07 kJs for lenses and combined collectors respectively. The highest values of useful heat gained were 0.104,0.194,0.244 and 0.289kJs for collectors with fins, regeneration, lenses and the combined collectors respectively. Figure 5-17 shows that the solar collector efficiencies obtained were directly proportional to the values of useful heat gain as a result of temperature changes through the various solar collector configurations. However, the rate of change of collector efficiency with useful heat gain as indicated by the slope of the curves varied with the type of collector configuration. The combined collector had the highest positive rate of change of efficiency with useful heat gain as shown by the slope of 2.878.

The rate of efficiency gain with useful heat for fined elements collector configuration (2.3114) superseded lenses (2.2082) and regeneration alone (2.2046). Although lower values of efficiency were recorded in this collector, the rate of available unit heat transfer to the air was increased by the fins and thus high rate of efficiency gain per useful heat gain than the lenses and regeneration configurations. This was attributed to interaction of air with increased surface area from the high density of warm finned elements. Moreover, the fins improved interaction of air by increased pressure drop beneath the collector plate and decelerated the movement of air in the collector which increased collector rate of useful heat transfer to the air per unit temperature rise. Similar findings were reported by Al-Neama & Farkas (2018) and Bahrehmand & Amer (2015).

The turbulence and friction forces between flowing air and surface of fins increased the temperature of the air (Jacobi & Shah 1995). This confirms the observation reported earlier where finned collector had a higher rate of efficiency gain per unit temperature compared to lenses and recirculation alone. This proves that a compromise between the various collector configurations was necessary to optimise the efficiency of the solar dryer. Therefore, from the gradients of Figure 5-17 the higher rates of efficiency gain with useful heat gain (2.878) was obtained for the combined collector. This was due to solar radiation concentration resulting to high temperature changes; improved heat transfer rate to the air by fins; and heat retention by

the effect of recirculation through multi-pass desiccant exhaust regeneration conduits. This collector configuration had the highest average efficiency at 61%.

Research by Amer *et al*. (2010) established that recycling of drying air can improved the dryer performance in the neighborhoods of 65%.

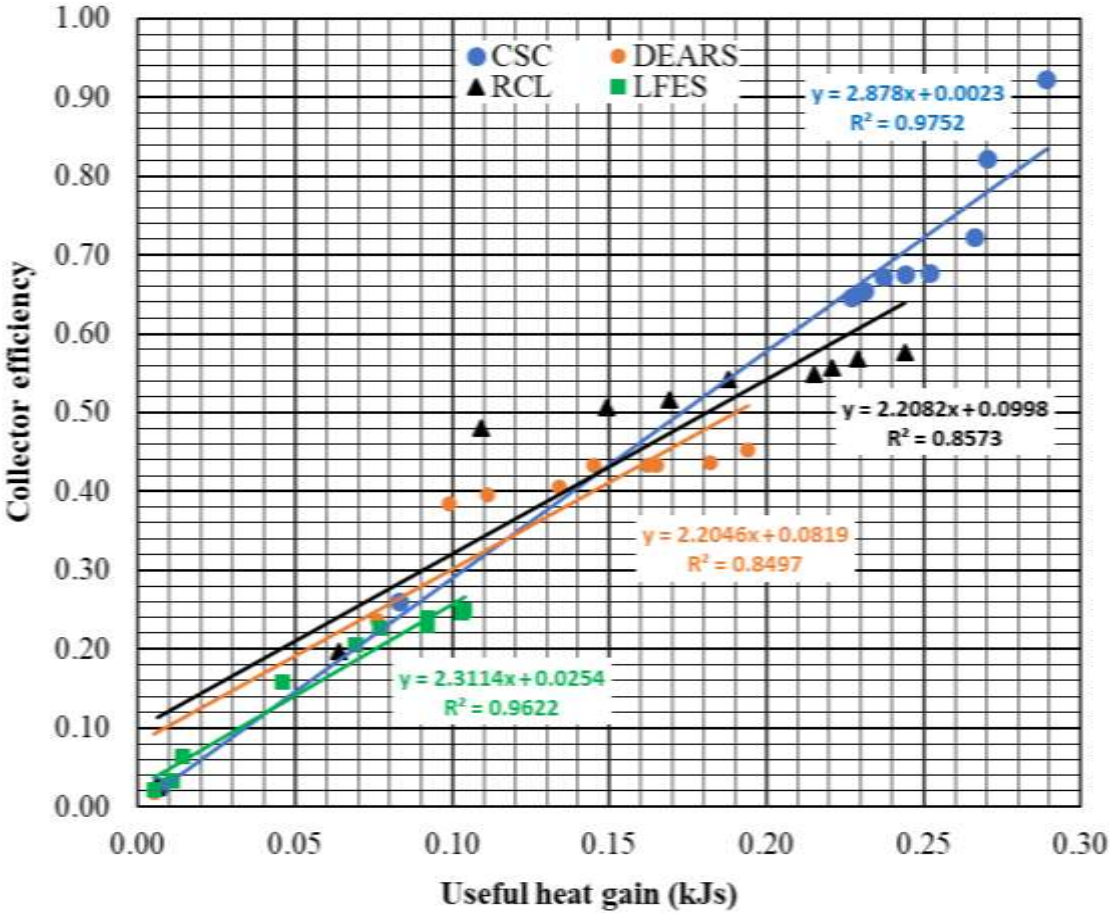

Figure 5-17: Influence of collector useful heat gain on collector efficiency

Further studies by Kareem *et al*. (2016) reported thermal collector efficiency of 59.96% for a solar air heating collector with multi-pass mode. The results of increased efficiency as a result of exhaust regeneration agree with findings, observation and suggestions of other researchers (Kareem *et al*., 2013; Velmurugan and Kalaivanan, 2013) where they reported improved performance and efficiency of multi-pass solar air heat collectors.

In this study, efficiency was improved by multi-pass regeneration of exhaust air pass. Moreover, incorporation of superabsorbent polymer desiccant in the multi-pass exhaust air desiccant regeneration (MPEADR) conduit had significant effect in improving the efficiency. A similar observation was reported by (White *et al*. 2011).

5.3.8 Collector efficiency and reduced temperature function (Δ T/I)

Figure 5-18 shows that the plot of collector performance against the reduced temperature function resulted to a linear expression of the form $y = -ax + b$. This represents a form of a relation between thermal efficiency (η) and the reduced temperature function (Ti- Ta)/ I) according to the model of slandered test for solar collectors by Duffie &Beckman (2013).

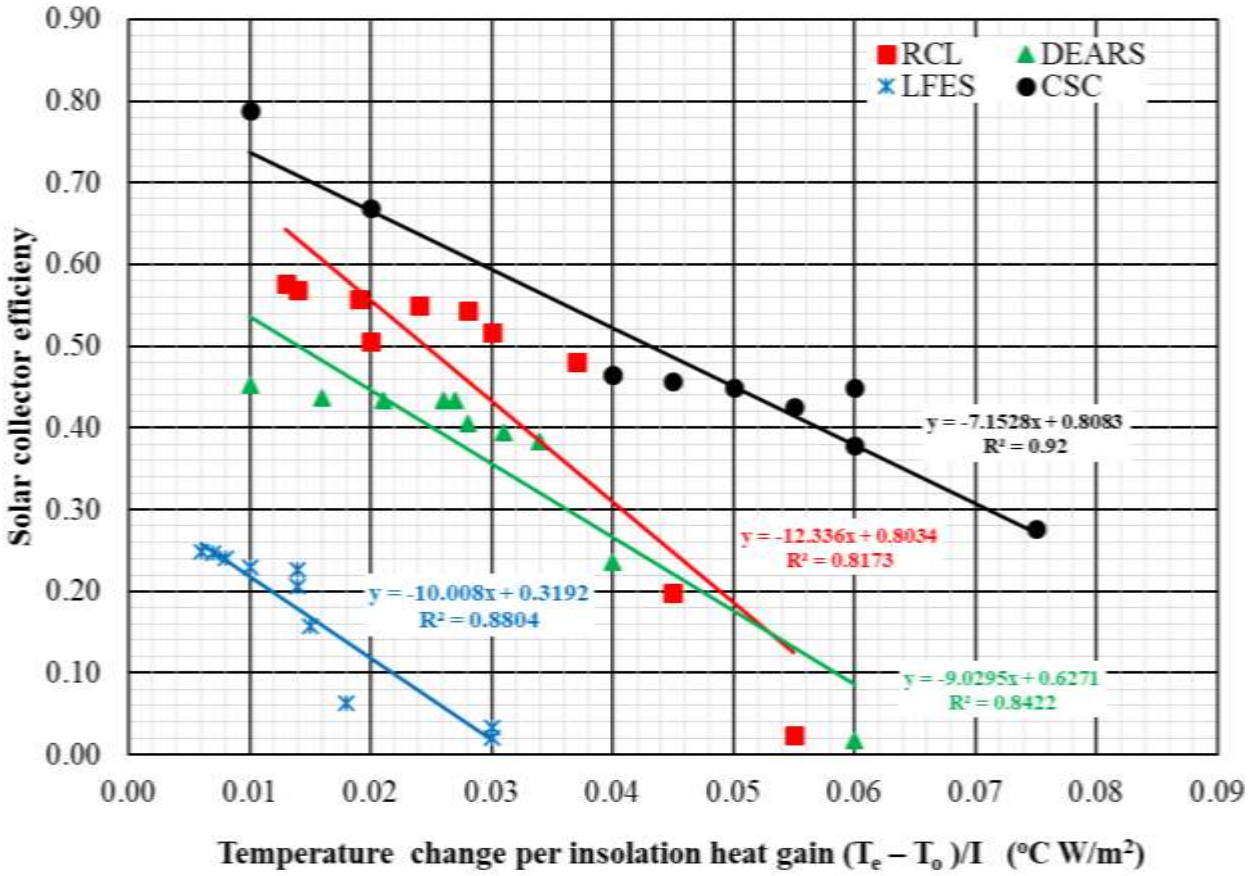

Figure 5-18: Thermal performance for various solar collector configurations

The obtained relationship was linear with different gradients for the various solar collector experimental configurations. This also agreed with the linear mathematical model for solar collectors developed by Al-Neama & Farkas (2018) rewritten as; $\eta = -a(\frac{T_i - T_a}{I})$+b and relates to Equation 3.12 (a) linear behaviour with a correlation coefficient R^2 between 0.82-0.92 for the four collector configurations. Research findings by Gonzalez *et al.* (2014) reported a linear behaviour with correlation coefficient R^2 =0.86 and collector efficiency range of 31% to 51%. A similar trend was reported by Al-Neama &Farkas (2018), Shemelin &Matuska (2017) and Allan *et al.* (2015). Studies by Struckmann (2008) reported that efficiency was a linear function (with negative slope) of pertinent parameters that defined the thermal conditions i.e. solar insolation, working fluid and ambient air temperatures.

The slope of the linear relationship related to the coefficients of heat losses from each of the solar collector configurations (Equation 3.11) as reported by Duffie and Beckman (2013). The heat loss coefficients were obtained by linear regression from the solar collector efficiencies and respective temperature changes for the four collector configurations as shown in Figure 5-18. The collector set up with combined radiation lenses, finned elements and exhaust air-desiccant recirculation conduits had lowest heat loss coefficient (7.1528) while the collector with radiation concentration lenses only manifested the highest coefficient of heat loss (12.336).The efficiency equation and heat loss constants are shown in Table 5.4.

Table 5.4: Solar collector performance models

Solar Collector Configuration	Efficiency Equation	Heat Loss	R^2 Value
Radiation concentration lenses	y = -12.336x + 0.8034	12.336	0.8173
Longitudinal finned elements surfaces	y = -10.008x + 0.3192	10.008	0.8804
Desiccant exhaust air regeneration	y = -9.0295x + 0.6271	9.0295	0.8422
CSC	y = -7.1528x + 0.8083	7.1528	0.92

The heat loss constants relate to collector thermal removal factor F_R and coefficient of heat losses U_L that vary with temperature as well as material constants such as transmission coefficients (τ) and absorption coefficient of the collector material (α).

Figure 5-18 showed that as the reduced temperature function ($\Delta T/I$) increases, the efficiency of the collector with radiation concentration lenses alone reduces significantly. This is due to high heat loss coefficient (12.336) and high heat dissipation to the environment as compared to LFES, DEARS and the CSC configurations.

The effects of collector plate absorbing surface temperature variation are twofold. The increasing collector plate temperature lead to gain of more of useful heat and in parallel with the same time, it would cause more heat losses. This was common in the RCL configuration since there was no exhaust recirculation, increased heat retention effect or increased air heat gain surface area compared to CSC and LFES configuration. Moreover, as high temperatures resulting from solar radiation concentration by the lenses caused rapid heating of the collector plate to achieve a sharp rise in temperature, the heat losses were commensurate as temperatures in the collector rose above the ambient conditions. This relates the effect of heat conductivity in materials where the thermal conductivity and heat losses vary indirectly with temperature. Thus, despite heating the air rapidly and achieving high temperature values, the radiation concentration lenses had highest heat loss constant compared to exhaust regeneration due to

heat losses to surrounding air and subsequent solar radiation fluctuations. Al-Neama and Farkas (2018) reported high heat losses using single pass ambient air into the solar collector due to effects of radiation fluctuations on the ambient air surroundings compared to double pass collector.

The LFES collector configuration had a lower heat loss coefficient (10.008) than RCL (12.3369) despite recording lower temperature changes compared to the latter. This is attributed to the effect of high rate of heat exchange as a result of increased heat transfer area, turbulence effect of air and increased friction and pressure drop through the high density of hot finned elements with increased surface temperature. This agrees with the higher rate of efficiency change with useful heat gained in LFES than RCL as observed earlier. Similar observation was presented by Bhushan & Singh (2010) as well as Kurtbas &Turgut (2006) on investigations of solar air heater performance where the fins increased heat transfer rate and pressure drop in the solar collector. Yang *et al*. (2014) reported that the instantaneous thermal efficiency could exceed 40% using finned elements at a solar insolation of 600 W/m^2.

The lowest heat loss coefficient (7.1528) of the collector with the combined configuration of lenses, finned elements and exhaust regeneration was 5.1832 lower than lenses configuration i.e. (12.336 -7.1528). This represented 42% lower heat losses than the configuration with the highest heat losses (RCL-12.336). This observation relates to waste heat recovery of the by the regeneration conduits. The collector configuration with combined lenses, finned elements and exhaust regeneration with lowest heat loss coefficient (7.1528) reaffirms the results obtained earlier where it maintained uniform temperature change with time from ambient conditions compared to other setups whose values dropped significantly during low radiation hours.

From the gradient of the lines in Figure 5-18, the combined collector with the lowest heat loss constant had the highest rate of useful heat gain with insolation as earlier reported. The low heat loss coefficient and an extended pull of high temperature changes after maximum insolation hour was related to the recirculation of every pass of air stream through exhaust air desiccant recirculation conduits (EADRC) back into the solar collector. This upholds the results obtained earlier where the combined collector configuration had significant higher range of temperature for longer hours and higher temperature change per insolation over time respectively. The effect of desiccant exhaust regeneration was earlier reported to maintain higher temperature changes from ambient conditions after the peak sunshine hours.

Moreover, the effect of regeneration has been found to have a significant positive effect on efficiency by having low heat loss coefficient due to regeneration and recirculation of every pass thus encouraging waste heat recovery. Al-Neama and Farkas (2018) reported lowest heat loss coefficient indicated by slope of performance curve for double pass recirculate solar collector compared to single pass collectors.

The combined configuration had regeneration conduits designed to direct exhaust warm air at the base of the collector plate with to directly interact with high density of high temperature finned elements surfaces between the collector plate and the back plate. Moreover, the useful energy gain is strongly dependent on the rate of convective and radiative heat transfer losses from the top surface of the solar collector plate.

As cited in literature, Bhatt *et al.* (2009); Agbo & Okoroigwe (2007) and Bhatt *et al.* (2017) the heat losses from the bottom as well as and the edges of the collector do exist but not significant compared to the losses from the top of the collector plate. This observation indicates that the low heat loss coefficient was majorly achieved by recirculation conduits designed to feedback exhaust regeneration into a high-density finned heat exchange zone beneath the collector plate surface where heat losses were low. Moreover, the flow vortices formed in the cross section of the curved recirculation conduits and beneath the collector plate enhanced heat transfer between the absorber surface and the air. Similar scenario was reported by Mahboub *et al.* (2016) where curved collector ducts created vortices and improved heat transfer.

The low heat loss constants in the configuration with desiccant exhaust-recirculation conduits also relates to psychrometric studies by Mbuge *et al*. (2016) where use of superabsorbent polymer desiccant extracted moisture from the air stream accompanied by a rise in temperature of about 4°C.

5.4 Grain drying experiments

5.4.1 Solar irradiance during grain drying experiments

Figure 5-19 shows the daily solar irradiance during the grain drying experiments on 11th and 12th October 2018. The solar irradiance gradually increased, reaching maximum of 845 W/m^2 and 865 W/m^2 at 13:30 hrs for day 1 and day 2 respectively and then decreases.

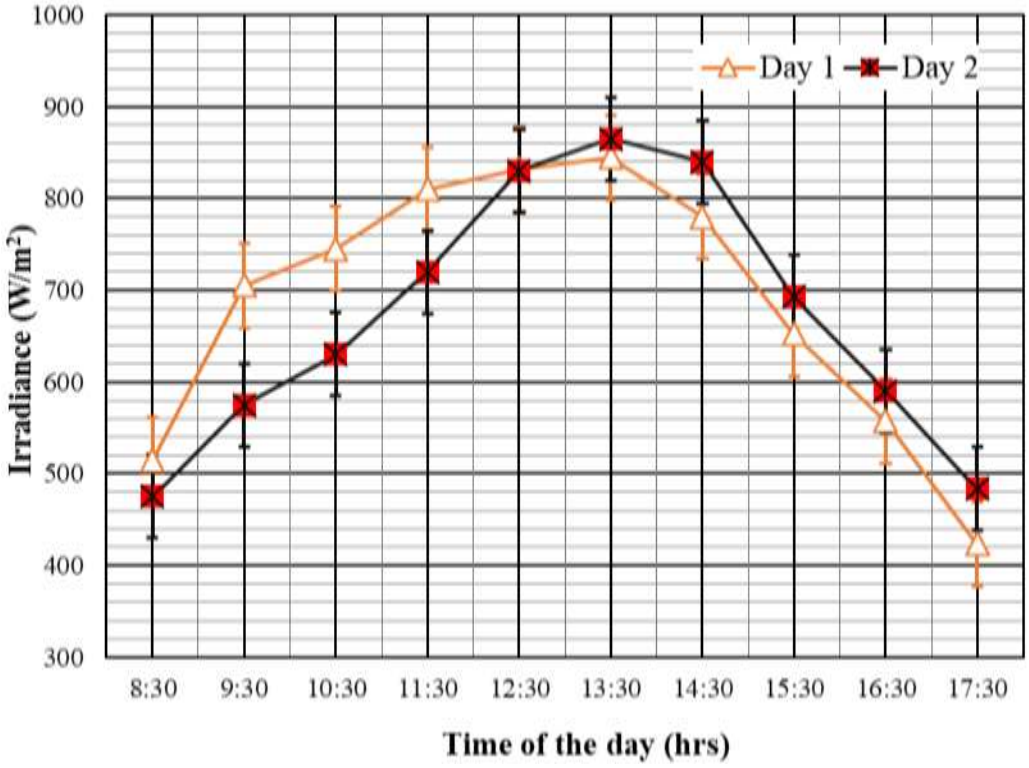

Figure 5-19: Daily solar irradiance during grain drying experiment

5.4.2 Variation of solar dryer temperature and relative humidity

Figure 5-20 shows average solar irradiance values, HSDD, open sun drying and single pass-inlet outlet dryer temperatures during the experiment's duration. The solar irradiance increases from 495W/m^2 at 8:30 am to higher values of 831W/m^2 at around noon, attains maximum peak value of 855 W/m^2 at 13:30hrs and 810 W/m^2 at 14:30 hrs and finally drops to 453 W/m^2 at 17:30hrs. Similar trend was reported by Tashtosh *et al.* (2014) where the total irradiation on the solar collector and the walls of the drying chamber versus time showed the peaks at 13:00hrs. These were the active solar irradiance hours, but a significant drop was noted between15:30hrs and 17:30hrs.

The ambient temperatures and HSDD as well as Single pass temperatures at the plenum varied greatly with solar irradiation (Figure 5-20). The maximum ambient (OASD) temperature at 13:30 hrs were 25.6°C. However, the temperature values reached as high as 43°C at the plenum inlet of the HSDD grain drying chamber and 33°C for the single pass (inlet outlet) dryer. Therefore, the HSDD dryer provides adequate conditions for significant moisture pick up from the grain drying chamber in the dryer than the single pass (inlet -outlet) dryer.

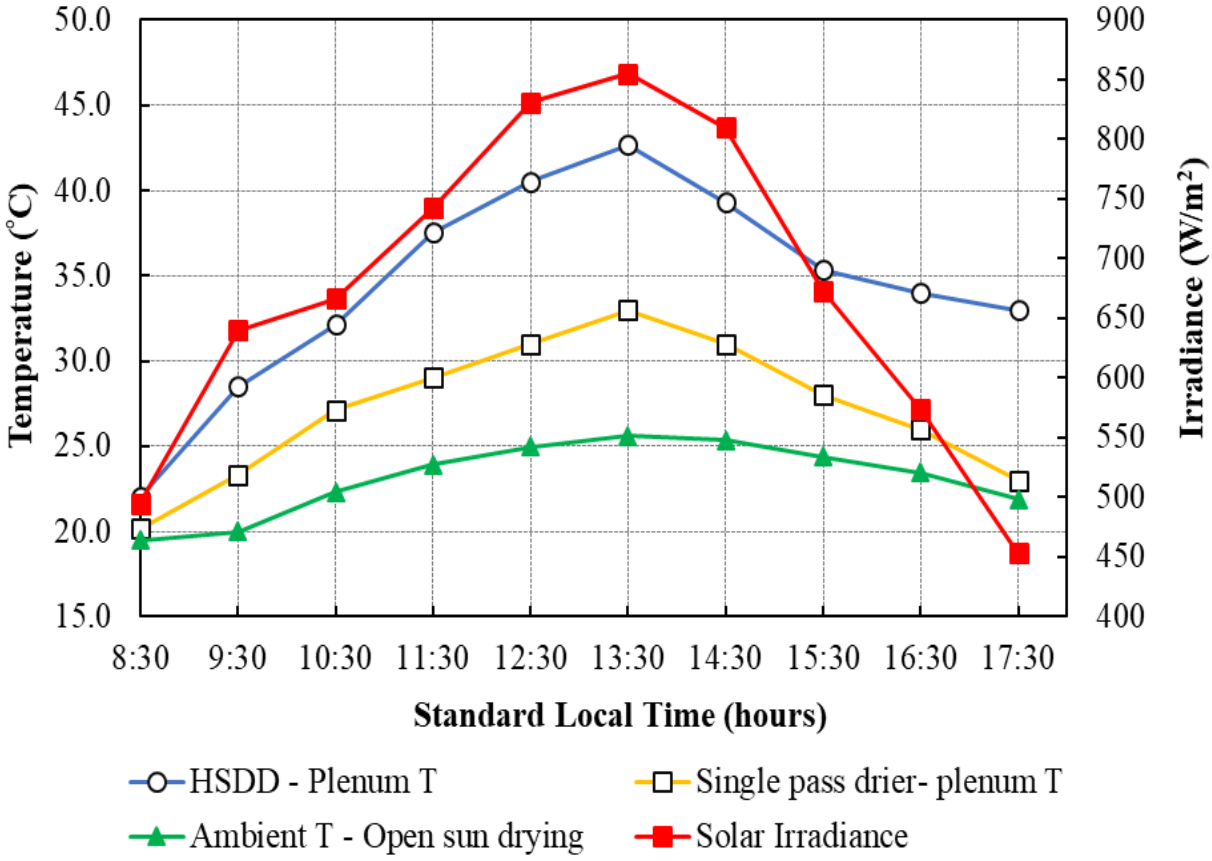

Figure 5-20: Distribution of dryer inlet (plenum) air temperature with irradiance

Drying studies by Al-Neama and Farkas (2018) reported a similar observation where the temperatures and relative humidity values of the air in double-pass solar air collectors were more suitable for grain drying compared to single-pass solar collectors.

After 15:30, the temperatures of the single pass dryer (inlet -outlet) and the ambient values fluctuate significantly compared to HSDD utilizing exhaust regeneration. Ambient drying temperatures of the open sun drying are low while relative humidity was high with low conditions of moisture sorption potential as shown in Figure 5-21.

Figure 5-21 shows that the relative humidity at the inlet plenum of HSDD were significantly lower than the single-pass (inlet -outlet) grain dryer and open sun drying. However, Figure 5-22 shows that during grain drying experiment, the HSDD had higher values of temperature at the dryer outlet than the ambient conditions drying. Moreover, the relative humidity values were higher at the exit of HSDD than the ambient relative humidity values. Similar observation was reported by Osodo *et al*. (2018) where they noted that the exhaust air, though moist, was at a higher temperature than ambient air temperatures of between 40 -55 °C.

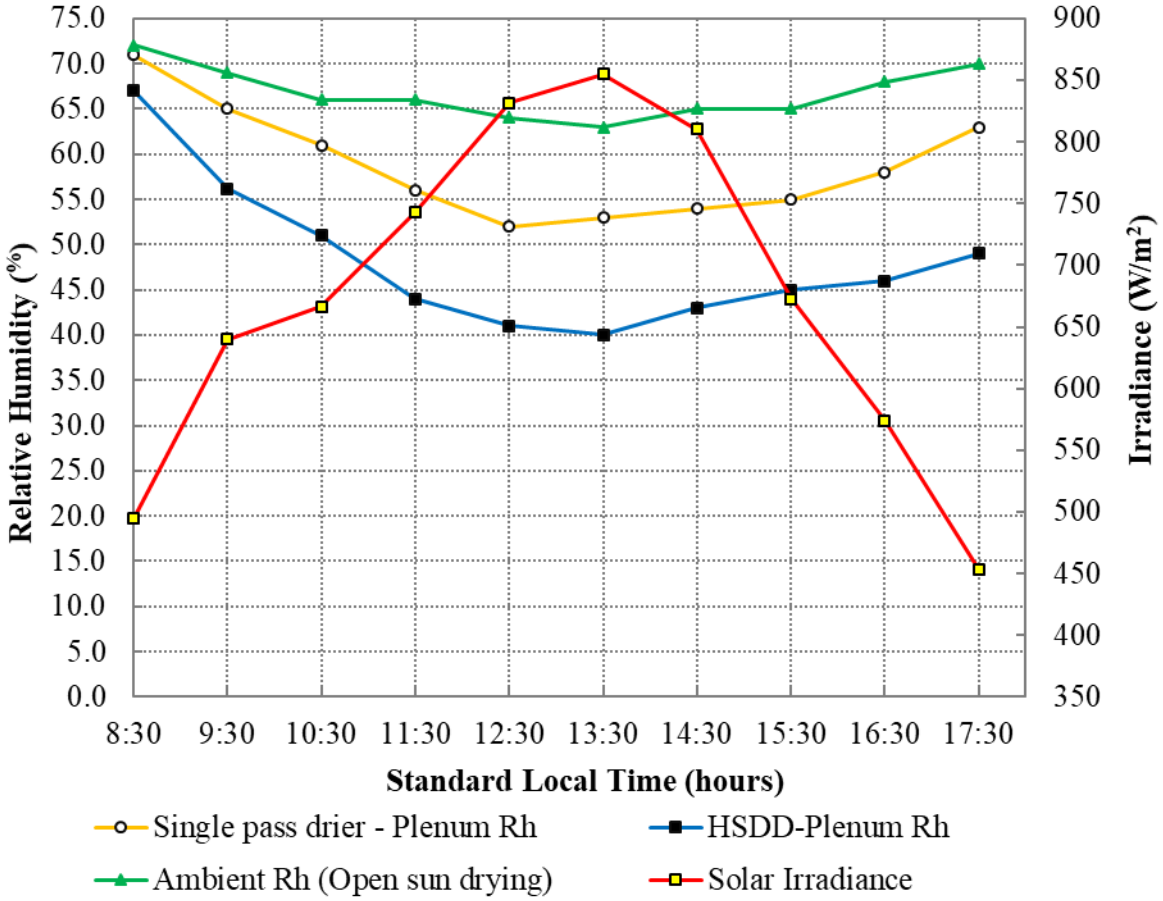

Figure 5-21: Variation of dryer relative humidity with irradiance during grain drying

Generally compared to plenum inlet curves (Figures 5-20,5-21and 5-22) the temperature values dropped substantially at the exit of the dryers while relative humidity values increased significantly. The HSDD dryer had the highest increase in relative humidity and decreased in temperature of the air between the grain chamber inlet at the plenum and the drying air outlet respectively. This is because the drying air in this dryer was confined to pick moisture from the drying grain as compared to ambient and single pass dryer. The outlet temperatures of HSDD were higher than ambient drying conditions because of regeneration effects.

Figure 5-22 indicates that as the as the air moved through the grain compartment it imparted heat to the grain while absorbing the humidity of the outermost layers, resulting to reduction in grain moisture and a significant rise in the humidity of the exhaust air. As moisture is being removed from grain it is absorbed by the drying air thereby increasing its humidity content. Similar observations were reported by Ngunzi (2014). The relative humidity curve of the HSDD shows a rapid increase between 8:30 and 13:30 and there after maintained a slow rate of reduction although at significant higher values than single pass and ambient relative humidity.

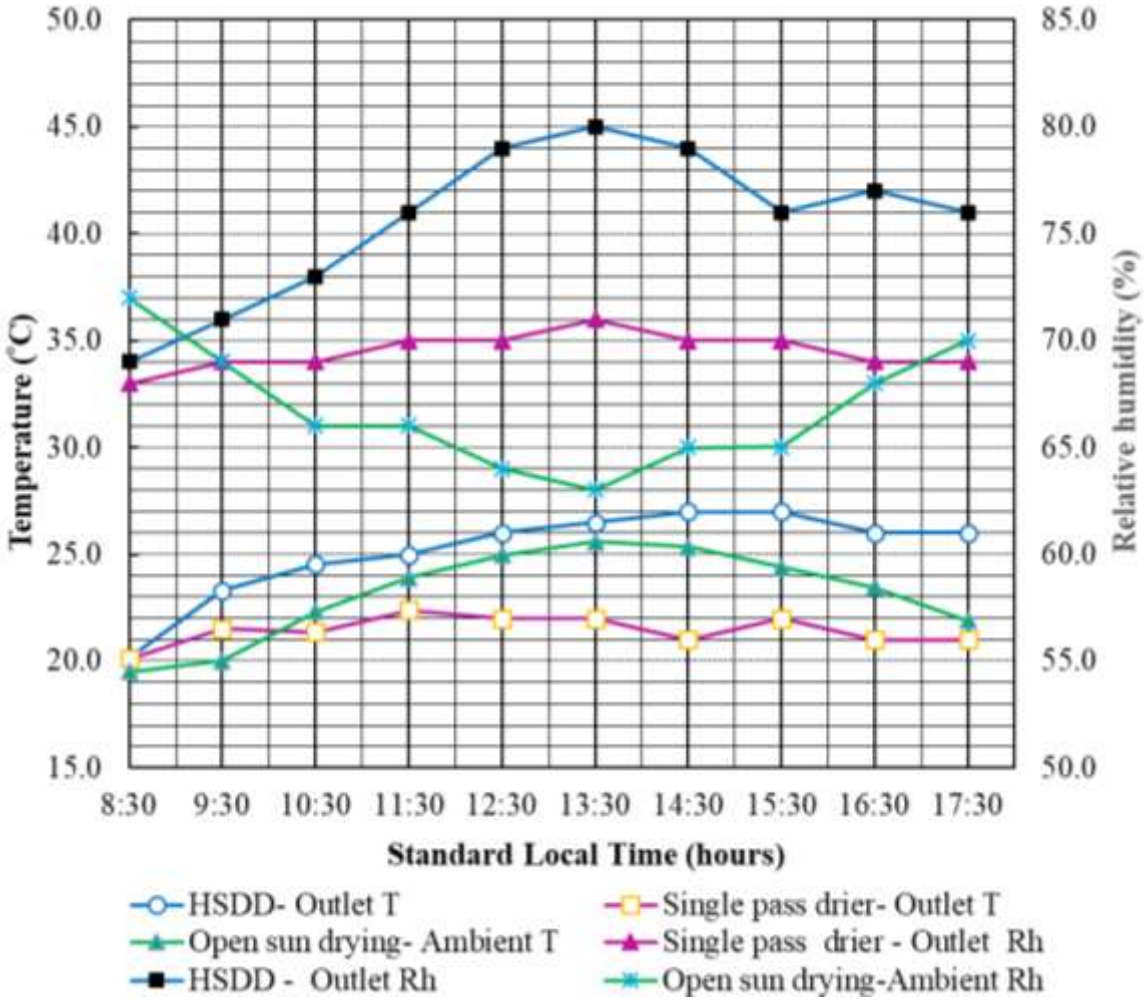

Figure 5-22: Variation of dryer outlet temperatures and relative humidity

During the initial drying hours there is a significant increase in humidity of the air due to faster rate of evaporation of water from the drying grain. This is related to the fact that the moisture of outer grain layers evaporates at a higher rate and is more easily removed compared to that of the internal layers.

Generally, the curves from Figures 5-21 shows that the air at dryer entrance had more capacity to catch the moisture from the grain than exit region (Figure 5-22). Similar scenario was reported by Al-Neama and Farkas (2018).

Drying experiments by Sundari *et al*. (2013) showed that the moisture removal was high initially due to high rates of removal of moisture content from the grain surface first and then gets reduced, with movement of moisture from the internal part to the periphery surfaces. This led to increased relative humidity during initial periods of drying in the enclosed dryer.

5.4.3 Grain drying curves

The variation of moisture content with time under ambient conditions for the open-air sun drying and for HSDD drying experiments is shown in Figure 5-23. The figure shows that the grain samples in both drying methods exhibited a declining pattern. This agrees with other studies where drying of most agricultural products often exhibit falling rate period (Velic *et al*.,2010; Karel & Lund, 2003 and Ramaswamy & Marcotte, 2006).

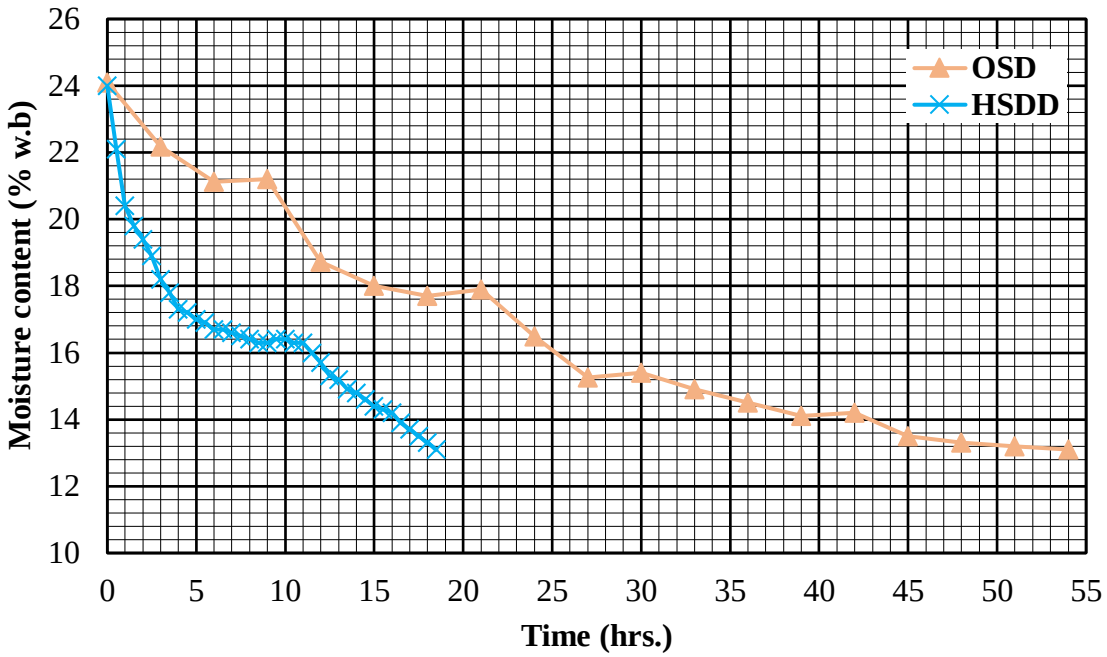

Figure 5-23: Variation of maize grain moisture content with time of drying

The graphical relationship of moisture course during drying time period was a typical maize grain drying curve as reported by Kituu *et al*. (2013), Gill *et al*. (2014), Coradi *et al*. (2016) and Dagde & Iminabo (2018). Moisture content variation with time over the dryer testing period showed a falling rate curve with a higher moisture removal pattern in the HSDD compared to open sun drying method. This was related to moisture sorption activity of the superabsorbent polymer material in the recirculation conduits as well as waste heat recovery. This was viewed as a significant improvement technique for saving energy in conventional maize grain dryers that release the exhaust hot air to the environment.

The initial moisture content of grain was 24.1% (w.b). Steady moisture content was reached after 18hrs and 54 hours for the HSCDD and OASD method respectively. Drying took place in a falling rate period with a higher moisture removal rate by the HSDD and significant reduction in drying time compared to OSD. Savings in time were achieved since it took only

18 hours to lower the moisture content of grain from 24.1% w. b to 13.1% w.b compared to 54 hours for the OSD. The drying time was reduced by about 70% using HSDD. Similar studies by Umogbai & Iorter (2013) reported three days to lower moisture content of maize from 30.3% w.b to 13.3% w.b using a solar dryer while OSD took 6 days to dry the cobs to 13.4 % w.b. It was deduced from this data that higher temperature induced higher moisture removal from the grains in the HSCDD compared to OSD.

The curves indicate higher drying pattern at initial stages than subsequent hours due to higher moisture concentration gradient that accelerate water migration from the grain kernels after which it gradually declines. Moreover, the moisture bound in the final drying period in a product usually demands more energy to extract than initially bound moisture, further slowing down the process. These results agree with drying literature. Moisture reduction is initially high and then gets reduced due to removal of moisture from the surface first followed by the movement of moisture from the interior of the grain to the surface (Sundari *et al*., 2013).

5.4.4 Grain drying rate

The rate of drying R_D decreased as drying time increased but tend to be constant with further increase in time. Drying rate curves shows that higher drying rates were achieved at first time intervals (Figure 5-24). It is evident HSCDD has a fast-drying rate than the OSD method and the drying time is reduced considerably**.** Results showed that moisture content decreased as drying time progresses for each drying method due to the increased vapour pressure in the grain kernel samples, which resulted to an increased diffusion rate of the internal moisture. Additionally, the R_D decreased as the moisture content reduced due to increase in the intra-particle resistance to migration of moisture to the surface of the grain kernels. This resistance effect was phenomenal in OSD compared to HSDD where drying conditions were more favourable.

Higher drying rates were achieved for the HSCDD at shorter time intervals compared to OSD method. The greater differences in temperature of the drying air and grain caused greater heat transfer to the grain kernels and rapid moisture removal from the grains. The drying rate increased with increased drying air temperatures which consequently decreased the drying time for the HSDD compared to OASD. Both drying systems had higher drying rates at initial drying time intervals that corresponded to high initial moisture content. The drying rate decreased with increase in drying time as a result of decreased rate of evaporation of moisture from grain kernels with progressive drying time.

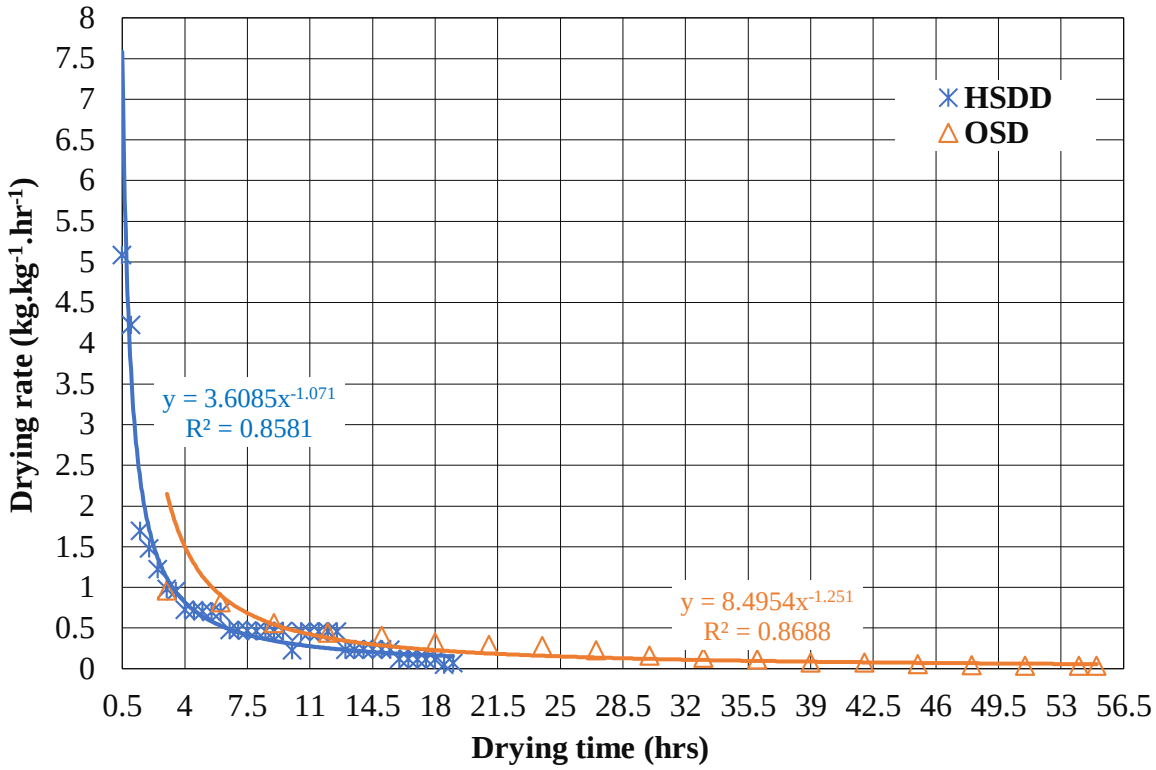

Figure 5-24: Variation of drying rate with drying time

Grain moisture content decreased with drying duration and the rate of reduction in moisture contents decreased as the drying time progressed (Fig 5-24) similar results were reported by Kim *et al*. (2015). Table 5.5 shows that the HSDD reduced the total drying time by 67% (54-18 hrs) and increased the drying rate by 199% (0.162-0.485kg/hr).

Table 5.5: Average dryer performance

Drying method	Mass of grain kg		Drying time (hrs.)	Drying rate (kg/hr)
	Initial mass	Final mass		
OSD	69	60.27	54	0.162
HSDD	69	60.27	18	0.485

Figure 5-25 shows the variation of drying rates with grain moisture content. Highest drying rates were obtained in the first-time interval then gradually declined. At about 13% M.C the drying rate for HSDD was uniform and did not change significantly indicating that the grain had achieved equilibrium. However, the OASD shows low initial drying rates due to ambient conditions during drying.

Drying rate curves shows that higher drying rates were achieved at first intervals of higher initial moisture contents and then declined to more less equalize. This relates to moisture

binding in the wet agricultural materials where free water is more easily removed at high moisture contents (Vitázek & Vereš 2013).

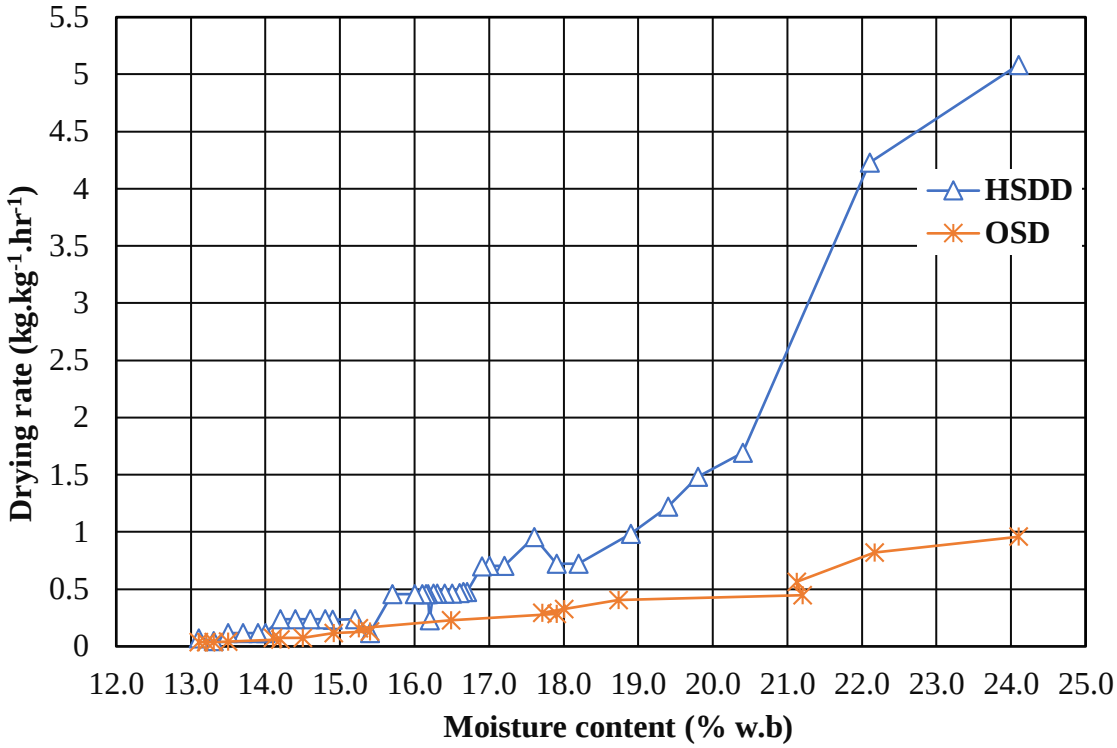

Figure 5-25: Variation of grain drying rates with moisture content

Figure 5-25 shows that the drying rate varied greatly with moisture content and decreased significantly in the initial stages (24.1% M.C) with decreasing moisture contents, and it is almost constant in the middle lower portion of the graph as the moisture content approached equilibrium. This was an indication of slower drying rate at lower moisture levels (Figure 5-26). This was corroborated with increase in the intra-particle resistance to internal moisture migration of grain kernels as the drying progresses. Thus, drying rate decreased continuously with decreasing moisture content due to increase in the intra-particle resistance to internal moisture migration of the grain kernels (Nwakuba,2017). Rapid drying rate in the HSDD than OSD was attributed to higher temperature differences of the drying air and maize kernels in the HSDD. Increased heat transfer coefficient influenced rapid heat and mass transfer rate. Similar observation was reported by Meesukchaosumran & Chitsomboon (2019). This further suggests that the moisture ratio gradient caused by temperature difference between the solid and drying medium for HSDD was steeper than the moisture diffusion gradient for OSD. This corroborates with Bhagyashree *et al*., (2013).

When the moisture levels approach 13% the capillary forces decline significantly and are no longer sufficient to overcome heat and mass transfer resistance and transport of the moisture

to surface of the grain kernels. This effect lowered the drying rate significantly which became constant at equilibrium of 13.1% with drying air. The variation of drying rate with moisture content for the two drying systems indicated that drying rate decreased exponentially with moisture content. Similar results were reported by Corrêa *et al*. (2011). The drying rate equations were found to be exponential with coefficient of determination R^2= 0.90 and 0.92 for HSDD and OSD respectively.

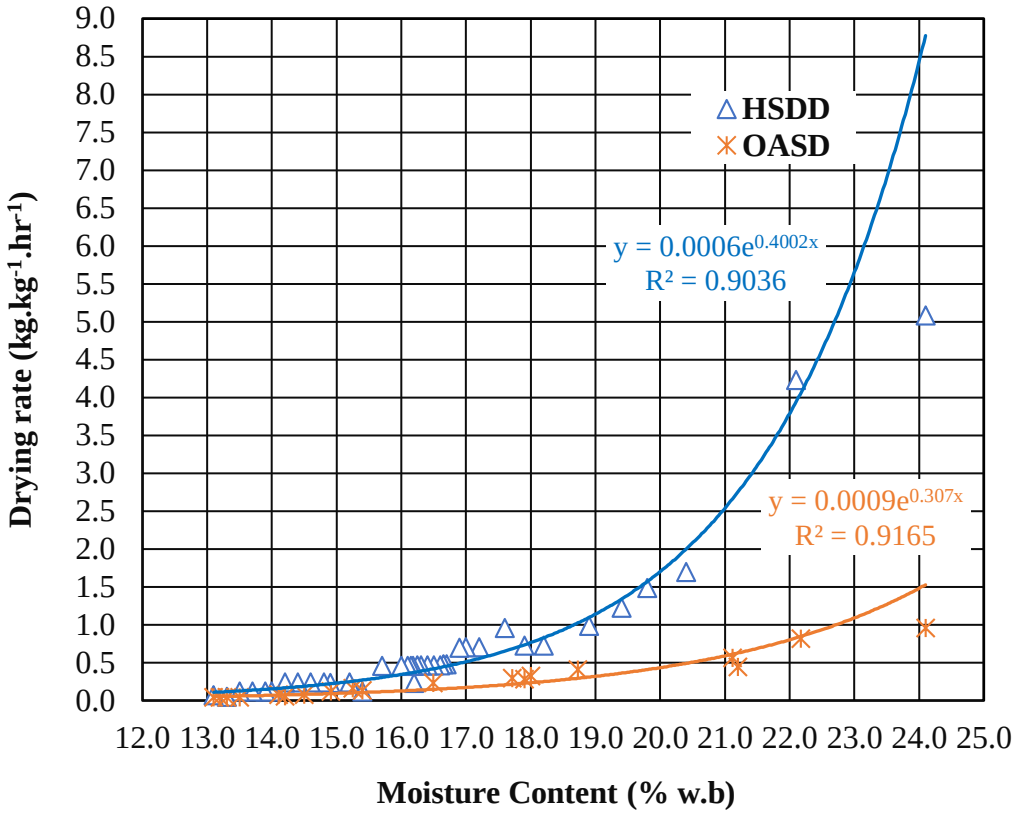

Figure 5-26: Drying rate trends and drying rate equations

5.4.5 Drying rate prediction

The complex operation of drying involves heat and mass transient along with several rate process of physical transformation that are functions of moisture content temperature and time. Therefore, knowledge of drying rate, minimum storage moisture content and time of drying are needed to maintain stability during storage, evaluate final product quality and stimulate the drying process. A relationship between drying rate and drying time and moisture content of the grain kernels in the HSDD was established. The predicted drying model was validated with experimental data, yielding a high value of coefficient of determination (R^2).

The equation of drying rate with drying time for HSDD in Figure 5-24 was verified and validated with the experimental drying rates data generated from the dryer. Figure 12 shows

that there was a strong linear correlation between predicted and experimental drying rates (R^2=0.925).

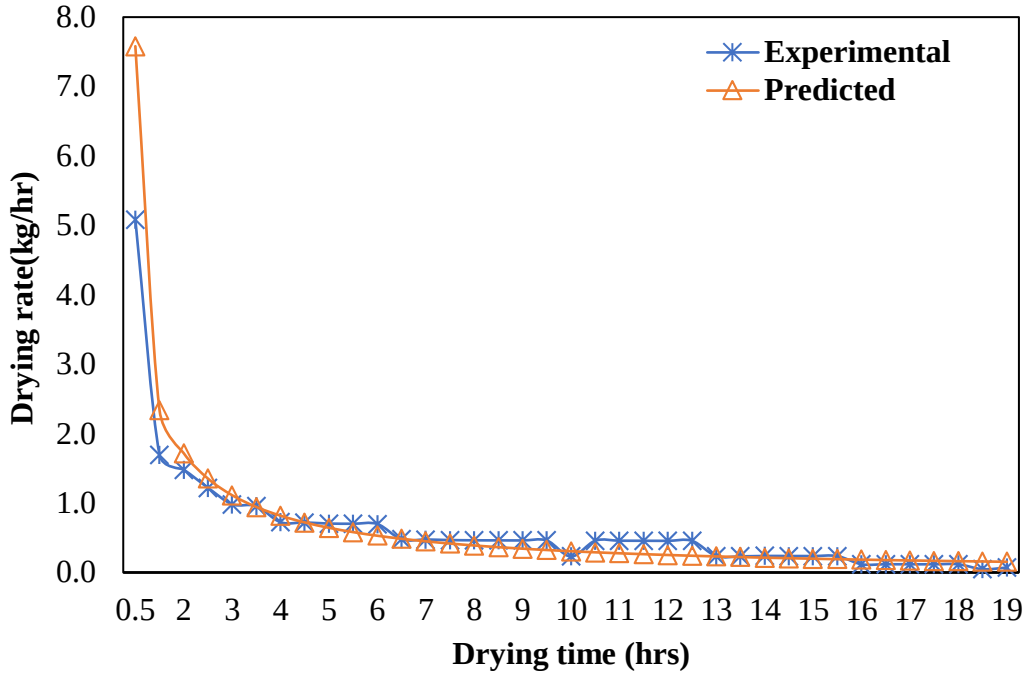

Figure 5-27: Drying rate prediction of the HSDD

High coefficients of determination of 92.5% between the predicted and experimental values showed that the model was good. The developed prediction equation established a model that can be used to predict drying rate in the HSCDD grain dryer with progressive drying time.

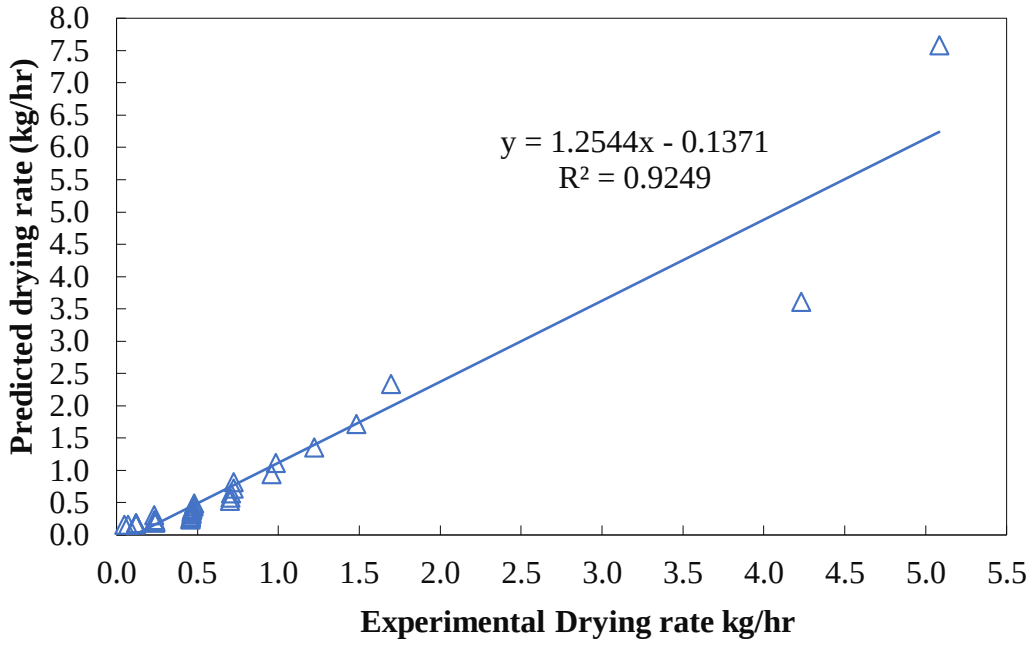

Figure 5-28: Validation of the predicted drying rate model of HSDD

5.4.6 Comparison of exhaust desiccant regeneration and single pass dryers

Figure 5-29 shows the variation of grain moisture content with drying time for the two-day drying experiments in the single pass dryer and desiccant exhaust regeneration dryer. The moisture loss was higher at the start of drying than towards the end of drying. The reduction in the drying was mainly due to reduction in moisture content as drying advances. A high moisture removal rate was indicated in the desiccant exhaust regeneration dryer. This was related to the activity of moisture sorption effect by the superabsorbent polymer desiccant material in the recirculation conduits. The drying rate in exhaust desiccant regeneration system was significantly higher due to the presence of superabsorbent polymer desiccant material. This dryer attained 13.1% mc about 8 hours earlier than the dryer without the desiccant recirculation system.

As shown in Figure 5-29, the falling rate period of moisture content with time was uniform and high in the dryer with desiccant exhaust regeneration system. This was attributed to homogeneous nature of drying air temperatures and relative humidity of the drying air media compared to the changing conditions of ambient inlet and outlet air dryer. There was consistent reduction in moisture content with time from interior to outer surface as drying progresses compared to intermittent pattern observed in the ambient air inlet outlet dryer. Similar observations were reported by Da Silva *et al*., (2014) and Da Silva *et al*., (2015). However, in both dryers the reduction of moisture content with time was observed in the initial drying intervals where initial moisture content was high and after which it gradually declined. This agrees with moisture binding in a wet agricultural material where free water is more easily removed (Can, 2000).

The grain moisture content of the dryer bin with desiccant exhaust air recirculation conduits and single pass dryer was compared statistically using student t test. The moisture content was statistically different at 95% confidence (P = 0.006). Therefore, P value of 0.006 indicates that a sufficient reason to conclude that the means for the two drying methods were significantly different thus rejecting the null hypothesis that the means from the two populations were the same. The value (0.6%) is way too low from the confidence interval of 0.05 (95%) set for the analysis. This was a notable improvement in preconditioning the drying air during the night as compared to ambient inlet-outlet dryer that in which the grain was susceptible to ambient rewetting.

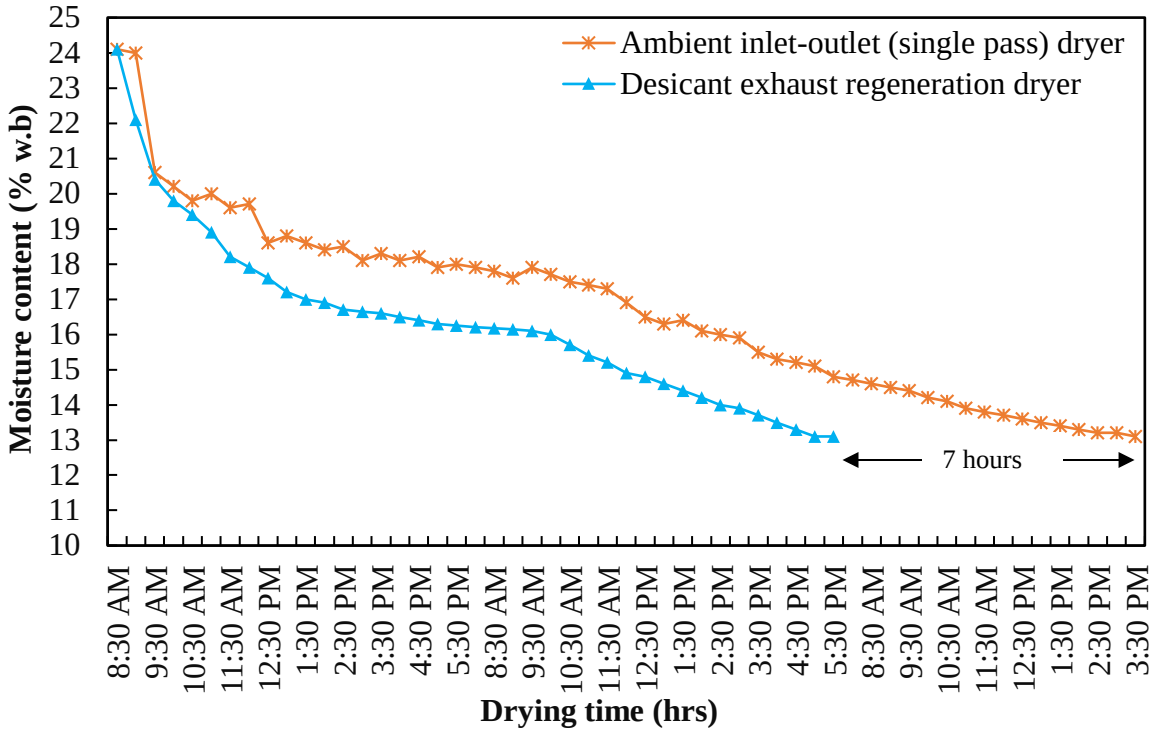

Figure 5-29: Grain moisture content variation with time for single pass and exhaust regeneration dryers

5.4.7 Drying kinetics of HSDD and moisture ratio models

HSDD moisture content datasets from maize drying experiments was converted into their respective moisture ratios and fitted to eighteen mathematical drying models listed in Table 3.1. To characterize the drying kinetics, experimental moisture ratio data were fitted to 18 commonly used drying models and regressed to evaluate goodness of fit by comparing coefficient of determination (R^2), root mean square error (RMSE) and sum of square error (SSE) using MATLAB (Version R2016a). Figure 5-30 shows that the experimental and theoretical moisture ratios decreased with drying time. The graph shows a typical drying curve generally obtained during drying of moist materials (Menges & Ertekin 2006; Bozkır 2006).

Regression results from Table 5-6 showed that R^2, SSE and RMSE values ranged from 0.7126 to 0.9676, 0.05655 to 0.5017, and 0.04078 to 0.118, respectively. The Two term model was ascertained to best describe the drying kinetics of maize grain in the HSDD with highest R^2, and lowest SSE and RMSE values of 0.9676, 0.05655, and 0.04078 respectively.

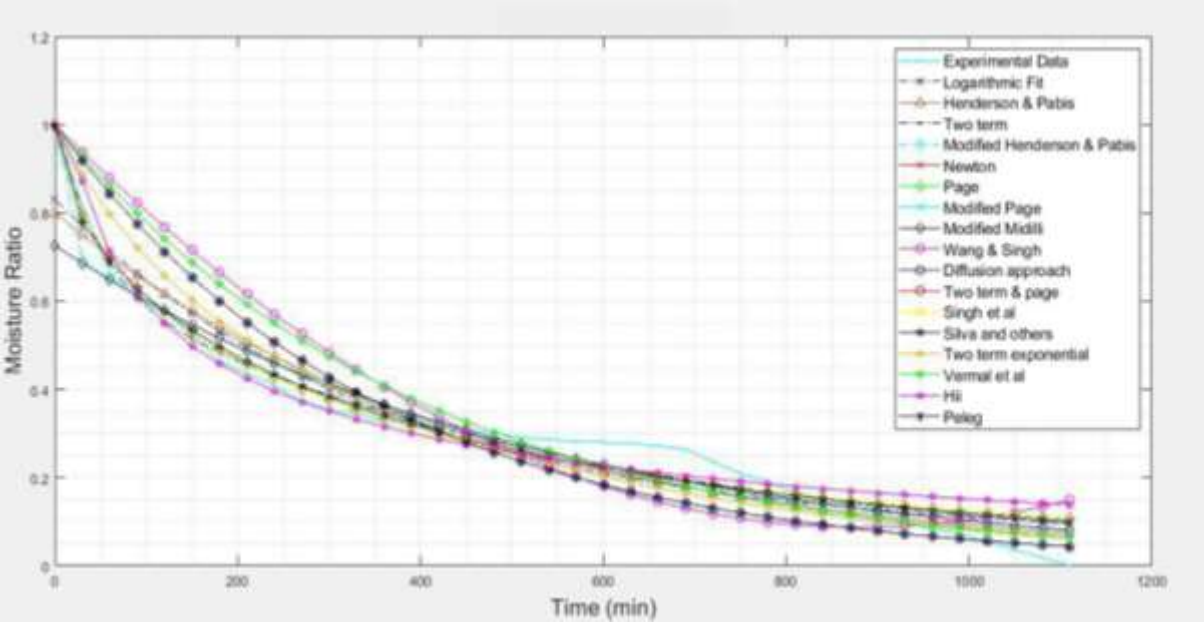

Figure 5-30: Experimental and predicted drying models

Experimental moisture ratio and the predicted Two term moisture ratio data was plotted and correlated shown in Figure 5-31. Validation of the proposed model indicated that there was a close correlation between the experimental and Two term predicted moisture ratio model values, with a high coefficient of determination R^2 value of 0.9692. This shows that the Two term model was the suitable model to satisfactorily describe the drying kinetics characteristics of maize grain in the HSDD.

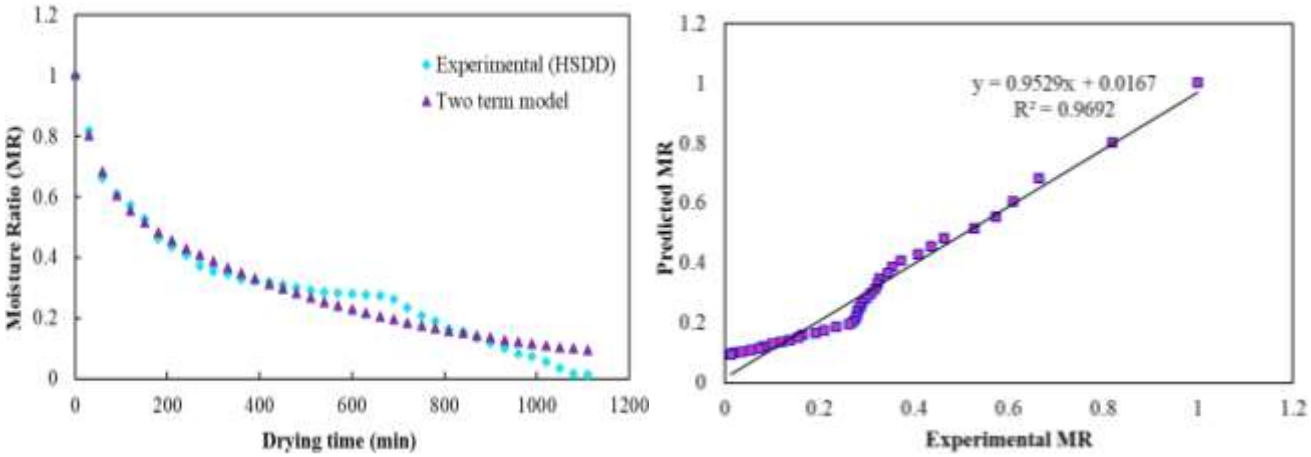

Figure 5-31: Comparison of experimental model and the predicted Two term drying model

Table 5.6: Model coefficients and regression analysis results of eighteen drying models

	Model name	Model coefficients	R^2	SSE	RMSE
1	Newton model	k = 0.002827	0.8428	0.2744	0.08611
2	Page model	k = 0.0269, n = 0.6299	0.9572	0.07468	0.04555
3	Modified page	n = 0.6299, k = 0.003213	0.9572	0.07468	0.04555
4	Henderson and Pabis	a = 0.8003, k = 0.002174	0.9236	0.1333	0.06084
5	Modified Henderson and Pabis	a = 0.7363, k = 0.001977 b = 0.4399, g = 0.8161 c = -0.1762, h = 0.8145	0.954	0.08033	0.0501
6	Logarithmic	a = 0.7713, k = 0.00272 c = 0.05931	0.9263	0.1286	0.06062
7	Midilli	a = 1, k = 0.8993 b = 0.0002535	0.8998	3.316	0.3078
8	Modified Midilli	a = 0.7411, k = 0.01854 b = -0.1478	0.9372	0.07331	0.04713
9	**Two term**	**a = 0.6507, b = 0.3535 k_o= 0.00174, k_1 = 0.0216**	**0.9676**	**0.05655**	**0.04078**
10	Two term-exponential	a = 0.1975, k = 0.01164	0.9159	0.1467	0.06384
11	Wang & Singh	a = -0.002072 b= 0.000001176	0.7126	0.5017	0.118
12	Diffusion approach	a = 0.1247, k = 0.003096 b = 0.9016	0.8431	0.2738	0.08845
13	Verma et al	a = 0.009094, g = 0.002486 k = 0.002648	0.7331	0.3114	0.09714
14	Peleg model	a = 184.8, b = 0.9589	0.9428	0.09979	0.05265
15	Two term and Page	a = 1, k = 0.02693, n = 0.6297, b = 0.0001924 h = 0.3532	0.9572	0.07468	0.04687
16	Hii and others model	a = 1.339, b = 0.5635 k_1 = 0.2492, k_2 = 0.2501 n = 0.3354	0.9242	0.08845	0.05342
17	Singh et al model	a = -0.02707, k = 0.003428	0.8753	0.2176	0.07774
18	Silva *et al* model	a = 0.0008359, b = 0.04098	0.9602	0.06951	0.04394

5.5 Statistical analysis results

From the summary statistics Table 5.7, the collector configuration that produced highest average temperatures (54.7638+- 10.2783SD) was CSC followed by RCL (50.177+-10.33SD), DEARS (43.378+-7.34SD) and LFES (33.4961+-6.50) respectively. The lowest average temperatures were recorded for the ambient drying conditions (23.752+-2.23SD) as shown in Table 5.7. Comparatively the boxes were tall indicating quite different temperature effect from

each of the configurations, moreover each of the whisker boxes was much higher or lower than another reporting a much difference in temperatures between the studied configurations. Comparatively the CSC has the highest values than corresponding individual configuration counterparts. The ambient whisker box is short indicating that the recorded overall temperatures had a higher level of agreement with each other (Fig 5-32).

Table 5.7: Summary statistics for collector configurations temperature datasets

Dryer	*Count*	*Average*	*Standard deviation*	*Coeff. of variation*	*Minimum*	*Maximum*	*Range*
LFES	254	33.4961	6.49703	19.3964%	19.0	46.0	27.0
Ambient	254	23.752	2.23109	9.39328%	18.0	28.0	10.0
RCL	254	50.1772	10.3296	20.5862%	19.0	65.0	46.0
CSC	254	54.7638	10.2783	18.7684%	19.0	71.0	52.0
DEARS	254	43.378	7.33817	16.9168%	19.0	57.0	38.0
Total	1270	41.1134	13.7546	33.4553%	18.0	71.0	53.0

There were statistical significance differences in mean of temperatures for the tested solar collector configurations at 95% confidence. i.e. $F_{0.05}(4,1265) = 641.38$, P=0.0000) as shown in ANOVA Table 5.8.

Table 5.8: ANOVA table for determination of statistically significant differences

Source	*Sum of Squares*	*Df*	*Mean Square*	*F-Ratio*	*P-Value*
Between groups	160796.	4	40199.1	641.38	0.0000
Within groups	79285.4	1265	62.6762		
Total (Corr.)	240082.	1269			

Since the P-value of the F-test is less than 0.05, there is a statistically significant difference between the means of the 5 variables at the 95.0% confidence level. Further analysis by multiple range test using Fisher's least significant difference (LSD) method determined the means that were significantly different from which others as shown in Table 5.9.

Table 5.9: Multiple range tests contrasting which means are significantly different from which others

	Count	*Mean*	*Homogeneous Groups*
Ambient	254	23.752	X
LFES	254	33.4961	X
DEARS	254	43.378	X
RCL	254	50.1772	X
CSC	254	54.7638	X

Method: Fisher's least significant difference procedure at 95.0 percent LSD. Similar column levels containing X's form a group of means within which there are no statistically significant differences.

Contrast	*Sig.*	*Difference*	*+/- Limits*
LFES - Ambient	*	9.74409	1.37689
LFES - RCL	*	-16.6811	1.37689
LFES - CSC	*	-21.2677	1.37689
LFES - DEARS	*	-9.88189	1.37689
Ambient - RCL	*	-26.4252	1.37689
Ambient - CSC	*	-31.0118	1.37689
Ambient - DEARS	*	-19.626	1.37689
RCL - CSC	*	-4.58661	1.37689
RCL - DEARS	*	6.79921	1.37689
CSC - DEARS	*	11.3858	1.37689

** denotes a statistically significant difference at 95.0% confidence level*

Group homogeneity and columns at different levels containing X^s were formed indicating statistically significant differences between the means of groups. Results showed significant differences at 95.0% confidence level between the means of temperatures from contrasted collector configuration as shown in Table 5.9.

Box Whisker plot showed a contrasted distribution characteristics and response pattern of temperature levels from the studied collector configurations. The summary of the range of visualization i.e. the lowest, mean, median and maximum temperature values of the quartile groups for various collector configurations were as shown in Figure 5-32.

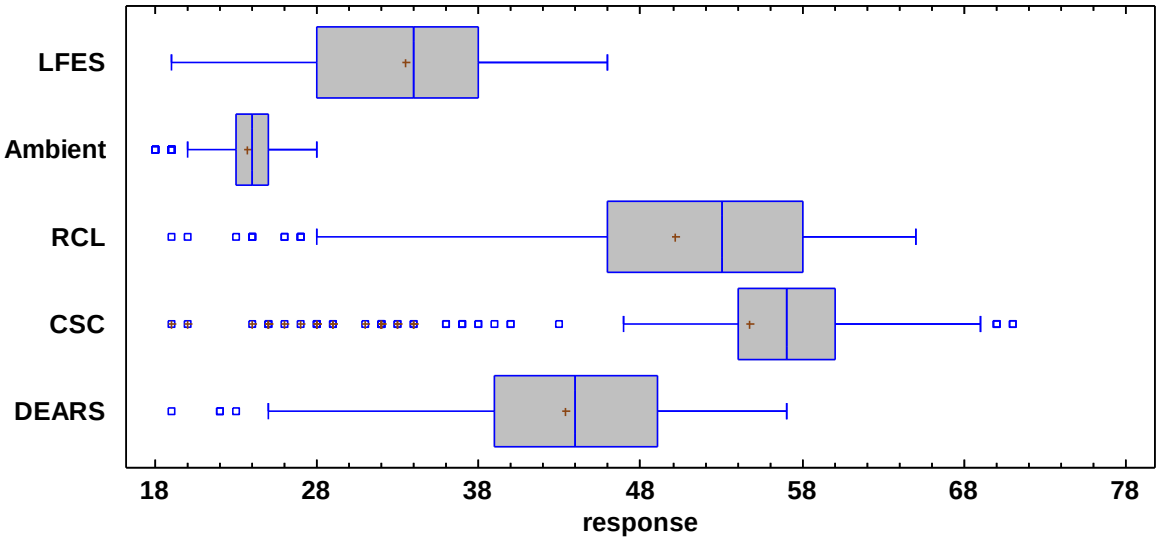

Figure 5-32. Box-Whisker plots summarizing the distribution of temperatures from different collector configurations.

The + sign and continuous line within the box represent the mean and median respectively while the left and right ends present the lower and upper quartiles with whisker lines presenting the lowest and the highest observations on the left side and right of Figure 5-32 respectively for various configurations.

T-test statistical analysis performed to compare the moisture content variation of single pass dryer and exhaust regeneration showed that the probability value (P=0.006) was less than the 0.05. The null hypothesis that the means of the two dryers are the same was therefore rejected and the alternative hypothesis that they were significantly different adopted.

CHAPTER SIX: CONCLUSIONS AND RECOMMENDATIONS

6.1 Conclusions

The performance of the hybrid solar desiccant dryer was optimized. The designed and tested prototype incorporated the established effects of RCL to achieve high temperatures, LFES to increase thermal contact and heat transfer rates and DEARS to enhance exhaust dehumidification and thermal recuperation of waste heat into the dryer to improve subsequent drying. The efficiency and performance of the tested solar collector dryer prototype was improved and grain drying experiments reviewed a significant increase in drying rates and reduced drying time compared to open sun drying.

Statistical analysis reviewed a significant change in drying temperatures of the optimized dryer. Regression analysis showed that the amongst eighteen different mathematical drying models, the Two term model characterised the drying kinetics of maize grain in the HSDD with highest R^2 and lowest *SSE* and *RMSE* values. The model also provides a theoretical basis for further understanding and predicting tempering effects during drying conditioning of grain dryers.

This study is useful in scaling-up dryer designs, optimization of drying process parameters and dryer performance enhancement to improve efficiency and reduce time loss and grain damage during drying for the benefit of grain and seed industry. The HSDD dryer can be piloted and adopted to meet the demands of small-scale farmers in developing countries.

Moreover, the compact enclosed solar dryer has the advantages of reducing the damages caused to the product by insect, birds, rodents, micro-organisms and the adverse climatic conditions compared to open sun drying. The drying rate models developed can be adopted by users of the dryer to assist in planning drying schedules.

6.2 Recommendations

- Further study can be carried out to evaluate grain quality and the nutrition value as well as aflatoxin levels of grain dried using HSDD compared with open sun drying to ascertain consumer quality.
- More research can be conducted to test the HSDD for dying of other maize grain varieties and agricultural legumes and cereal grains such as beans.

- Further studies on optimization of drying chamber configuration and airflow distribution, temperature and velocity profiles for reduced energy consumption and drying time can be performed
- During grain drying experiments presence of moisture on the walls of the drying chamber was noted. Further research should be conducted for possibilities of a wide range of momentary dryer operation conditions and storage geometries that occur in the grain drying chamber to reduce heterogeneity and homogenise humidity and temperature distribution of the air in the drying chamber.

REFERENCES

Abdullah, A. L., Misha, S., Tamaldin, N., & Mohd, M. A. (2019). A Review: Parameters affecting the PVT collector performance on the thermal, electrical, and overall efficiency of PVT system.

Adelaja, A.O., Ogunmola, B.Y., & Akolade, P.O. (2009). Development of a photovoltaic powered forced convection solar dryer, Advanced Materials Research Journal, 2009, 62-64, pp. 543-548.

Agbo, S. N., & Okoroigwe, E. C. (2007). Analysis of thermal losses in the flat-plate collector of a Thermosyphon Solar water Heater. *Research Journal of Physics*, *1*(1), 35-41.

Ahn, J.G., Kim, J.H., & Kim, J.T. (2015). A study on experimental performance of air-type PV/T collector with HRV, Energy Procedia Journal, 6th International Building Physics Conference, 78, pp. 3007 – 3012

Aissa, W., Ei-Sallak, M., & Elhakem, A. (2014). Performance of solar dryer chamber used by convective drying of Spong-Cotton, *Thermal Science*, 18, S451-S462.

Akinola, A.O., & Fapetu, O.P. (2006). Exergetic Analysis of a Mixed-Mode Solar Dryer. J. Engin. Appl. Sci. 1: 205-10.

Akpinar, E. K. (2006). Determination of suitable thin layer drying curve model for some vegetables and fruits. *Journal of food engineering*, *73*(1), 75-84.

Akpinar, E.K., & Koçyiğit, F. (2010). Energy and exergy analysis of a new flat-plate solar air heater having different obstacles on absorber plates, Applied Energy Journal, 87, pp. 3438–3450.

Aldabbagha, L.B.Y., Egelioglu, F., Al-Khawajah, M.F. (2010). The effect of partitioning single pass mesh wire packed bed solar air heater, 7th international conference on heat transfer, fluid mechanics and thermodynamics, 19-21 July, Antalya, Turkey.

Allan, J., Dehouche, Z., Stankovic, S., & Mauricette, L. (2015). Performance testing of thermal and photovoltaic thermal solar collectors. *Energy Science & Engineering*; 3(4): 310–326.

Al-Neama, M.A., & Farkas, I. (2015). Performance enhancement of solar air collectors, Book of Abstracts, 14th International Workshop for Young Scientists (BioPhys Spring 2015), Gödöllő, Hungary, May 27-29, 2015, pp. 40-4.

Al-Neama, M.A., & Farkas, I. (2018). Evaluation of Temperature and Relative Humidity Stratifications in a Solar Drying Chamber. Journal of Scientific and Engineering Research, 2018, 5(10):59-65 ISSN: 2394-2630.

Al-Neama, M.A., & Farkas, I. (2018). Utilization of Solar Air Collectors for Product's Drying Processes. Journal of Scientific and Engineering Research, 2018, 5(2):40-56 ISSN: 2394-2630.

Al-Neama, M.A., Farkas, I. (2016). Modelling of a modular indirect natural convection solar dryer, 11th International Conference on Solar Energy for Buildings and Industry, EuroSun2016, Palma (Mallorca), Spain, October 11-14, pp. 660-669.

Alobaid, M., Hughes, B., Heyes, A., & O'Connor, D. (2018). Determining the effect of inlet flow conditions on the thermal efficiency of a flat plate solar collector. *Fluids*, *3*(3), 67.

Alqadhi, A., Misha, S., Rosli, M.A.M., & Akop, M.Z. (2017). Design and Simulation of an optimized mixed mode solar dryer integrated with desiccant material. International Journal of Mechanical & Mechatronics Engineering. IJMME-IJENS Vol:17 No:06.

Amer, B. M. A., Hossain, M. A., & Gottschalk, K. (2010). Design and performance evaluation of a new hybrid solar dryer for banana. *Energy conversion and management*, *51*(4), 813-820.

Ankit, S. G., & Dilip, G. (2014). Testing and Performance of the Convex Lens Concentrating Solar Power Panel Prototype. *International Journal of Emerging Technology and Advanced Engineering* Vol.04, Issue 6, June 2014, ISSN 2250-2459.

Aravindh, M., & Sreekumar, A. (2014). Experimental and economic analysis of a solar matrix collector for drying application. Current Science (00113891), 107(3), pp. 350-355.

Aregbesola, O. A., Ogunsina, B. S., Sofolahan, A. E., & Chime, N. N. (2015). Mathematical modeling of thin layer drying characteristics of dika (Irvingia gabonensis) nuts and kernels. *Nigerian Food Journal*, *33*(1), 83-89.

Armel, F.Z., Lessoy, T. Z., Niamkey, J.A., & Sebastian, L. N. (2015). The effect of sun drying on nutritive. African Journal of Science and Research, pp. 24-31.

Armstrong, P. R., McNeil, S., Manu, N., Bosomtwe, A., Danso, J. K., Osekre, E., & Opit, G. (2017). Development and evaluation of a low-cost probe-type instrument to measure the equilibrium moisture content of grain. *Applied engineering in agriculture*, *33*(5), 619-627.

ASABE Standards. 2008. S352.2 APR1988 (R2008): Moisture measurement - Unground grains and seeds. St. Joseph, Mich.: ASABE.

ASABE Standards. 2009. D245.6 OCT 2007: Moisture relationships of plant based agricultural products. St. Joseph, Mich.: ASABE.

Ayadi, M., Mabrouk, S. B., Zouari, I., & Bellagi, A. (2014). Kinetic study of the convective drying of spearmint. *Journal of the Saudi Society of Agricultural Sciences*, *13*(1), 1-7.

Badgujar, V.R. (2012). An experimental investigation of solar dryer with regenerative desiccant material for multicrops. International Journal of Engineering Research and Applications (IJERA) ISSN: 2248-9622 Vol. 2, Issue 3, May-Jun 2012, pp.3144-3149.

Bagheri, N., Tarabi, N., & Javadikia, H. (2015). Development and evaluation of an adaptive neuro-fuzzy interface models to predict performance of a solar dryer. Agricultural Engineering International: CIGR Journal, 17(2), pp. 112-121.

Bahrehmand, D., & Ameri, M. (2015). Energy and exergy analysis of different solar air collector systems with natural convection. *Renewable Energy*, *74*, 357-368.

Bake, M., Shukla, A., Liu, S., & Agrawal, A. (2019). A systematic review on parametric dependencies of transpired solar collector performance. *International Journal of Energy Research, 43*(1), 86-112.

Bala, B. K., Morshed, M. A., & Rahman, M. F. (2009). Solar drying of mushroom using solar tunnel dryer. International Solar Food Processing Conference, pp. 1-11.

Banout, J., Ehl, P., Havlik, J., Lojka, B., Polesny, Z., & Verner, V. (2011) Design and performance evaluation of a Double-pass solar dryer for drying of red chilli (Capsicum annum L.). Solar Energy, 85(3), pp. 506-515.

Belessiotis, V., & Delyannis, E. (2011). Solar drying. Solar Energy, 85: 1665–1691.

Belessiotis, V., Kalogirou, S., & Delyannis, E. (2016). *Thermal Solar Desalination: Methods and Systems*. Elsevier.

Bennamoun, L. (2013). Integration of photovoltaic cells in solar drying systems. *Drying technology*, *31*(11), 1284-1296.

Bhagyashree, P., Vanita, B., & Sneha, D. (2013). Thin layer drying of long pepper (Piper longum L.). *Journal of Spices and Aromatic Crops, 22*(1), 31-37.

Bhatt, M. K., Gaderia, S. N., & Channiwala, S. A. (2009). Experimental investigations on top loss coefficients of solar flat plate collector at different tilt angle. *World Acad Sci Eng Technol, 79*, 432-436.

Bhatt, M. K., Gaderia, S. N., & Channiwala, S. A. (2017). Experimental Investigations on Top Loss Coefficients of Solar Flat Plate Collector at Different Tilt Angle. I: World Academy of Science, Engineering and Technology [Elektronisk artikkel]. 2011 [Hentet 2013-10-15]; 55. *Tilgjengelig fra: http://www. waset. org/journals/waset/v55. php*.

Bhattacharyya, T., Anandalakshmib, R., & Srinivasan, K., (2017). Heat Transfer Analysis on Finned Plate Air Heating Solar Collector for its Application in Paddy Drying. Energy Procedia, pp. 353-360.

Bhushan, B., & Singh, R. (2010). A review on methodology of artificial roughness used in duct of solar air heaters. *Energy*, *35*(1), 202-212.

Bola, F., Bukola, A. F., Olanrewaju, I. S., & Adisa, S. B. (2013). Design parameters for a small-scale batch in-bin maize dryer, Agricultural Sciences, 4(5B), pp. 90-95.

Bolaji, B.O. & Olalusi, A.P. (2008). Performance Evaluation of a Mixed Mode Solar Dryer. *AU.J.T* 11(4):225-231

Bolaji, B.O. (2005). Development and performance evaluation of box-type absorber solar air collector for crop drying, Journal of Food Technology, 3(4), 515–600.

Bozkır, O. (2006). Thin layer drying and mathematical modelling for washed dry apricots. *Journal of food engineering*, *77*(1), 146-151.

Can, A. (2000). Drying kinetics of pumpkinseeds, International Journal of Energy Research, 24, pp. 965-975.

Chabane, F., Moummi, N., & Benramache, S. (2013). Experimental analysis on thermal performance of a solar air collector with longitudinal fins in a region of Biskra, Algeria. *Journal of Power Technologies*, *93*(1), 52-58.

Chayjan, R. A., Parian, J. A., & Esna-Ashari, M. (2011). Modeling of moisture diffusivity, activation energy and specific energy consumption of high moisture corn in a fixed and fluidized bed convective dryer. *Spanish Journal of Agricultural Research*, *9*(1), 28-40.

Chen, C. H., Hsu, C. Y., Chen, C. C., & Chen, S. L. (2015). Silica gel polymer composite desiccants for air conditioning systems. *Energy and buildings*, *101*, 122-132.

Chen, C. H., Hsu, C. Y., Chen, C. C., Chiang, Y. C., & Chen, S. L. (2016). Silica gel/polymer composite desiccant wheel combined with heat pump for air-conditioning systems. *Energy*, *94*, 87-99.

Chramsa-ard, W. Jindaruksab, S., Sirisumpunwonga, C., & Sonsareea, S. (2013). Performance evaluation of the desiccant bed solar dryer. Elsevie Energy Procedia 34 (2013) 189 – 197.

Coradi, P. C., Milane, L. V., Dias, C. F., & Baio, F. H. R. (2016). Mathematical modeling of drying maize grains in different temperatures. *Revista Brasileira de Milho e Sorgo*, *14*(2), 247-259.

Corrêa, P. C., Botelho, F. M., Oliveira, G. H. H., Goneli, A. L. D., Resende, O., & Campos, S. D. C. (2011). Mathematical modeling of the drying process of corn ears. *Acta Scientiarum. Agronomy*, *33*(4), 575-581.

Costa, S. J. (2014). Reducing Food Losses in Sub-Saharan Africa. *An 'Action Research'Evaluation Trial from Uganda and Burkina Faso*.

Da Silva, W. P., e Silva, C. M., Gama, F. J., & Gomes, J. P. (2014). Mathematical models to describe thin layer drying and to determine drying rate of whole bananas. *Journal of the Saudi Society of Agricultural Sciences*, *13*(1), 67-74.

Da Silva, W. P., Rodrigues, A. F., e Silva, C. M. D., de Castro, D. S., & Gomes, J. P. (2015). Comparison between continuous and intermittent drying of whole bananas using empirical and diffusion models to describe the processes. *Journal of Food Engineering*, *166*, 230-236.

Dagde, K.K & Iminabo, J.T, (2018). Determination of kinetic parameters for thin layer drying of corn, International Research Journal of Advanced Engineering and Science, Volume 3, Issue 4, pp. 119-124.

Darvishi, H., Farhang, A., & Hazbavi, E. (2012). Mathematical modeling of thin layer drying of shrimp. *Global Journal of Science Frontier Research Mathematics and Decision Sciences*, *12*(3), 82-90.

Delgado, S.E., Martinez-Flores, H.E., Garnica-Romo, M.G., Aranda-Sanchez, J.I., Sosa-Aguirre, C.R., Cortes-Penagos, C.D.J., & Fernandez-Munoz, J.L. (2013). Optimization of solar dryer for the dehydration of fruits and vegetables, Journal of Food Processing and Preservation ISSN 1745-4549.

Demir, V., Gunhan, T., Yagcioglu, A. K., & Degirmencioglu, A. (2004). Mathematical modelling and the determination of some quality parameters of air-dried bay leaves. *Biosystems engineering*, *88*(3), 325-335.

Duffie, J., & Beckman, W. (2013). Solar Engineering of Thermal Processes, Fourth edition, John Wiley & Sons, New Jersey, USA.

Ekechukwu, O. & Norton, B., (1999). Review of solar-energy drying systems II: an overview of solar drying technology. *Energy Conversion & Management*, pp. 615-655. *40*(6), 615-655.

Elsafi, A. M., & Gandhidasan, P. (2015). Comparative study of double-pass flat and compound parabolic concentrated photovoltaic–thermal systems with and without fins. *Energy conversion and management*, *98*, 59-68.

El-sebaii, A.A., Aboul-enein, S., Ramadan, M.R.I., & EL-gohary, H.G. (2002). Experimental investigation of an indirect type natural convection solar dryer. Ener. Convers. Manag. *43*, 2251–2266.

Emelue, H. U., Omehe, N., Oghome, P., & Amanze, K. (2014). Design and Construction of Cabinet Solar Dryers British Journal of Applied Science & Technology 5(3): 270-284, 2015, Article no. BJAST.2015.026 ISSN: 2231-0843.

Erenturk, K., Erenturk, S., & Tabil, L. G. (2004). A comparative study for the estimation of dynamical drying behavior of Echinacea angustifolia: regression analysis and neural network. *Computers and Electronics in Agriculture*, *45*(1-3), 71-90.

Erenturk, S., Gulaboglu, M. S., & Gultekin, S. (2004). The thin-layer drying characteristics of rosehip. *Biosystems Engineering*, *89*(2), 159-166.

Ertekin, C., Yaldiz, O. (2004). Drying of eggplant and selection of a suitable thin layer drying model, Journal of Food Engineering, 63, pp. 349-359.

FAO/AfDB, (2009). Framework Paper on Postharvest Loss Reduction in Africa. UN

Farkas, I. (2013). Integrated Use of Solar Energy for Crop Drying. Drying Technology, 31(8), pp. 866-871.

Fathima, H. A., Priya, K., Sudakar, B.T., Devabalaji, K.R., Rekha, M., Rajalakshmi, K., & Shilaja, C. (2014). Problems in conventional energy sources and subsequent shift to green energy. *International Journal of Innovative Research in Science, Engineering and Technology.*Volume 3, February 2014.

Fernando, J. A. K. M., & Amarasinghe, A. D. U. S. (2016). Drying kinetics and mathematical modeling of hot air drying of coconut coir pith. *SpringerPlus*, *5*(1), 807.

Fudholi, A, Sopian K, Ruslan M.H, Alghoul, M. A, & Sulaiman, M.Y. (2010). Review of solar dryers for agricultural and marine products. Renew Sust Energy Rev 14:1–30.

Fudholi, A., Othman, M. Y., Ruslan, M. H., Yahya, M., Zaharim, A., & Sopian, K. (2011). The effects of drying air temperature and humidity on drying kinetics of seaweed. *Recent Research in Geography, Geology, Energy, Environment and Biomedicine*, 129-133.

Gan, P. L., & Poh, P. E. (2014). Investigation on the effect of shapes on the drying kinetics and sensory evaluation study of dried Jackfruit. *International Journal of Science and Engineering*, *7*(2), 193-198.

Gill, R. S., Singh, S., & Singh, P. P. (2014). Design and development of desiccant seed dryer with airflow inversion and recirculation. *Journal of food science and technology*, *51*(11), 3418-3424.

Gill, R. S., Sukhmeet, S., & Parm, P. S. (2012). Solar Dryer for Powder Drying, Drying Technology, 30:14, 1666-1673, DOI: 10.1080/07373937.2012.704468.

Gluesenkamp, K., & Radermacher, R. (2011). Heat-activated cooling technologies for small and micro combined heat and power (CHP) applications. In *Small and Micro Combined Heat and Power (CHP) Systems* (pp. 262-306). Woodhead Publishing.

Gonzalez, S.M., Larsen,S.F., Hernandez,A., & Lesino,G. (2014). Thermal evaluation and modelling of a double-pass solar collector for air heating. Energy Procedia 57 (2014) 2275– 2284.

Goyal, R. K., Kingsly, A. R. P., Manikantan, M. R., & Ilyas, S. M. (2007). Mathematical modelling of thin layer drying kinetics of plum in a tunnel dryer. *Journal of Food Engineering*, *79*(1), 176-180

Guan, Z., Wang, X., Li, M., & Jiang, X. (2013). Mathematical modeling on hot air drying of thin layer fresh tilapia fillets. *Polish journal of food and nutrition sciences*, *63*(1), 25-33.

Gulandaz, A., Ali, R., Hasan, M., Jahan, N., Rahman, M., & Alam, N. (2015). Performance evaluation of modified hybrid solar dryer for paddy seed. International Journal of Postharvest Technology and Innovation, Vol. 5, No. 2, 2015.

Hanif, M. U. H. A. M. M. A. D., Khattak, M. K., Rahman, M., Khan, M., Amin, M., & Ramzan, M. (2014). Performance evaluation of a flat plate solar collector as a dryer for chillies and tomatoes. *J. Sci. Tech. and Dev*, *33*(2), 63-67.

Hematian, A., & Bakhtiari, A.A. (2015): Efficiency analysis of an air solar flat plate collector in different convection modes, International Journal of Green Energy, 12(9), pp. 881-887.

Henriksson, R., & Gustafsson, G. (1986). Use of solar collectors for drying agricultural crops and for heating farm buildings. *Energy in agriculture*, *5*(2), 139-150.

Hii, C.L., Law, C.L., Cloke, M., & Suzannah, S. (2009). Thin layer drying kinetics of cocoa and dried product quality, *Biosyst. Eng.*, vol. 102, no. 2, pp. 153–161.

Hodali, R., & Bougard, J. (2001). Integration of desiccant unit in crops solar drying installation: optimization by numerical simulation, Energy Conversion and Management 42 (2001) 1543–1558.

Hodges, R. (2009). Supplying Cereal Grain Postharvest Losses Information: The Examples of ALPHIS (African Postharvest Loss Information System).

Hossain, M. A., Amer, B. M. A., & Gottschalk, K. (2008). Hybrid Solar Dryer for Quality Dried Tomato Drying Technology,26:12,1591 — 1601.

Hottel, H.C., & Whillier, A. (1954). Evaluation of flate-plate solar collector performance," Transactions of Conference on the Use of Solar Energy, vol. 3, 1954.

Ibrahim, A., Othman, M. Y., Ruslan, M. H., Alghoul, M., Yahya, M., Zaharim, A., & Sopian, K. (2009). Performance of photovoltaic thermal collector (PVT) with different absorbers design. *WSEAS Transactions on Environment and Development, 5*(3), 321-330.

Ibrahim, Z., Ibarahim, Z., Yatim, B., Ruslan M.H. (2013). Thermal efficiency of single-pass solar air collector, AIP Conference Proceedings, 1571, pp. 90-94.

IFPRI. (2010). Aflatoxins in Kenya: an overview. Afla control project note 1, July 2010. Available online on**:** *http://programs.ifpri.org/afla/afla.asp.*

Iwe, M., Okoro, C., Eke, A. B., & Agiriga, A. (2019). Mathematical modelling of thin layer solar drying of Ighu. *Agricultural Engineering International: CIGR Journal*, *20*(4), 149-156.

Jacobi, A. M., & Shah, R. K. (1995). Heat transfer surface enhancement through the use of longitudinal vortices: a review of recent progress. *Experimental Thermal and Fluid Science*, *11*(3), 295-309.

Jain, D., & Tiwari, G. (2003). Thermal aspects of sun drying of various crops. Energy, 28(25), pp.37-54.

Janjai, S., &Tung, P. (2005). Performance of a solar dryer using hot air from roof-integrated solar collectors for drying herbs and spices. Renew Energy 30:2085–2095.

Jaruk, S., & John, S. R. (2007). Moisture transfer in solid food materials: a review of mechanisms, models, and measurements. *International Journal of Food Properties.* Retrieved from https://doi.org/10.1080/10942910601161672.

Johan, N. (2005). Optical Design and Characterization of Solar Concentrators for Photovoltaic. Department of Architecture and Built Environment, Division of Energy and Building Design, Lund University, Lund. ISSN 1651-8136 ISBN 91-85147-15-X.

Jradi, M., & Riffat, S. (2012). Medium temperature concentrators for solar thermal applications. *International Journal of Low-Carbon Technologies, 9*(3), 214-224.

Kalogirou, S. (2007). Recent patents in solar energy collectors and applications. *Recent Patents on Engineering*, *1*(1), 23-33.

Kang'ethe, E. (2011). Situation analysis: Improving food safety in the maize value chain in Kenya. *Report prepared for FAO. College of Agriculture and Veterinary Science, University of Nairobi, Nairobi*.

Karanja, D. D. (1996). *An economic and institutional analysis of maize research in Kenya* (No. 1096-2016-88394).

Kareem, M. W., Habib, K., Ruslan, M. H., & Saha, B. B. (2017). Thermal performance study of a multi-pass solar air heating collector system for drying of Roselle (Hibiscus sabdariffa). *Renewable Energy*, *113*, 281-292.

Kareem, M. W., Habib, K., Sopian, K., & Irshad, K. (2016). Performance evaluation of a novel multi-pass solar air heating collector. *Procedia engineering*, *148*, 638-645.

Kareem, M.W., Habib, K., Sulaiman, S.A. (2013). Comparative study of single pass collector and double pass solar collector filled with porous media, Asian Journal of Scientific Research, 6(3), pp. 445-455.

Karel, M., & Lund, D. B. (2003). *Physical principles of food preservation: revised and expanded* (Vol. 129). CRC Press.

Kaur, K., & Singh, A. K. (2014). Drying kinetics and quality characteristics of beetroot slices under hot air followed by microwave finish drying. *African Journal of Agricultural Research*, *9*(12), 1036-1044.

Kaygusuz, K. (2011). Energy services and energy poverty for sustainable rural development. *Renewable and sustainable energy reviews*, *15*(2), 936-947.

Kenya National Bureau of Statistics. (2014). Economic Survey, 2014; Production of maize ('000'MT) in Kenya (1972 - 2008) Data source: Republic of Kenya. Economic Surveys (various issues). Nairobi: Government Printer.

Kim, O. W., Kim, H., Kim, W., Lee, H. J., & Han, J. W. (2015). Simulation of Wheat Circulating Cross-flow Dryer. *Journal of Biosystems Engineering*, *40*(3), 232-237.

Kituu, G. M., Ngunzi, V. K., Mugucia, S. W., & Mutwiwa, U. N. (2013). Simulation model for predict drying in the automated grain dryer.

Kokate, D. H., Kale, D. M., Korpale, V. S., Shinde, Y. H., Panse, S. V., Deshmukh, S. P., & Pandit, A. B. (2014). Energy conservation through solar energy assisted dryer for plastic processing industry. *Energy Procedia*, *54*, 376-388.

Kumar, A., Singh, R., Prakash, O., & Shutosh, A. (2014). Review on global solar drying status. Agricultural Engineering International: CIGR Journal, 16(4), pp. 161-177.

Kumar, D., & Kalita, P. (2017). Reducing postharvest losses during storage of grain crops to strengthen food security in developing countries. *Foods (Basel, Switzerland)*, *6*(1), 8. doi:10.3390/foods6010008

Kumar, M., Sansaniwal, S. K., & Khatak, P. (2016). Progress in solar dryers for drying various commodities. *Renewable and Sustainable Energy Reviews*, *55*, 346-360.

Kurtbas, I., & Turgut, E. (2006). Experimental investigation of solar air heater with free and fixed fins: efficiency and exergy loss, International Journal of Science & Technology, 1(1), pp. 75-82.

Law, T. (2013). *The future of thermal comfort in an energy-constrained world*. Springer Science & Business Media.

Leon, M., & Kumar, S. (2006). Mathematical modeling and thermal performance analysis of unglazed transpired solar collectors. Elsevier, September, pp. 62-75.

Lingayat, A., Chandramohan, V.P. & Raju, V.R.K. (2017). Design, Development and Performance of Indirect Solar Dryer for Banana Drying. *Energy Procedia* 109: 409-416.

Mahboub, C., Moummi, N., Brima, A., & Moummi, A. (2016). Experimental study of new solar air heater design, International Journal of Green Energy, 13(5), pp. 521-529.

Maheshwari, G., (2014). Solar drying – psychrometry. *IOSR Journal of Applied Chemistry (IOSR-JAC) ISSN: 2278-5736, PP 54-57. www.iosrjournals.org*

Maia, C., Ferreira, A., Valle, R., & Cortez, M. (2009). Analysis of the Airflow in a Prototype of a Solar Chimney Dryer. Heat Transfer Engineering, 30(5), pp. 393-399.

Mbithi, L.M. (2000). Agricultural policy and maize production in Kenya: Universiteit Gent, Unpublished Ph.D Thesis.

Mbuge, D.O., Renata, N., Livine, O.N., Serge, P.K., Ranajit, B., William, M.M., Baldwyn, T., & Raffaele, M. (2016). Application of superabsorbent polymers (SAP) as desiccants to dry maize and reduce aflatoxin contamination. Journal of food science and technology, 53(8), pp. 3157-3165.

Mc Doom, I.A., Ramsaroop, R., Saunders, R., & Kai, A.T. (1999). Optimization of solar crop drying, *Renewable Energy*, 16, 749-752.

Meesukchaosumran, S., & Chitsomboon, T. (2019). Dimensionless variable groups for the free-fall grain dryer. *International Journal of Agricultural and Biological Engineering*, *12*(4), 197-204.

Meisami-Asl, E., Rafiee, S., Keyhani, A., & Tabatabaeefar, A. (2010). Determination of suitable thin layer drying curve model for apple slices (variety-Golab). *Plant Omics*, *3*(3), 103.

Menges, H. O., & Ertekin, C. (2006). Mathematical modeling of thin layer drying of Golden apples. *Journal of Food Engineering*, *77*(1), 119-125.

Mewa, E. A., Okoth, M. W., Kunyanga, C. N., & Rugiri, M. N. (2019). Experimental evaluation of beef drying kinetics in a solar tunnel dryer. *Renewable energy*, *139*, 235-241.

Midilli, A., Kucuk, H., & Yapar, Z. (2002). A new model for single-layer drying. *Drying technology*, *20*(7), 1503-1513.

Misha, S., Mat, S., Ruslan, M.H., Salleh, E., & Sopian, K. (2016). Performance of a solar-assisted solid desiccant dryer for oil palm fronds drying. Sol Energy 132:415–429.

Misha,S., Mat,S., & Ruslan, M. (2014). Performance Test of Solar Assisted Solid Desiccant Dryer. Computer Applications in Environmental Sciences and Renewable Energy, pp. 174-179.

Mrema, G., Gumbe, L., Chepete, H., & Agullo, J. (2012). Farm structures in the tropics: Design and development, Rome: FAO/CTO.

Mrema, G.C., Gumbe, L.O., Chepete, H.J., & Agullo, J.O. (2011). Rural structures in the tropics: design and development. ISBN 978-92-5-107047-5.

Mulokozi, G., & Svanberg, U. (2003). Effect of traditional open sun-drying and solar cabinet drying on carotene content and vitamin A activity of green leafy vegetables. Plant Foods for Human Nutrition, 58(3), pp. 1-15.

Munira, A., Sultan, U., & Iqbal, M. (2013). Development and performance evaluation of a locally fabricated portable solar tunnel dryer for drying of fruits, vegetables and medicinal plants. Pak J Agric Sci 50:493–498.

Naphon, P. (2005). On the performance and entropy generation on double pass solar air heater with Fins. Renewable Energy, pp. 1345-1357.

Naveen Kumar B.K., Sushma, M.S., & Raveesha. S. (2016). Convex lens with transparent glass solar water heating system. International Journal of Research in Engineering and Technology 2319-1163, 2321-7308.

Ngindu, A., Johnson, B.K, Kenya, P.R, Ngira, J.A, Ocheng, D.M, Nandwa, H., Omondi, T.N, Jansen, A.J, Ngare, W., Kaviti, J.N, Gatei, D., & Siongok, T.A. (1982). Outbreak of acute hepatitis caused by aflatoxin poisoning in Kenya. Lancet, Volume 319, p. 1346–1348.

Ngunzi, V. (2014, May). Simulation Model for Predict Drying in the Automated Grain Dryer. In *Scientific Conference Proceedings*.

Norton B. (2017) Characteristics of Different Systems for the Solar Drying of Crops. In: Prakash O., Kumar A. (eds) Solar Drying Technology. Green Energy and Technology. Springer, Singapore

Nwakuba, N. R. (2017). A mathematical model for predicting the drying rate of cocoa bean (Theobroma cacao L.) in a hot air dryer using dimensional analysis. *Agricultural Engineering International: CIGR Journal*, *19*(3), 195-202.

Nyariki, W. O., Mulati, D. M., & Maina, D. M. (2016). Design and Characterization of a Hybrid Flat Plate Photovoltaic-Thermal System. In *Proceedings of Sustainable Research and Innovation Conference* (pp. 262-268).

Ohijeagbon, I. O., Ogunfowora, L. I., Omale, J. I., & Ameh, P. (2016). Energetic performance analysis of drying agricultural products with solar tracking. Nigerian Journal of Technology (NIJOTECH) vol. 35, no. 4, October 2016 pp. 825 – 830.

Okoth, S., & Kola, M., (2012). Market samples as a source of chronic aflatoxin exposure in Kenya. African Journal of Health Sciences, Volume 20, pp. 56-61.

Oloo, F., Olang, L., & Strobl, J. (2016). Spatial Modelling of Solar Energy Potential in Kenya. International Journal of Sustainable Energy Planning and Management Vol. 06 2016 17-30.

Omofunmi, O.E., & Alli, A.A. (2016). Performance Evaluation and Comparison Studies on Drying Characteristics of Sliced Plantain and Maize. British Journal of Applied Science & Technology 15(4): 1-7, 2016, Article no. BJAST.24682 ISSN: 2231-0843, NLM ID: 101664541.

Omolola, A. O., Jideani, A. I., & Kapila, P. F. (2014). Modeling microwave drying kinetics and moisture diffusivity of Mabonde banana variety. *International Journal of Agricultural and Biological Engineering*, *7*(6), 107-113.

Ong, S., Campbell, C., Denholm, P., Margolis, R., & Heath, G. (2013). *Land-use requirements for solar power plants in the United States* (No. NREL/TP-6A20-56290). National Renewable Energy Lab. (NREL), Golden, CO (United States).

Onwude, D. I., Hashim, N., Janius, R. B., Nawi, N. M., & Abdan, K. (2016). Modeling the thin layer drying of fruits and vegetables: A review. *Comprehensive reviews in food science and food safety*, *15*(3), 599-618.

Osodo, B. O. (2018). *Simulation and Optimisation of a Drying Model for a Forced Convection Grain Dryer* (Doctoral dissertation, Kenyatta University).

Osodo, B., Nyaanga, D., Kiplagat, J. & Muguthu, J. (2018). Optimum Air Velocity, Air Temperature and Maize Layer Thickness for Highest Moisture Removal Rate and Drying Efficiency in a Forced Convection Grain Dryer. *American Journal of Food Science and Technology*, vol. 6, no. 6: 263-273. doi: 10.12691/ajfst-6-6-6.

Padmanaban, G., Palani, P. K., & Murugesan, M. (2017). Performance of a desiccant assisted packed bed passive solar dryer for copra processing. *Thermal science*, pp. S419-s426.

Perez, R., & Perez, M. (2009). A fundamental look at energy reserves for the planet. *The IEA SHC Solar Update*, *50*(2).

Pirasteh, A., Saidur, R., Rahman, S.M.A., & Rahim, N.A. (2014). A review on development of solar drying applications. Renew Sust Energy Rev 31:133–148.

Poole, L. (2001). *Concentrating solar power: Energy from mirrors* (No. DOE/GO-102001-1147; NREL/BR-810-28751). National Renewable Energy Lab., Golden, CO (US).

Prakash, O. & Kumar, A., (2017). Solar Drying Technology: Concept, Design, Testing, Modeling, Economics, and Environment. s.l.: Springer.

Prasad, J., Prasad, A., & Vijay, V. K. (2006). Studies on the drying characteristics of Zingiber officinale under open sun and solar biomass (hybrid) drying. *International journal of green energy*, *3*(1), 79-89.

Prasartkaew, B., & Kumar, S. (2014). Design of a renewable energy-based air-conditioning system. *Energy and Buildings*, *68*, 156-164.

Probert, R. J. (2003). Seed viability under ambient conditions, and the importance of drying. *Seed conservation: turning science into practice*, 337-365.

Proszak-Miąsik, D., & Rabczak, S. (2017). Impact of solar radiation change on the collector efficiently. *Journal of Ecological Engineering*, *18*(1).

Punlek, C., Pairintra, R., Chindaraksa, S., & Maneewan, S. (2009). Simulation design and evaluation of hybrid PV/T assisted desiccant integrated HA-IR drying system (HPIRD). *Food and Bioproducts Processing*, *87*(2), 77-86.

Querikiol, E. M., & Taboada, E. B. (2018). Drying kinetics of mango byproducts in a greenhouse-type solar dryer using a wireless weighing scale. *International Journal of Applied Engineering Research*, *13*(22), 15933-15943.

Rajkumar, P., Kulanthaisami, S., Raghavan, G. S. V., Gariépy, Y., & Orsat, V. (2007). Drying kinetics of tomato slices in vacuum assisted solar and open sun drying methods. *Drying Technology*, *25*(7-8), 1349-1357.

Ramani, B.M, Akhilesh, G. & Ravi, K. (2010). Performance of a double pass solar air collector. *Solar Energy* 2010; 84; 11; 1929-37.

Ramaswamy, H. & Marcotte, M. (2006. Food Processing - Principles and Applications. London: Taylor and Francis Group.

Rayaguru, K., & Routray, W. (2012). Mathematical modeling of thin layer drying kinetics of stone apple slices.

Rembold, F., Hodges, R., Bernard, M., Knipschild, H., & Léo, O. (2011). The African postharvest losses information system (APHLIS). *European Union, Luxembourg*.

Román, F., Mbuge, D. O., & Hensel, O. (2019). Modeling the effect of a superabsorbent polymer material as desiccant in maize drying using CFD. *Drying Technology*, *37*(11), 1441-1453.

Sadeghi, G., Taheri, O., & Mobadersani, F. (2012). New technologies of Solar Drying Systems for Agricultural and Marine Products. s.l., s.n.

Saeed, I. E., Sopian, K., & Abidin, Z. Z. (2008). Drying characteristics of Roselle (1): mathematical modeling and drying experiments. *Agricultural Engineering International: CIGR Journal*.

Sahdev, R. K., Kumar, M., & Dhingra, A. K. (2016). A review on applications of greenhouse drying and its performance. *Agricultural Engineering International: CIGR Journal*, *18*(2), 395-412.

Sámano, D.E., Martinez-Flores, H. E., Garnica-Romo, M. G., Aranda-Sanchez, J. I., Sosa-Aguirre, C. R., De Jesús Cortés-Penagos, C. O. N. S. U. E. L. O., & Fernández-Muñoz, J. L. (2013). Optimization of solar dryer for the dehydration of fruits and vegetables. *Journal of food processing and preservation*, *37*(5), 489-495.

Sami, S., Rahimi, A., & Etesami, N. (2014). Economical optimization of an indirect solar cabinet dryer based on mathematical modelling. *Environmental Engineering & Management Journal (EEMJ)*, *13*(10).

Sayibu, S.W., & Ampadu, O.M. (2015). Effectiveness of Biogas Production from Slaughter Waste using Two Mixing Ratios (Waste: Water Ratio of 1: 1 and 1: 2), *5*(2).

Sencan, A., & Özdemir, G. (2007). Comparison of thermal performances predicted and experimental of solar air collector, Journal of Applied Sciences, 7(23), pp. 3721-3728.

Seshachalam, K., Thittipalayam, A., & Selvaraj, V. (2017). Drying of Carrots Slices in a Tripple Pass Solar Dryer. Thermal Science, pp. S389-S398.

Shanmugam, V., & Natarajan, E. (2006). Experimental investigation of forced convection and desiccant integrated solar dryer. *Renew Energy*, 31(8):1239–51.

Shanmugam, V., & Natarajan, E. (2007). Experimental study of regenerative desiccant integrated solar dryer with and without reflective mirror. *Appl Therm Eng*, 27(8–9):1543–51.

Sharma, A., Chen, C. R., & Lan, N. V. (2009). Solar-energy drying systems: A review. *Renewable and sustainable energy reviews*, *13*(6-7), 1185-1210.

Sharma, S. P., Saha, S.N. (2017). Thermohydraulic performance of double flow solar air heater with corrugated absorber, International Journal of Energy and Power Engineering, 11(7), pp.855-861.

Sharma, V.K., Colangelo, A., Spagna, G., & Pistocchi, F. (1994). Preliminary economic appraisal of solar air heating system used for drying of agricultural products. *Energy Convers Manage*, 35(2):105–10.

ShazibUddin, M.D., Parvez, M., & Enamul, H. (2016). Construction and Performance Study of a Rock Bed Integrated Green House Type Solar Air Heater with Solar Dryer. IOSR Journal of Environmental Science, Toxicology and Food Technology (IOSR-JESTFT) e-ISSN: 2319-2402, p- ISSN: 2319-2399.Volume 10, Issue 5 Ver. I (May. 2016), PP30-36.

Shemelin, V., & Matuska, T. (2017). Detailed Modeling of Flat Plate Solar Collector with Vacuum Glazing. *International Journal of Photoenergy*, *2017*.

Singh, P.P., Singh, S., & Dhaliwal, S.S. (2006). Multi-shelf domestic solar dryer. Energy Convers Manage 47(13–14):1799–1815.

Singh, S., & Kumar, S. (2012). New approach for thermal testing of solar dryer: development of generalized drying characteristic curve. *Solar energy*, *86*(7), 1981-1991.

Smitabhindu, R., Janjai, S., & Chankong, V. (2008). Optimization of a solar-assisted drying system for drying bananas, *Renewable Energy*, 33, 1523-1531.

Soponronnarit, S. (2017). Review of research and development work on forced convection solar drying in Thailand. *International Energy Journal*, *10*(1).

Sreekumar, A. (2010). Techno-economic analysis of a roof-integrated solar air heating system for drying fruit and vegetables. Energy Convers Manag 51:2230–2238.

Srikiatden, J., & Roberts, J. S. (2007). Moisture transfer in solid food materials: A review of mechanisms, models, and measurements. *International Journal of Food Properties*, *10*(4), 739-777.

Steiner, M, Siefer, G., Schmidt, T., Wiesenfarth, M., Dimroth, F., & Bett, A.W. (2016). 43% Sunlight to Electricity Conversion Efficiency Using CPV. IEEE J. Photovolt. 2016, 6, 1020–1024.

Struckmann, F. (2008). Analysis of a flat-plate solar collector. *Heat and Mass Transport, Project Report, 2008MVK160*.

Sundari, A.R.U., Neelamegam, P., & Subramanian, C.V. (2013). An experimental study and analysis on solar drying of bitter ground using an evacuated tube air collector in Thanjavur, Tamil Nadu, India, International conference on solar energy photovoltaic.

Tashtosh, G. M., Jaradat, M., Zuraiakt, S., & Aljarah, M. (2014). A mathematical model of indirect solar drying of dairy products (Jameed). *Energy and Environmental Engineering*, *2*(1), 1-13.

Tefera, T. (2012). Post-harvest losses in African maize in the face of increasing food shortage. *Food security*, *4*(2), 267-277. Springer

Temp, A. (2011). Impact of Air Temperature on Relative Humidity-A study. Available at https://www.coa.gov.in/show_img.php?fid=98 . Last accessed 31st March 2019.

Timsina, K., Dahal, P., Bradford, K. J., Kunusoth, K., Van Asbrouck, J., Pandey, I., ... & Shivakoti, G. (2014). Impacts of a new post-harvest drying technology on the horticultural seed value chain in Nepal. In *Selected paper presented at the 29th international horticultural congress* (pp. 17-22).

Tiwari, A. (2016). A review on solar drying of agricultural produce. *Journal of Food Processing and Technology*, *7*(9), 623.

Tiwari, G. N., Bhatia, P. S., Singh, A. K., & Sutar, R. F. (1994). Design parameters of a shallow bed solar crop dryer with reflector. *Energy conversion and management*, *35*(6), 535-542.

Tonui, K. S., Mutai, E. B. K., Mutuli, D. A., Mbuge, D. O., & Too, K. V. (2014). Design and evaluation of solar grain dryer with a back-up heater. *Research Journal of Applied Sciences, Engineering and Technology*, *7*(15), 3036-3043.

Toshniwal, U., Karale, S.R (2013). A review paper on Solar Dryer, International Journal of Engineering Research and Applications (IJERA), 3(2), pp. 896-902.

Tsoutsos, T., Frantzeskaki, N., & Gekas, V. (2005). Environmental impacts from the solar energy technologies. *Energy Policy*, *33*(3), 289-296.

Umayorupagam, P.A., Edwin, M. (2017). Experimental investigations on thermal performance of solar air heater with different absorber plates, International Journal of Heat And Technology, 35(2), pp. 393-397.

Umogbai, V. I., & Iorter, H. A. (2013). Design, construction and performance evaluation of a passive solar dryer for maize cobs. *African Journal of Food Science and Technology*, *4*(5), 110-115.

Velic, D., Ackar, D., Mujic, I., Subaric, D., Bilic, M., & Jokic, S. (2010). Influence of drying temperature on drying kinetics and physico-chemical properties of two chestnut varieties (Castanea sativa Mill.). *Acta horticulturae*.

Velmurugan, P., Kalaivanan, R. (2013). Effect of diverse stream patterns on the performance of solar air heater, International Journal of Mechanical Engineering and Robotics Research, 2(1), pp. 65-70.

VijayaVenkata Raman, S., Iniyan, S., & Goic, R. (2012). A review of solar drying technologies. *Renewable and sustainable energy reviews*, *16*(5), 2652-2670.

Vitázek, I., & Vereš, P. (2013). Drying rate of grain maize. *Acta Technologica Agriculturae*, *16*(2), 31-34. 10.2478/ata-2013-0008.

Vlachos, N. A., Karapantsios, T. D., Balouktsis, A. I., & Chassapis, D. (2002). Design and testing of a new solar tray dryer, drying technology. An International Journal, 20:6, 1243-1271.

Waewsak, J. Chindaruksa, S., & Punlek, C. (2006). A mathematical modeling study of hot air drying for some agricultural products. Thammasat International Journal of Science and Technology, 11(1): 14-20.

Weiss W. & Buchinger, J. (2012). *Solar Drying.* Training Course within the Scope of the Project Establishment of a Production, Sales and Consulting Infrastructure for Solar Thermal Plants in Zimbabwe. Australian Development Cooperation, Institute of Sustainable Technologies, Australia

White, S. D., Goldsworthy, M., Reece, R., Spillmann, T., Gorur, A., & Lee, D. Y. (2011). Characterization of desiccant wheels with alternative materials at low regeneration temperatures. *International Journal of Refrigeration*, *34*(8), 1786-1791.

Winkler, H., Simões, A. F., La Rovere, E. L., Alam, M., Rahman, A., & Mwakasonda, S. (2011). Access and affordability of electricity in developing countries. *World development*, *39*(6), 1037-1050.

World Bank (2010). *Missing Food: The case of postharvest grain losses in Sub*- Saharan Africa.

Yang, M., Wang, P., Yang, X., & Shan, M. (2012). Experimental analysis on thermal performance of a solar air collector with a single pass, Building and Environment Journal, 56, pp. 361-369.

Yang, M., Yang, X., Li, X., Wang, Z., & Wang, P. (2014). Design and optimization of a solar air heater with offset strip fin absorber plate. *Applied Energy*, 113, 1349-1362.

Yeh, H. M. (2014). Effect of Pass Number on Collector Efficiency in Downward-Type Multipass Solar Air Heaters. Journal of Applied Science and Engineering, 17(2), pp. 175-184.

Zarezade, M., & Mostafaeipour, A. (2016). Identifying the effective factors on implementing the solar dryers for Yazd province, Iran. *Renewable and Sustainable Energy Reviews*, *57*, 765-775.

Zelzouli, K., Guizani, A., Sebai, R., & Kerkeni, C. (2012). Solar thermal systems performances versus flat plate solar collectors connected in series. *Engineering*, *4*(12), 881.

Zenoozian, M. S., Feng, H., Razavi, S. M. A., Shahidi, F., & Pourreza, H. R. (2008). Image analysis and dynamic modeling of thin layer drying of osmotically dehydrated pumpkin. *Journal of Food processing and Preservation*, *32*(1), 88-102.

Zhang, L. Z. (2013). Conjugate heat and mass transfer in heat mass exchanger ducts. *Elsevier.*

Zorya, S., Morgan, N., Diaz Rios, L., Hodges, R., Bennett, B., Stathers, T., ... & Lamb, J. (2011). Missing food: The case of postharvest grain losses in sub-Saharan Africa.

APPENDIX

Appendix A: Design drawings

Figure 8-1: Dryer bin compartment dimensions

Appendix B:Dryer description

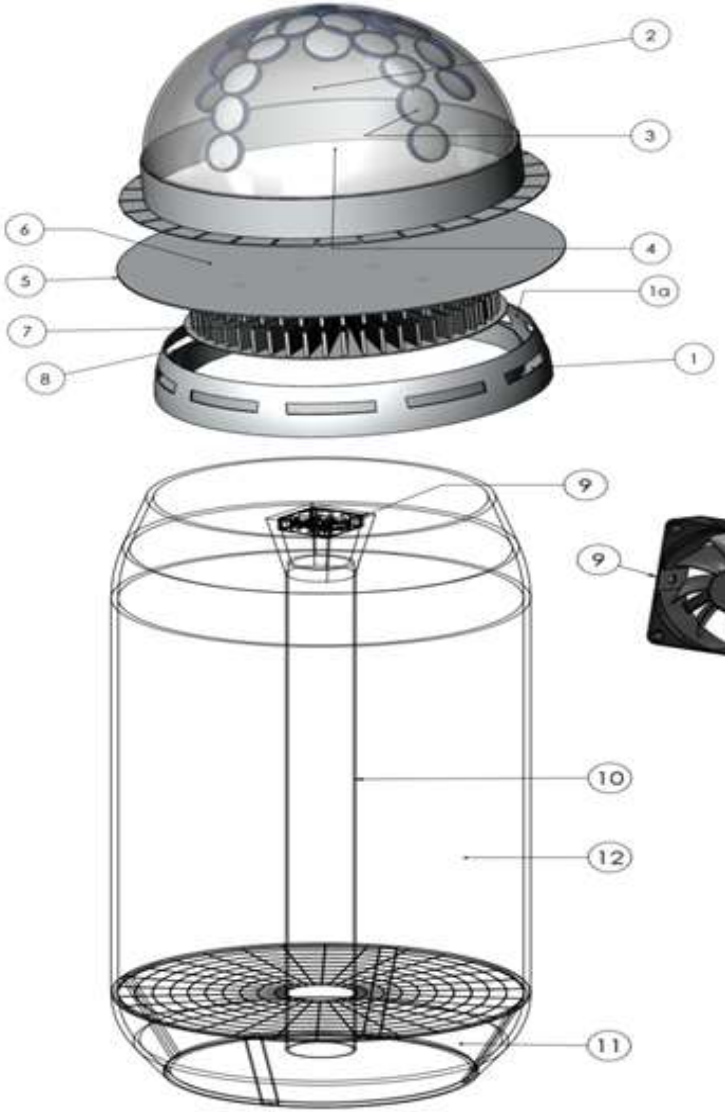

No.	Description
1	Ambient/Recirculate Air Inlet
1a	Air inlet channel to the finned elements
2	Acrylic glazing (2mm transmits 90% infrared)
3	Array of Convex lenses radiation concentrators
4	Evacuated space (Prevent heat loss)
5	Black coated collector and solar concentrator surface
6	Black coated collector plate
7	Extended surfaces (High density of finned elements)
8	Back plate
9	Centrifugal fan
10	Air conduit
11	Plenum chamber
12	Grain drying chamber

Figure 8-2: Solar dryer components

Appendix C:Solar collector components

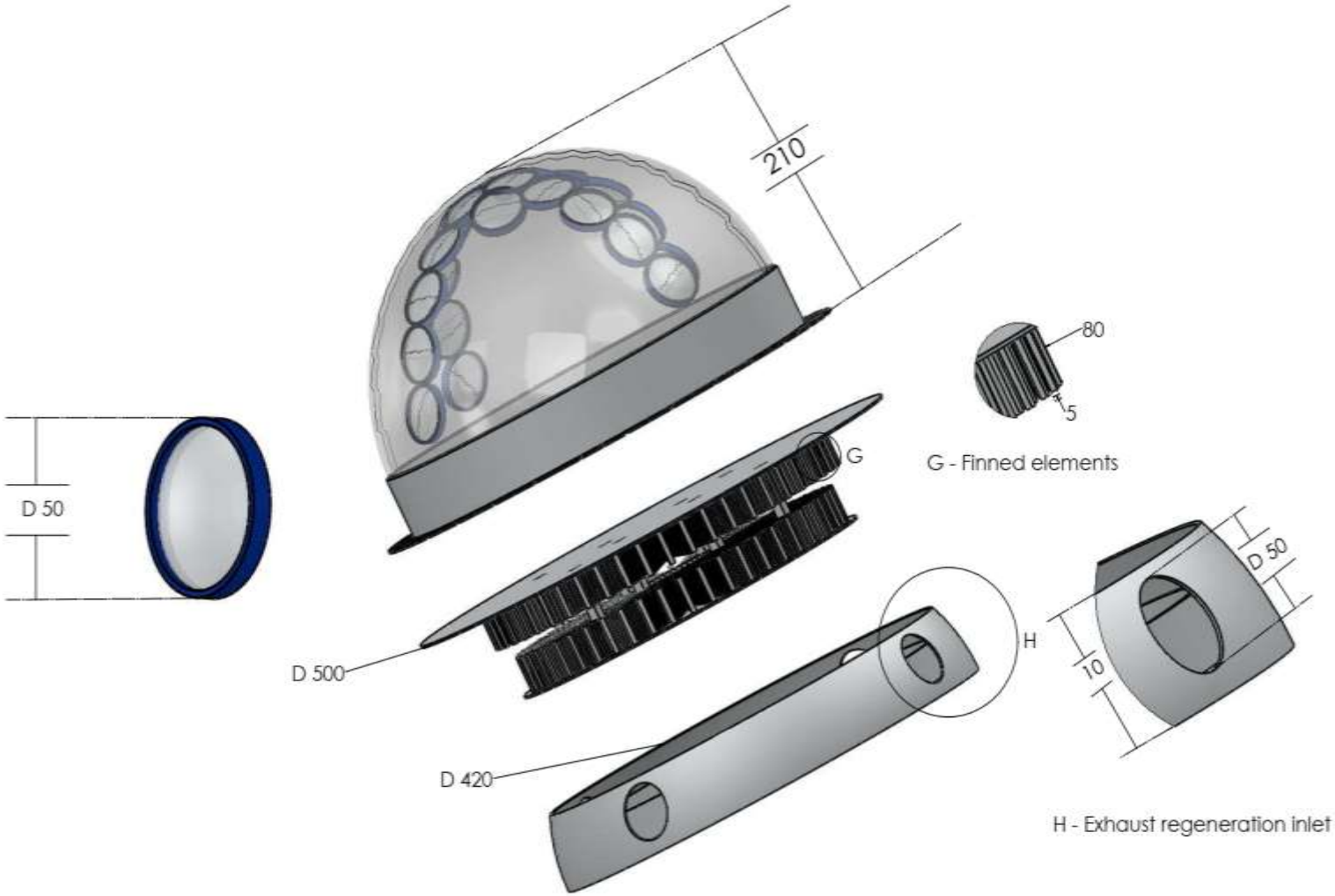

Figure 8-3: Solar collector with exhaust degeneration inlets

Appendix D:Exhaust air regeneration desiccant lined conduit

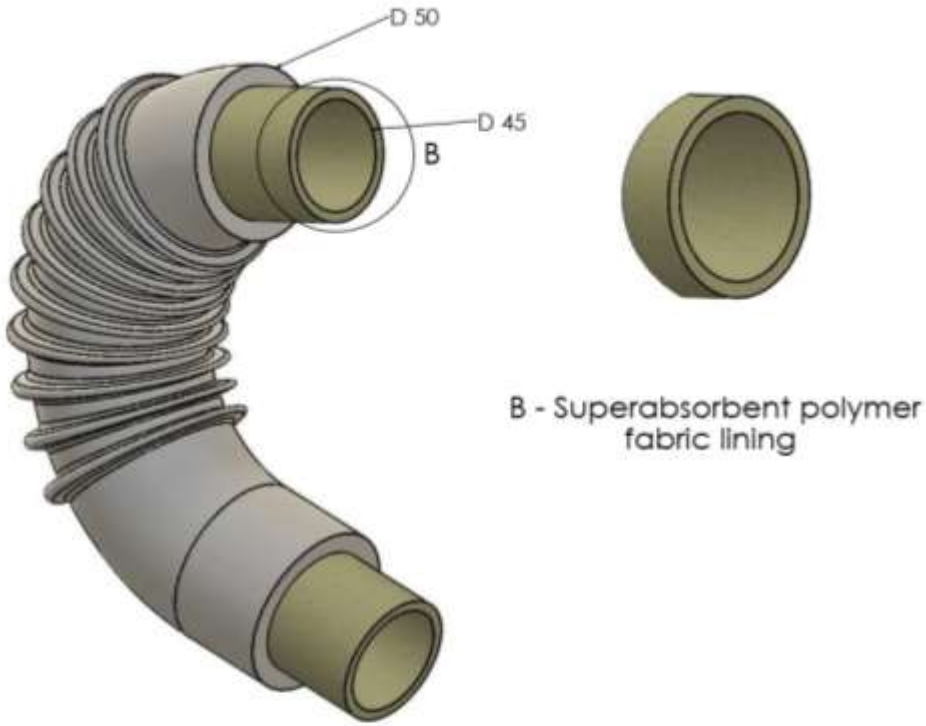

Figure 8-4: Exhaust desiccant recirculation system

Appendix E:Interior dryer components

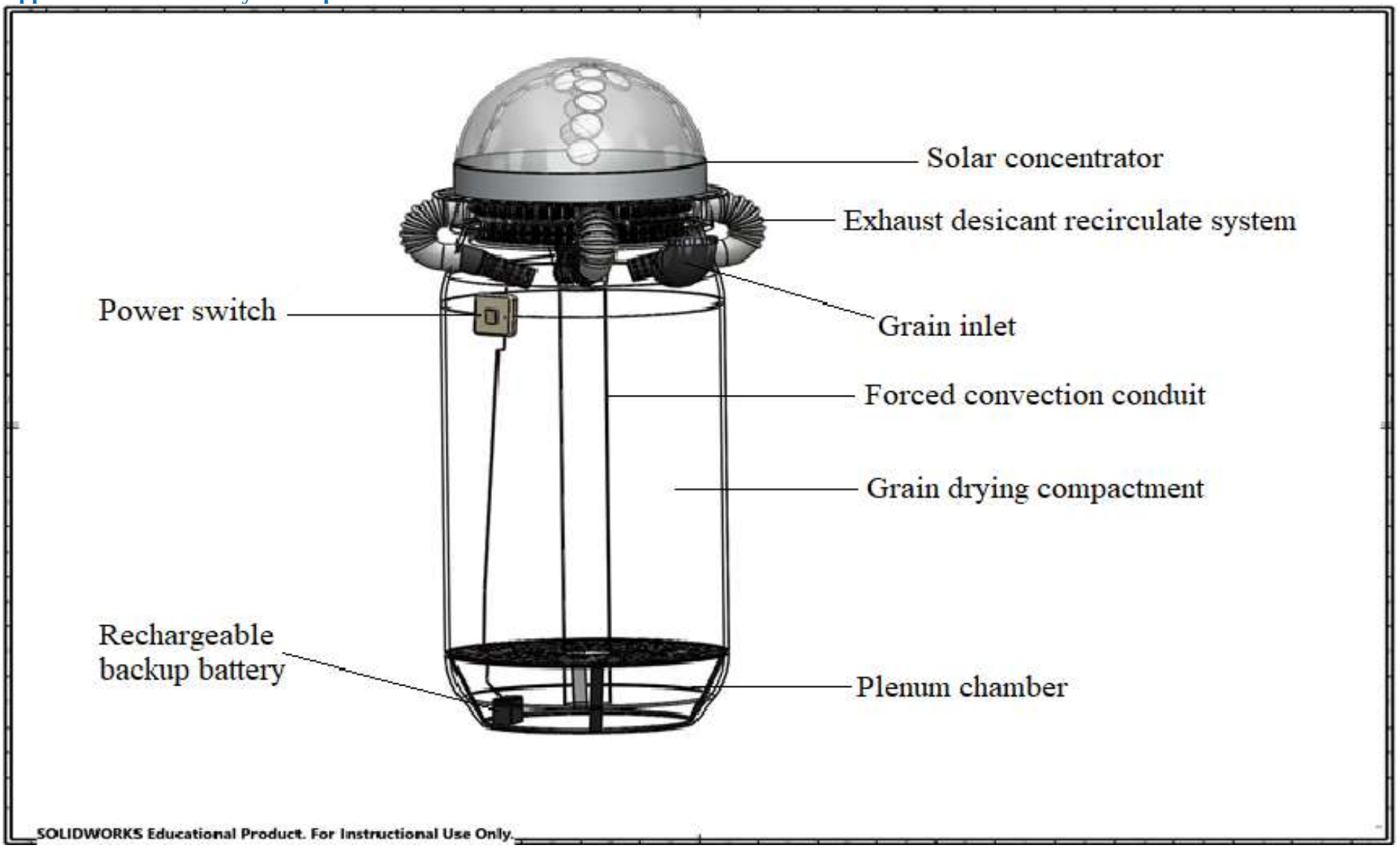

Figure 8-5: Wireframe view of the interior dryer components

Appendix F: Conceptual fabrication framework

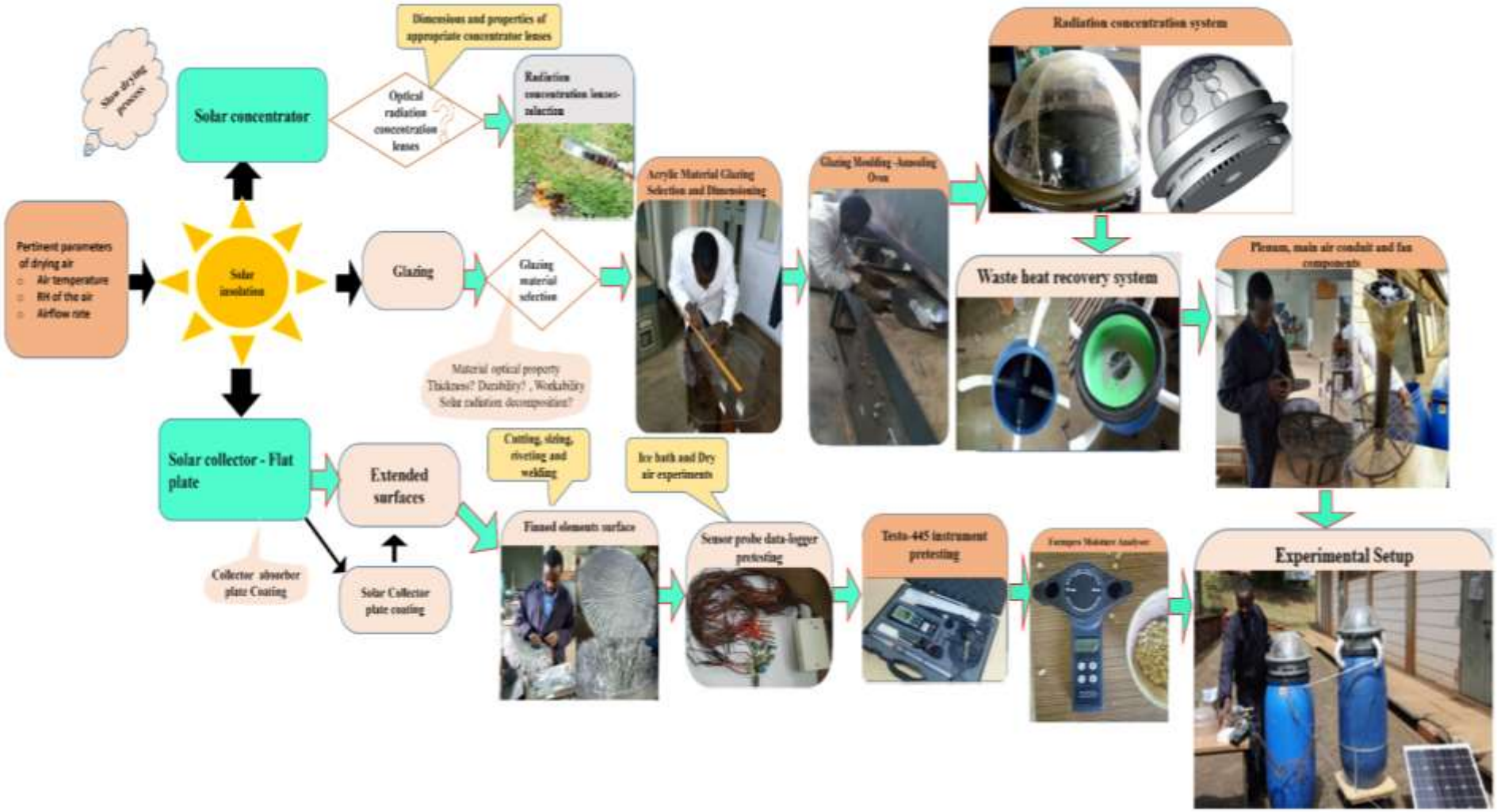

Plate 8-1: Conceptual fabrication framework

Appendix G: Exhaust recirculation dryer inlets

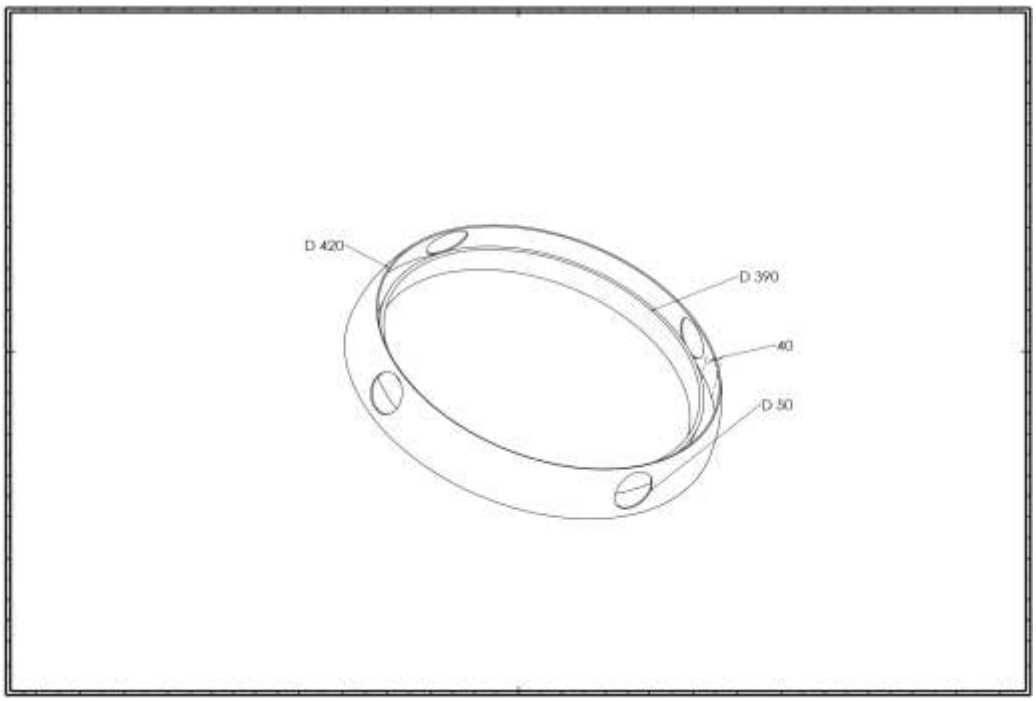

Figure 8-6: Exhaust regeneration inlets

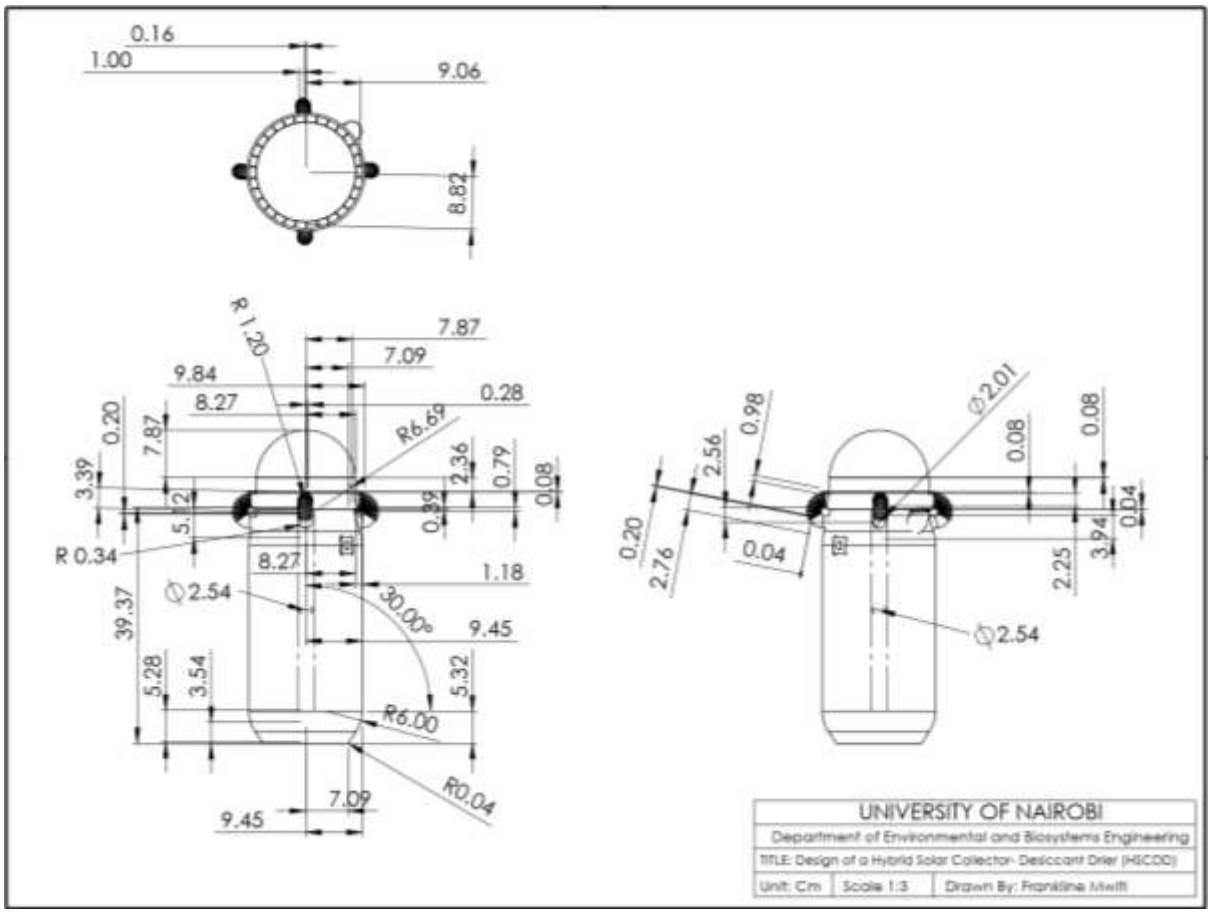

Figure 8-7: Detailed drawing of the Hybrid solar desiccant dryer

Appendix H: Hybrid solar dryer dimensions

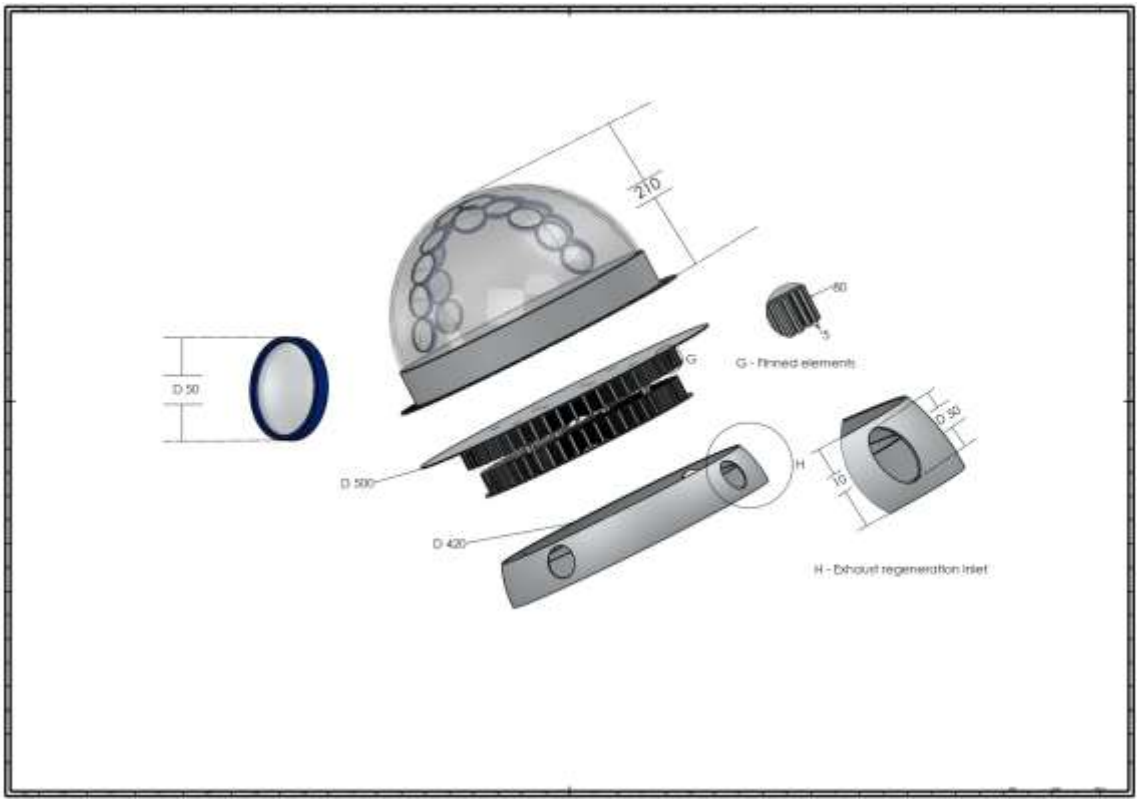

Figure 8-8: Solar collector dimensions

Appendix I: Air flows within the drying chamber

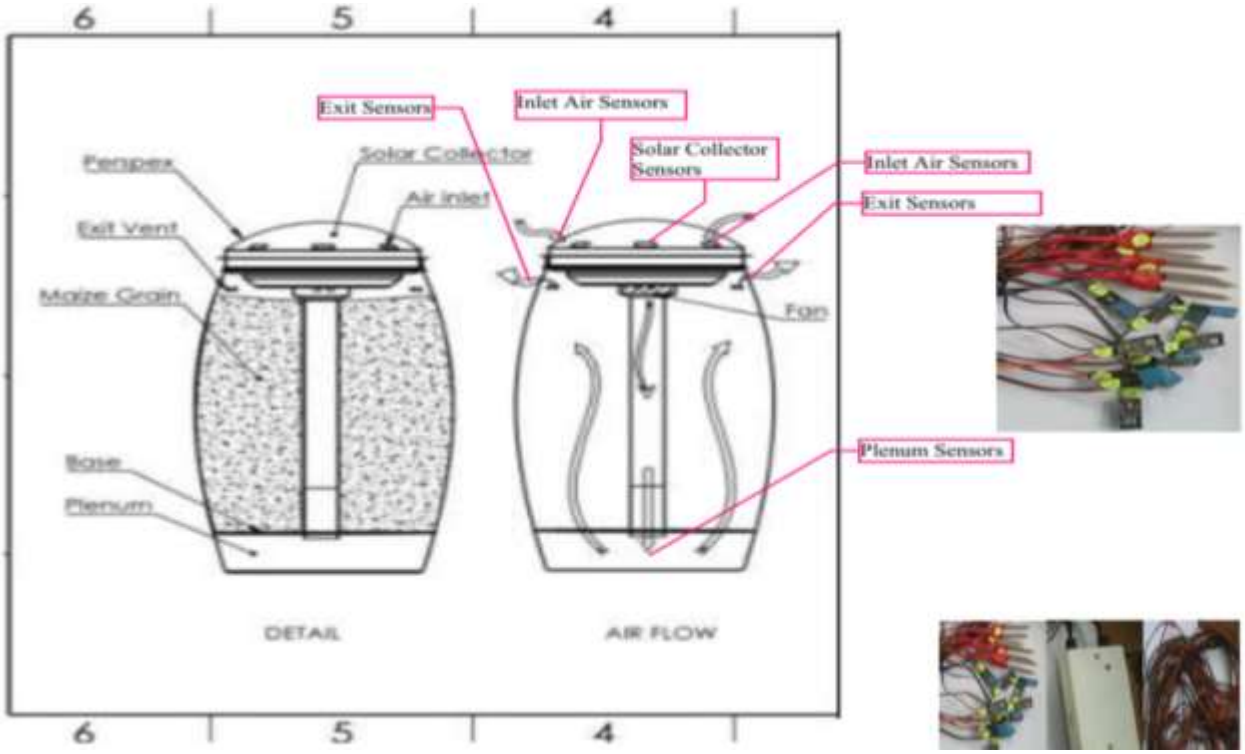

Plate 8-2: Air flow through grain drying chamber

Appendix J: Initially existing dryer bin

Plate 8-3: Initial existing dryer bin

Appendix K: Workshop fabrication works

Plate 8-4: Moulding solar collector glazing in annealing oven and Fabrication of collector plate and finned elements surfaces

Plate 8-5: Exhaust regeneration conduits fabrication

Plate 8-6(a): Plenum system fabrication

Plate 8-6(b): Solar concentrator plate heating by radiation concentration lenses

Appendix L: Preparation of grain drying experiments

Plate 8-7: Grain drying experimentation

Appendix M: Exhaust air regeneration and inlet-outlet (single pass) dryer

Plate 8-8: Desiccant exhaust recirculation dryer and Ambient inlet-outlet dryer (single pass)

Appendix N:Finished product Hybrid-solar desiccant maize grain dryer

Plate 8-9: Finished product fabricated hybrid solar desiccant dryer

Appendix O: Average daily solar irradiance for Kabete-October 2018

Table 8.1: Average daily radiation in Kabete

Day of the month	Solar Irradiance (w/m^2)	Day of the month	Solar Irradiance (w/m^2)
1	750	17	770
2	700	18	600
3	830	19	530
4	850	20	550
5	750	21	610
6	650	22	510
7	750	23	600
8	720	24	520
9	770	25	500
10	800	26	590
11	850	27	530
12	820	28	550
13	780	29	500
14	760	30	540
15	720	31	580
16	780	Average irradiance	670

Appendix P: Hourly temperatures for various solar collector configurations

Table 8.2: Average temperature values with time

Time (hrs.)	Ambient	Fins	Lenses	Regeneration	Integration of Fins, Lenses and exhaust Regeneration
8:00	19.9	20.6	20.7	20.5	20.8
9:00	21.5	22.9	29.9	31.5	32.5
10:00	22.3	31.5	44.6	41.4	52.2
11:00	23.9	36.0	52.2	45.2	57.1
12:00	25.0	38.7	55.1	49.0	60.5
13:00	26.9	40.5	59.1	52.5	65.0
14:00	25.3	37.4	54.4	47.0	60.4
15:00	24.4	34.6	49.2	42.0	56.6
16:00	23.5	28.5	43.1	37.1	54.7
17:00	22.1	24.0	36.5	34.1	52.5
Average	23.48	31.47	44.48	40.03	51.23

Appendix Q: Hourly relative humidity values for various solar collector configurations

Table 8.3: Relative humidity for various solar collector configurations

Time (Hrs.)	Ambient	Fins	Lenses	Recirculation	Integration of Fins, Lenses and Recirculation
8:00	70	70	70	69	68
9:00	68	68	62	58	50
10:00	65	63	49	52	41
11:00	61	52	38	43	34

12:00	58	50	34	38	29
13:00	57	47	32	35	27
14:00	61	51	33	39	29
15:00	60	52	35	41	31
16:00	63	55	40	47	34
17:00	68	60	46	53	36

Appendix R: Variation of temperature and relative humidity values

Table 8.4: Variation of temperature and relative humidity for various collector configurations

Ambient conditions		**Finned elements**		**Radiation concentration lenses**		**Exhaust air regeneration**		**Fins, lenses and exhaust air regeneration**	
T(°C)	RH (%)	T(°C)	RH (%)	T(°C)	RH (%)	T(°C)	RH (%)	T(°C)	RH (%)
20	70	21	70	21	70	21	69	21	68
22	68	23	68	30	62	32	58	32	50
22	68	24	63	37	51	34	53	52	41
23	63	29	55	43	40	37	47	53	34
22	65	31	60	45	49	41	52	55	37
24	61	35	52	49	35	42	41	57	31
24	61	36	52	52	38	45	43	57	34
25	58	37	50	54	32	47	38	60	29
25	60	39	51	55	34	49	39	61	29
27	57	41	47	59	31	53	35	65	28

Appendix S: Hourly temperature changes for various solar collector configurations

Table 8.5: Temperature changes for solar collector configurations

Time (hrs.)	**Fins**	**Lenses**	**Regeneration**	**Integration of Lens, Fins and Regeneration**
8:00	0.7	0.8	0.6	0.9
9:00	1.4	8.4	10.0	11.0
10:00	9.1	22.3	19.1	29.9
11:00	12.1	28.3	21.3	33.2
12:00	13.7	30.2	24.0	35.6
13:00	13.6	32.2	25.6	38.1
14:00	12.1	29.1	21.7	35.1
15:00	10.2	24.8	17.6	32.2
16:00	6.0	19.6	14.6	31.2
17:00	1.9	14.4	13.0	30.4
Average	8.1	21.0	16.8	27.8

Appendix T: Hourly changes in relative humidity for various solar collector configurations

Table 8.6: Changes in relative humidity

Time (hrs.)	Fins	Lenses	Recirculation	Integration of Lens, Fins and Regeneration
8:00	1	0	-1	-2
9:00	0	-6	-10	-17
10:00	-3	-16	-14	-25
11:00	-9	-23	-18	-27
12:00	-8	-24	-20	-29
13:00	-10	-26	-22	-29
14:00	-10	-29	-22	-32
15:00	-8	-25	-19	-30
16:00	-8	-23	-16	-29
17:00	-8	-17	-15	-29
Average	-6	-19	-16	-25

Appendix U: Changes in temperature and relative humidity

Table 8.7: Solar collector changes in temperature and relative humidity

Finned elements surfaces		Exhaust air regeneration		Radiation concentration lenses		Fins, lenses and exhaust air regeneration	
ΔT	ΔRh	ΔT	ΔRh	ΔT	ΔRh	ΔT	ΔRh
1	0	1	1	1	0	1	2
1	1	10	10	8	6	11	17
2	3	13	14	15	16	30	25
6	8	15	15	20	17	30	27
9	8	18	16	22	23	31	29
10	9	19	18	25	23	32	29
12	9	21	19	28	24	33	29
12	9	22	20	29	25	35	29
14	10	24	22	30	26	36	30
14	10	26	22	32	29	38	32

Appendix V: Solar collector performance calculations and analysis

The rate of useful heat gain from the solar collector was found by calculating the amount of heat energy extracted and carried by the stream of air mass that passed through the various collector configurations using equation (3.7). The air mass flow rate ṁ is found by multiplying the density of air (ρ) and the volumetric air flow rate, ṽ. The rate of volumetric air flow is found by product of air flow duct area (collector inlet) A_{duct} and the air speed V measured and recorded by the digital Testo-445 anemometer probe.

Therefore $\dot{m} = \rho * v * A_{duct}$

The instantaneous thermal efficiency (η) of the solar collector is represented by the ratio of the instantaneous useful heat collected by the air (Q_u) to the instantaneous total amount of radiation received at the solar collector plate area A_c during the experimental period.

i.e. $\eta = \frac{Q_u}{G*A_c}$

the area of inlet duct is calculated as;

Where; A= cross sectional area of inlet duct

Considering the four 2 inches inlet ducts area; 3.14x(0.0508/2) x(0.508/2))x4 =0.008103m^2

V = velocity at inlet air flow into the system (measured) in m/s =0.76 m/s

ρ_a = density of air in kg/m^3 (literature) = 1.225kg/m^3

mass flow rate = 0.008103x0.76x1.225 =0.007544 kg/s

Specific heat capacity of dry air (1.006 KJ/kg.K)

Considering solar insolation of 859 w/m^2 on the solar collector plate of 0.5m^2 and a change in air collector temperature of 38.1°C, then

$Q_u = \dot{m} * C_P * \Delta T$ = 0.007544*1006*38.1= 289.15W

Therefore, the instantaneous thermal efficiency η**,** of the solar air collector using Equation3.9. is:

$\eta = \frac{Q_u}{G*A_c} = \frac{289.15}{859*0.5}$ *100%= 67.3%

Appendix W: Solar collector useful energy

Table 8.8: Useful energy from solar air collectors

Time (hrs.)	**Solar irradiance (W/m²)**	**Useful energy absorbed, MCpΔt (kJs)**							
		Finned Elements Surfaces		**Exhaust Regeneration**		**Radiation Concentration Lenses**		**Finned Elements, Radiation Lenses and Exhaust Regeneration**	
		ΔT	MCP ΔT	ΔT	MCP ΔT	ΔT	MCP ΔT	ΔT	MCP ΔT
8:00	497	0.7	0.005	0.6	0.005	0.8	0.006	0.9	0.007
9:00	643	1.4	0.011	10	0.076	8.4	0.064	11	0.083
10:00	669	9.1	0.069	19.1	0.145	22.3	0.169	29.9	0.227
11:00	746	12.1	0.092	21.3	0.162	28.3	0.215	33.2	0.252
12:00	835	13.7	0.104	24	0.182	30.2	0.229	35.6	0.270
13:00	859	13.6	0.103	25.6	0.194	32.2	0.244	38.1	0.289
14:00	814	12.1	0.092	21.7	0.165	29.1	0.221	35.1	0.266
15:00	676	10.2	0.077	17.6	0.134	24.8	0.188	32.2	0.244

16:00	576	6	0.046	14.6	0.111	19.6	0.149	31.2	0.237
17:00	455	1.9	0.014	13	0.099	14.4	0.109	30.4	0.231
Average	677	8.1	0.061	16.8	0.127	21.0	0.159	27.8	0.211

Appendix X: Solar collector efficiency and insolation

Table 8.9: Solar collector efficiency and temperature changes per insolation

Finned elements surface		**Exhaust Regeneration**		**Radiation concentration lenses**		**Finned elements, Radiation lenses and exhaust-air-desiccant regeneration**	
Efficiency $\eta = Q_u/AI$	$\Delta t / I$	Efficiency $\eta = Q_u/AI$	$\Delta t / I$	Efficiency $\eta = Q_u/AI$	$\Delta t / I$	Efficiency $\eta = Q_u/AI$	$\Delta t / I$
0.021	0.006	0.018	0.010	0.024	0.013	0.027	0.010
0.033	0.007	0.236	0.016	0.198	0.014	0.260	0.020
0.206	0.008	0.433	0.021	0.506	0.019	0.678	0.040
0.246	0.01	0.433	0.026	0.576	0.024	0.676	0.040
0.249	0.014	0.436	0.027	0.549	0.028	0.647	0.045
0.240	0.014	0.452	0.028	0.569	0.030	0.673	0.050
0.226	0.015	0.405	0.031	0.543	0.020	0.655	0.060
0.229	0.018	0.395	0.034	0.557	0.037	0.723	0.055
0.158	0.03	0.384	0.040	0.516	0.045	0.822	0.060
0.063	0.03	0.433	0.060	0.480	0.055	0.923	0.075
Average η 0.167		0.363		0.452		0.608	

Appendix Y: Solar irradiance and efficiency for various collector configurations

Table 8.10: Irradiance and solar collector efficiency

Solar Irradiance (W/M^2)	**Efficiency**			
	Finned Elements Surface	**Exhaust Regeneration**	**Radiation Concentration Lenses**	**Integration of Finned Elements, Radiation Lenses and Exhaust Regeneration.**
497	0.021	0.018	0.024	0.027
643	0.033	0.236	0.198	0.260
669	0.206	0.433	0.506	0.678
746	0.246	0.433	0.576	0.676
835	0.249	0.436	0.549	0.647
859	0.240	0.452	0.569	0.673
814	0.226	0.405	0.543	0.655
676	0.229	0.395	0.557	0.723
576	0.158	0.384	0.516	0.822
455	0.063	0.433	0.480	0.923
Average				
677	0.167	0.363	0.452	0.608

Appendix Z: Change in temperature and collector efficiency

Table 8.11: Changes in temperature and collector efficiency

Finned Elements Surfaces		Exhaust Regeneration		lenses		Fins, Lenses and Exhaust Regeneration	
ΔT	**Efficiency, η**	**ΔT**	**Efficiency, η**	**ΔT**	**Efficiency, η**	**ΔT**	**Efficiency, η**
0.7	0.021	0.6	0.018	0.8	0.02	0.9	0.027
1.4	0.033	10	0.236	8.4	0.20	11	0.26
9.1	0.206	19.1	0.433	14.4	0.48	29.9	0.647
12.1	0.246	21.3	0.433	19.6	0.51	30.4	0.655
13.7	0.249	24	0.436	22.3	0.52	31.2	0.673
13.6	0.24	25.6	0.452	24.8	0.54	32.2	0.676
12.1	0.226	21.7	0.405	28.3	0.55	33.2	0.678
10.2	0.229	17.6	0.395	29.1	0.56	35.1	0.723
6	0.158	14.6	0.384	30.2	0.57	35.6	0.822
1.9	0.063	13	0.433	32.2	0.58	38.1	0.923

Appendix AA: Collector efficiency and useful heat gain

Table 8.12: Useful heat gain and collector efficiency

Finned element surfaces		Exhaust air Regeneration		Radiation concentration Lenses		Combined lenses, fins and exhaust regeneration	
Heat gain Qu	**Efficiency η**	**Heat gain Qu**	**Efficiency η**	**Heat gain Qu**	**Efficiency η**	**Heat gain Qu**	**Efficiency η**
0.005	0.02	0.005	0.02	0.006	0.02	0.007	0.03
0.011	0.03	0.076	0.24	0.064	0.20	0.083	0.26
0.014	0.06	0.099	0.38	0.109	0.48	0.227	0.65
0.046	0.16	0.111	0.40	0.149	0.51	0.231	0.66
0.069	0.21	0.134	0.41	0.169	0.52	0.237	0.67
0.077	0.23	0.145	0.43	0.188	0.54	0.244	0.68
0.092	0.23	0.162	0.43	0.215	0.55	0.252	0.68
0.092	0.24	0.165	0.43	0.221	0.56	0.266	0.72
0.103	0.25	0.182	0.44	0.229	0.57	0.27	0.82
0.104	0.25	0.194	0.45	0.244	0.58	0.289	0.92

Appendix BB: Solar insolation during grain drying

Table 8.13: Average hourly solar irradiance values during drying experiments

TIME (24Hrs)	SOLAR IRRADIANCE (w/m^2)	
	Day 1	**Day 2**
0830	515	475
0930	705	575
1030	745	630

1130	810	720
1230	833	830
1330	845	865
1430	780	840
1530	653	693
1630	558	590
1730	423	483

Appendix CC: Loaded grain inlet dryer temperatures and relative humidity

Table 8.14: Variation of dryer inlet (plenum) air temperatures and relative humidity

Appendix DD: Loaded grain outlet dryer temperatures and relative humidity

Table 8.15: Variation of dryer outlet temperatures and relative humidity

TIME	Average Solar Irradiance	Exhaust-Recirculation Dryer Outlet		Single Pass Dryer (inlet-outlet dryer) Outlet		Ambient Air (Open sun drying)	
		T	RH	T	RH	T	RH
8:30	495	20.2	69.0	20.1	68.0	19.5	72.0
9:30	640	23.3	71.0	21.5	69.0	20.0	69.0
10:30	666	24.5	73.0	21.4	69.0	22.3	66.0
11:30	743	25.0	76.0	22.4	70.0	23.9	66.0
12:30	831	26.0	79.0	22.0	70.0	25.0	64.0
13:30	855	26.5	80.0	22.0	71.0	25.6	63.0
14:30	810	27.0	79.0	21.0	70.0	25.3	65.0
15:30	673	27.0	78.0	22.0	70.0	24.4	65.0
16:30	574	26.0	77.0	21.0	69.0	23.5	68.0
17:30	453	26.0	76.0	21.0	69.0	21.9	70.0

Appendix EE: Natural open-air sun drying data

Table 8.16: Open sun drying data

Day	Time	M.C (%) W.b	Day	Time	M.C (%) W.b
Day 1	11:00	24.1	**Day 4**	11:00	15.25
	14:00	22.17		14:00	15.4
	17:00	21.12		17:00	14.91
Day 2	11:00	21.2	**Day 5**	11:00	14.5
	14:00	18.73		14:00	14.1
	17:00	18		17:00	14.2
Day 3	11:00	17.71	**Day 6**	11:00	13.5
	14:00	17.9		14:00	13.3
	17:00	16.49		17:00	13.2, 13.1

Table 8.17: OASD grain drying rate

Moisture content (% w.b)	D_R ($kg.kg^{-1}.hr^{-1}$)	Moisture content (% w.b)	D_R ($kg.kg^{-1}.hr^{-1}$)
24.1	0.9583	15.4	0.1319
22.2	0.8183	14.9	0.1154
21.1	0.5644	14.5	0.0762
21.2	0.4462	14.1	0.0761
18.7	0.4062	14.2	0.0584
18.0	0.3252	13.5	0.0402
17.7	0.2938	13.3	0.0384
17.9	0.2821	13.2	0.0380
16.5	0.2289	13.1	0.0380
15.3	0.1582		

Table 8.18: HSDD grain drying rate

Moisture content (% w.b)	D_R ($kg.kg^{-1}.hr^{-1}$)	Moisture content (% w.b)	D_R ($kg.kg^{-1}.hr^{-1}$)
24.1	5.0834	16.2	0.2300
22.1	4.2286	16.2	0.4589
20.4	1.6944	16.2	0.4578
19.8	1.4813	16.1	0.4567
19.4	1.2207	16.0	0.4557
18.9	0.9826	15.7	0.4557
18.2	0.7235	15.4	0.1180
17.9	0.7209	15.2	0.2357
17.6	0.9565	14.9	0.2324
17.2	0.7046	14.8	0.2383
17.0	0.7021	14.6	0.2371
16.9	0.6980	14.4	0.2368
16.7	0.4771	14.2	0.2366
16.7	0.4754	14.0	0.1188
16.6	0.4670	13.9	0.1187
16.5	0.4637	13.7	0.1182
16.4	0.4626	13.5	0.1181
16.3	0.4615	13.3	0.0472
16.3	0.4605	13.1	0.0708

Appendix FF: DEARD and SPD grain drying rate

Table 8.19: Predicted and experimental drying rate values for HSCDD

Time (hrs.)	Moisture content (% w.b)	Experimental drying rate (kg/hr.)	Predicted drying rate (kg/hr.)	Time (hrs.)	Moisture content (% w.b)	Experimental drying rate (kg/hr.)	Predicted drying rate (kg/hr.)

0.5	24.1	5.0834	7.5811	10.0	16.2	0.2300	0.3064
1.0	22.1	4.2286	3.6085	10.5	16.18	0.4589	0.2908
1.5	20.4	1.6944	2.3374	11.0	16.15	0.4578	0.2767
2.0	19.8	1.4813	1.7176	11.5	16.1	0.4567	0.2638
2.5	19.4	1.2207	1.3525	12.0	16.0	0.4557	0.2521
3.0	18.9	0.9826	1.1126	12.5	15.7	0.4557	0.2413
3.5	18.2	0.9565	0.9433	13.0	15.4	0.2357	0.2314
4.0	17.9	0.7235	0.8176	13.5	15.2	0.2324	0.2222
4.5	17.6	0.7209	0.7207	14.0	14.9	0.2383	0.2137
5.0	17.2	0.7046	0.6438	14.5	14.8	0.2371	0.2058
5.5	17.0	0.7021	0.5813	15.0	14.6	0.2368	0.1985
6.0	16.9	0.6980	0.5296	15.5	14.4	0.2366	0.1916
6.5	16.7	0.4771	0.4861	16.0	14.2	0.1188	0.1852
7.0	16.7	0.4754	0.4490	16.5	14.0	0.1187	0.1792
7.5	16.6	0.4670	0.4170	17.0	13.9	0.1182	0.1736
8.0	16.5	0.4637	0.3892	17.5	13.7	0.1181	0.1683
8.5	16.4	0.4626	0.3647	18.0	13.5	0.1180	0.1633
9.0	16.3	0.4615	0.3430	18.5	13.3	0.0472	0.1586
9.5	16.3	0.4605	0.3237	19.0	13.1	0.0708	0.1541

Appendix GG: DEARD and SPD grain moisture content variation with drying time

Table 8.20: Grain moisture content variation with time

Date	Time (hour)	Grain moisture content (% w.b)	
		Desiccant exhaust regeneration dryer (DEARD)	Ambient air inlet -outlet dryer (SPD)
11th Oct 2018	8:30	24.1	24.1
	9:00	22.1	24
	9:30	20.4	20.6
	10:00	19.8	20.2
	10:30	19.4	19.8
	11:00	18.9	20
	11:30	18.2	19.6
	12:00	17.9	19.7
	12:30	17.6	18.6
	13:00	17.2	18.8
	13:30	17	18.6
	14:00	16.9	18.4
	14:30	16.7	18.5
	15:00	16.6	18.1
	15:30	16.6	18.3
	16:00	16.5	18.1
	16:30	16.4	18.2
	17:00	16.3	17.9
	17:30	16.2	18

12th Oct 2018	8:00	16.2	17.9
	8:30	16.1	17.8
	9:00	16.1	17.6
	9:30	15.9	17.9
	10:00	15.8	17.7
	10:30	15.7	17.5
	11:00	15.4	17.4
	11:30	15.2	17.3
	12:00	14.9	16.9
	12:30	14.8	16.5
	13:00	14.6	16.3
	13:30	14.4	16.4
	14:00	14.2	16.1
	14:30	14.0	16
	15:00	13.9	15.9
	15:30	13.7	15.5
	16:00	13.5	15.3
	16:30	13.3	15.2
	17:00	13.1	15.1
	17:30	13.1	14.8
13th Oct 2018	8:00		14.7
	8:30		14.6
	9:00		14.5
	9:30		14.4
	10:00		14.2
	10:30		14.1
	11:00		13.9
	11:30		13.8
	12:00		13.7
	12:30		13.6
	13:00		13.5
	13:30		13.4
	14:00		13.3
	14:30		13.2
	15:00		13.2
	15:30		13.1

Table 8.21: HSDD experimental moisture ratio data

HSDD		
Time (min)	**MC**	**MR**
0	24.1	1.000
30	22.1	0.818
60	20.4	0.664
90	19.8	0.609
120	19.4	0.573

150	18.9	0.527
180	18.2	0.464
210	17.9	0.436
240	17.6	0.409
270	17.2	0.373
300	17.0	0.355
330	16.9	0.345
360	16.7	0.327
390	16.7	0.323
420	16.6	0.318
450	16.5	0.309
480	16.4	0.300
510	16.3	0.291
540	16.25	0.286
570	16.2	0.282
600	16.18	0.280
630	16.15	0.277
660	16.1	0.273
690	16.0	0.264
720	15.7	0.236
750	15.4	0.209
780	15.2	0.191
810	14.9	0.164
840	14.8	0.155
870	14.6	0.136
900	14.4	0.118
930	14.2	0.100
960	14.0	0.082
990	13.9	0.073
1020	13.7	0.055
1050	13.5	0.036
1080	13.3	0.018
1110	13.1	0.000

Appendix HH: T- test

The two dryers are here by compared statistically using a student T-test. The null hypothesis was that the two samples have got no significant differences. If the probability value is less

than the 0.05, then we reject the null hypothesis that the two means of the two populations means are the same. Thus, they are significantly different. Below is the output.

Two-sample t-test

Variates: Singlepass_dryer and Exhaust_regeneration_dryer.

Test for equality of sample variances

Test statistic F = 1.43 on 38 and 38 d.f.

Probability (under null hypothesis of equal variances) = 0.28

Table 8.22: T- test summary

	Sample Size	**Mean**	**Variance**	**Standard deviation**	**Standard error of mean**
Single pass dryer	39	16.03	7.493	2.737	0.4383
Exhaust regeneration dryer	39	17.65	5.254	2.292	0.3670

Difference of means: *-1.626*
Standard error of difference: *0.572*

95% confidence interval for difference in means: (-2.764, -0.4870)
Test of null hypothesis that mean of Single pass dryer is equal to mean of Exhaust regeneration dryer.
Test statistic t = -2.84 on 76 d.f.
Probability = 0.006

Appendix II: Small-scale traditional maize drying methods.

Appendix JJ: Superabsorbent polymer material safety data sheet

Printing date 04/17/2014 *Reviewed on 04/09/2014*

1 Identification

· **Product identifier**
· **Trade name: Super Absorbent Polymer**
· **Application of the substance / the preparation:** Absorb water and retaining water

· **Details of the supplier of the safety data sheet**
· **Manufacturer/Supplier:**
QINGDAO ST-ARN IMP & EXP CO.,LTD
NO.56 HongKong Middle Rd, Qingdao, China
Tel: 0086-532-86120912
Fax: 0086-532-83888779

· **Further information obtainable from:** QINGDAO ST-ARN IMP & EXP CO.,LTD
· **Emergency telephone number:**
Cynthia Liu
Tel: 13791941101
· **Email:** starn@st-arn.com
· **Reference Number:** QDHG201400929; SHAHG1405590901

2 Hazard(s) identification

· **Hazard description:** Not applicable.
· **Information pertaining to particular dangers for man and environment:**
The product is not classified as dangerous according to OSHA Hazard Communication standard (29 CFR 1910.1200)
· **Classification system:**
The classification is according to the latest edition of the OSHA Hazard Communication Standard (29 CFR 1910.1200), and extended by company and literature data.
· **NFPA ratings (scale 0 - 4)**

Health = 0
Fire = 0
Reactivity = 0

· **HMIS-ratings (scale 0 - 4)**

Health = 0
Fire = 0
Reactivity = 0

3 Composition/information on ingredients

· **Chemical characterization: Mixtures**
· **Description:** Mixture of the substances listed below with nonhazardous additions.

· **Dangerous components:** Not applicable

· **Non dangerous components:**

9003-04-7	Sodium polyacrylate	96.0%
7732-18-5	water	4.0%

4 First-aid measures

· **Description of first aid measures**
· **After inhalation:**
Supply fresh air; consult doctor in case of complaints.
In case of unconsciousness place patient stably in side position for transportation.
· **After skin contact:**
Wash with water and soap and rinse thoroughly.
If skin irritation continues, consult a doctor.

(Contd. on page 2)

Appendix KK: Model fitting data

Table 8.23: Drying kinetics model fitting data

Model No		1	2	3	4	5	6	7	8	9	10	11	12	13	14	15	16	17	18
Time (min)	Experimental M. R	Newton model	Page model	Modified page	Henderson & Pabis	Modified Henderson and pabis	Logarithmic	Midilli	Modified midilli	Two term	Wang & Singh model	Diffusion approach	Two term and Page	Singh model	Peleg model	Hii *et al* model	Verma *et al*	Two term exponential	Silva *et al*
0	1.0000	1.0000	1.0000	1.0000	0.8003	1.0000	0.8306	1.0000	0.7263	1.0042	1.0000	1.0000	1.0002	1.0000	1.0000	1.0025	1.0000	1.0000	1.0000
30	0.8182	0.9187	0.7952	0.7952	0.7498	0.6939	0.7703	0.0076	0.6862	0.8025	0.9389	0.9186	0.7951	0.9051	0.8595	0.8716	0.9281	0.8883	0.7792
60	0.6636	0.8440	0.7014	0.7015	0.7024	0.6539	0.7148	0.0152	0.6483	0.6829	0.8799	0.8439	0.7013	0.8197	0.7524	0.7105	0.8614	0.7973	0.6924
90	0.6091	0.7754	0.6326	0.6327	0.6581	0.6163	0.6636	0.0228	0.6124	0.6070	0.8230	0.7752	0.6326	0.7429	0.6680	0.6156	0.7994	0.7218	0.6288
120	0.5727	0.7123	0.5776	0.5777	0.6165	0.5808	0.6164	0.0304	0.5785	0.5545	0.7683	0.7122	0.5776	0.6739	0.5998	0.5491	0.7419	0.6579	0.5774
150	0.5273	0.6544	0.5317	0.5318	0.5776	0.5473	0.5728	0.0380	0.5464	0.5151	0.7157	0.6542	0.5317	0.6119	0.5436	0.4985	0.6886	0.6029	0.5340
180	0.4636	0.6012	0.4924	0.4925	0.5411	0.5158	0.5327	0.0456	0.5160	0.4830	0.6651	0.6010	0.4923	0.5562	0.4964	0.4581	0.6391	0.5549	0.4965
210	0.4364	0.5523	0.4581	0.4582	0.5070	0.4861	0.4957	0.0532	0.4873	0.4553	0.6167	0.5521	0.4580	0.5063	0.4562	0.4248	0.5931	0.5123	0.4633
240	0.4091	0.5074	0.4277	0.4279	0.4750	0.4581	0.4616	0.0608	0.4602	0.4305	0.5705	0.5072	0.4277	0.4615	0.4216	0.3966	0.5505	0.4743	0.4337
270	0.3727	0.4661	0.4006	0.4008	0.4450	0.4318	0.4302	0.0684	0.4345	0.4078	0.5263	0.4660	0.4006	0.4214	0.3915	0.3723	0.5109	0.4399	0.4070
300	0.3545	0.4282	0.3763	0.3764	0.4169	0.4069	0.4012	0.0760	0.4102	0.3866	0.4842	0.4281	0.3763	0.3854	0.3650	0.3511	0.4742	0.4087	0.3827
330	0.3455	0.3934	0.3542	0.3543	0.3906	0.3835	0.3745	0.0837	0.3872	0.3667	0.4443	0.3933	0.3542	0.3533	0.3416	0.3324	0.4401	0.3801	0.3605
360	0.3273	0.3614	0.3341	0.3342	0.3659	0.3614	0.3499	0.0913	0.3654	0.3480	0.4065	0.3613	0.3341	0.3245	0.3208	0.3156	0.4084	0.3538	0.3401
390	0.3227	0.3320	0.3157	0.3158	0.3428	0.3406	0.3272	0.0989	0.3448	0.3302	0.3708	0.3320	0.3157	0.2988	0.3020	0.3006	0.3790	0.3295	0.3213
420	0.3182	0.3050	0.2987	0.2989	0.3211	0.3210	0.3062	0.1065	0.3254	0.3134	0.3372	0.3050	0.2988	0.2760	0.2852	0.2869	0.3518	0.3071	0.3039
450	0.3091	0.2802	0.2831	0.2832	0.3009	0.3025	0.2869	0.1141	0.3070	0.2974	0.3057	0.2802	0.2832	0.2556	0.2698	0.2745	0.3265	0.2863	0.2878
480	0.3000	0.2574	0.2687	0.2688	0.2819	0.2851	0.2691	0.1217	0.2896	0.2823	0.2764	0.2574	0.2687	0.2375	0.2559	0.2631	0.3030	0.2669	0.2728
510	0.2909	0.2365	0.2553	0.2554	0.2641	0.2686	0.2527	0.1293	0.2731	0.2679	0.2492	0.2365	0.2553	0.2214	0.2431	0.2526	0.2812	0.2490	0.2588
540	0.2864	0.2173	0.2428	0.2429	0.2474	0.2532	0.2376	0.1369	0.2575	0.2543	0.2240	0.2173	0.2429	0.2072	0.2314	0.2430	0.2610	0.2323	0.2457
570	0.2818	0.1996	0.2312	0.2313	0.2318	0.2386	0.2237	0.1445	0.2428	0.2414	0.2010	0.1997	0.2313	0.1946	0.2206	0.2340	0.2422	0.2167	0.2334
600	0.2800	0.1834	0.2203	0.2205	0.2171	0.2249	0.2109	0.1521	0.2289	0.2291	0.1802	0.1834	0.2204	0.1835	0.2107	0.2256	0.2248	0.2022	0.2219
630	0.2773	0.1685	0.2102	0.2103	0.2034	0.2119	0.1990	0.1597	0.2157	0.2174	0.1614	0.1685	0.2102	0.1738	0.2014	0.2178	0.2087	0.1887	0.2111

660	0.2727	0.1548	0.2007	0.2008	0.1906	0.1997	0.1881	0.1673	0.2032	0.2064	0.1447	0.1549	0.2007	0.1653	0.1928	0.2105	0.1937	0.1761	0.2010
690	0.2636	0.1422	0.1917	0.1918	0.1786	0.1882	0.1780	0.1749	0.1914	0.1959	0.1302	0.1423	0.1918	0.1579	0.1848	0.2037	0.1797	0.1643	0.1914
720	0.2364	0.1306	0.1833	0.1834	0.1673	0.1774	0.1688	0.1825	0.1803	0.1859	0.1178	0.1307	0.1834	0.1516	0.1773	0.1972	0.1668	0.1534	0.1824
750	0.2091	0.1200	0.1754	0.1755	0.1567	0.1671	0.1602	0.1901	0.1697	0.1765	0.1075	0.1201	0.1754	0.1461	0.1703	0.1912	0.1548	0.1431	0.1739
780	0.1909	0.1102	0.1679	0.1680	0.1468	0.1575	0.1523	0.1977	0.1597	0.1675	0.0993	0.1104	0.1680	0.1414	0.1638	0.1854	0.1437	0.1336	0.1659
810	0.1636	0.1013	0.1608	0.1610	0.1376	0.1485	0.1451	0.2053	0.1503	0.1590	0.0933	0.1014	0.1609	0.1374	0.1576	0.1800	0.1333	0.1247	0.1583
840	0.1545	0.0930	0.1542	0.1543	0.1289	0.1399	0.1384	0.2129	0.1414	0.1509	0.0893	0.0932	0.1542	0.1341	0.1518	0.1749	0.1238	0.1164	0.1511
870	0.1364	0.0855	0.1479	0.1480	0.1207	0.1318	0.1322	0.2205	0.1329	0.1432	0.0875	0.0856	0.1479	0.1314	0.1463	0.1700	0.1149	0.1086	0.1443
900	0.1182	0.0785	0.1419	0.1420	0.1131	0.1243	0.1265	0.2281	0.1249	0.1359	0.0878	0.0787	0.1420	0.1292	0.1411	0.1654	0.1066	0.1014	0.1378
930	0.1000	0.0721	0.1362	0.1363	0.1060	0.1171	0.1212	0.2358	0.1174	0.1290	0.0902	0.0723	0.1363	0.1276	0.1362	0.1610	0.0989	0.0946	0.1317
960	0.0818	0.0663	0.1309	0.1309	0.0993	0.1104	0.1164	0.2434	0.1102	0.1224	0.0947	0.0664	0.1309	0.1263	0.1315	0.1568	0.0918	0.0883	0.1259
990	0.0727	0.0609	0.1257	0.1258	0.0930	0.1040	0.1119	0.2510	0.1035	0.1162	0.1013	0.0610	0.1258	0.1255	0.1271	0.1528	0.0852	0.0824	0.1204
1020	0.0545	0.0559	0.1209	0.1210	0.0871	0.0980	0.1078	0.2586	0.0971	0.1103	0.1101	0.0561	0.1210	0.1250	0.1229	0.1489	0.0791	0.0769	0.1152
1050	0.0364	0.0514	0.1163	0.1164	0.0816	0.0924	0.1040	0.2662	0.0910	0.1047	0.1209	0.0515	0.1163	0.1248	0.1189	0.1453	0.0734	0.0718	0.1102
1080	0.0182	0.0472	0.1119	0.1120	0.0765	0.0870	0.1005	0.2738	0.0853	0.0994	0.1339	0.0473	0.1120	0.1249	0.1151	0.1418	0.0681	0.0670	0.1055
1110	0.0000	0.0434	0.1077	0.1078	0.0717	0.0820	0.0973	0.2814	0.0799	0.0943	0.1490	0.0435	0.1078	0.1253	0.1114	0.1384	0.0632	0.0625	0.1009

TERMINOLOGIES

Optimization

Optimization is a process, or methodology of making a designed system achieve maximum functionality, effectiveness and efficiency as much as possible by enhancing some specified set of parameters without violating some constraints. It involves finding alternatives with the most effective and highest achievable performance compromise under the prevailing constraints, by maximizing desired parameters and minimizing undesired ones. Optimisation attains the highest or maximum result while considering the costs or expense.

Hybrid

A hybrid system employs a combination of techniques, methods approaches and conceptual models to investigate a problem from different functionalities. Hybrid dryer is a typical hybrid drying system with two or more different modes of energy sources so that it has functionalities or qualities of both for sustainable energy provision round the clock. Hybrid power system uses one or more renewable energy sources or more than one renewable.

Desiccant

A hygroscopic substance that induces or sustains a state of dryness (desiccation) in its vicinity by absorbing water. It dehumidifies air to remove moisture that degrades and destroys moisture sensitive products such as grain. Application of desiccant drying systems for the drying of freshly harvested cereal grains is done in order to remove the moisture and provide safe levels of storage. Desiccants dehumidify by eliminating or lowering humidity of the air to create and sustain a dry, moisture-free environment.

Solar collector

A device that collects and/or concentrates solar radiation from the Sun. Flat plate solar collectors have a transparent glazing as a cover on the absorber collector plate. Solar radiation penetrates the transparent glazing material and heat the plate. The hot plate transfers the heat to air that is held between the glazing and collector absorber plate. The plates are painted with special coatings designed with good conductors and absorbers of heat better than normal black paints.

Dryer performance

The effectiveness of air heating and dehumidification to improve moisture removal process from a substance. The performance of a dryer is referred by preconditioning the air parameters

such as temperature and relative humidity to enhance heat and mass transfer from a product through drying or dehydration. High dryer performances results to high drying rates.

Finned element surface

Finned elements are extended surfaces that protrude from an object to increase the rate of heat transfer to or from the air. Fins increase the temperature difference between an object and the air by increasing surface area and enhancing convection heat transfer rate to provide economical solution to heat transfer problems.

Radiation concentration lenses

Radiation concentration lenses are devices that work on the basic principle of focusing the sun. Lenses increase the amount of solar radiation energy per unit area by concentration of the scattered or direct solar radiation through intensification of sunlight and solar energy from the sun into one focal point. Generally, intense sunlight results in higher temperatures, which increases the rate at which heat can be trapped efficiently. Radiation concentration lenses systems generate solar power by using mirrors or lenses to concentrate a large area of sunlight, or solar thermal energy, onto a small areas.

Desiccant exhaust air regeneration

In a desiccant exhaust air regeneration system, exhaust air from the process is recycled back to the workplace through a desiccant material. Dehumidification of exhaust air takes place in the desiccant regeneration system. This reduces the energy needed for tempering cold incoming air because the recycled air contains the heat that was present in the workplace when it was removed. A system that makes optimum use of recirculated air is the most efficient method of recovering heat from the exhaust air. Thus, it leads to a lowering in the energy cost. An additional benefit is the lowering of the capacity requirements for the plant heating system. The regeneration of exhaust air for drying is feasible with the use of a desiccant material (Kothari *et al*., (2009).

Data logger

An electronic device for monitoring and recording data over time using in-built sensor. Data is automatically monitored and record based on environmental conditions over time, allowing relevant parameters to be measured, documented, analyzed and validated. The data logger contains a sensor to receive the information and a computer chip to store it. The stored

information in the data logger memory is transferred to a computer for analysis. Data loggers monitor a range of parameters such as temperature and relative humidity

Solar insolation

Solar insolation is the power per unit area received from the Sun in the form of electromagnetic radiation in the wavelength range of the measuring instrument. The solar irradiance integrated over time is called solar irradiation, insolation, or solar exposure. However, in practice insolation is often used interchangeably with irradiance.

Open-air sun drying (OASD)

Natural open sun drying takes place when grain is exposed to the sun and wind by placing it on mats, racks, or on the ground. The advantage of drying products directly open-air is that almost no costs for fuel and appliances have to be spent by the farmer. However, the dried products are often of lower quality due to varying temperature levels and contamination of the products with dust, vermin's and leaves.

Useful heat

Useful heat is heat stored above room temperature in a solar heating system. It is the portion of final energy of the air which is available for the respective use during final conversion after losses. Maximum heat gains occur when the whole collector configuration temperature is highest.